

**Fermilab**

TM-1155  
1183.000

**THE DESIGN OF THE MAGNETIZED MUON SHIELD  
FOR THE PROMPT NEUTRINO FACILITY**

**C. Baltay, N. Bosek, J. Couch, B. Cox,  
D. Cossairt, R. Fast, E. Leung, J. Lindberg, S. Oh,  
M. Peters, I. Pless, J. Spitzer, R. Stefanski and  
J. K. Walker**

**October 12, 1982**

CONTENTS

- I. Preface
  - II. Introduction and Summary
  - III. Description of the Muon Flux Computational Procedures
  - IV. Calculation of the E-613 Shield
  - V. Muon Shield Designs for the Prompt Neutrino Facility
  - VI. Muon Fluxes Associated with the Proton Beam Transport
  - VII. Comparison of Designs and Conclusions
- Appendix

I. PREFACE

This report covers the work of many individuals and it is appropriate to identify the main areas of responsibility and contributions.

1. Program Development

a) M. Peters and J. K. Walker.....Fermilab

b) C. Baltay and J. Spitzer.....Columbia

c) S. Oh and I. Pless.....MIT

2. Muon Flux Measurements for E-613 were analyzed and provided by

S. Childress and B. Roe.....Michigan

3. Radiation Calculations

D. Coissart and J. Couch

4. Mechanical and Electrical Design for Magnetized Muon Shield

N. Bosek, B. Cox, R. Fast and E. Leung

5. Target Box Design

J. Lindberg

6. Coordination

R. Stefanski and J. K. Walker

## II. Introduction and Summary

The main technical challenge in the design of the prompt neutrino beam is the magnetized muon shield. Two satisfactory alternate designs have been developed for such a shield during this past year and the background muon fluxes have been calculated by three independent programs at Columbia, Fermilab, and MIT. The background muon fluxes have been calculated to be satisfactory in all of the detectors that might use the beam (i.e., the 32-in. and the 15-ft. bubble chambers, as well as counter detectors located in or near Lab E and Lab C).

- 1) A conventional iron magnet system with an air gap in the central regions of high muon flux. This design is an improvement over a previous solid iron design in that it eliminates or minimizes the uncertainties due to inelastic scattering and electromagnetic trident production by the large flux of muons traversing the shield (see Figs. 1 and 2).
- 2) A design using an 8.4m long 50 kG superconducting magnet (see Fig. 3).

A large amount of detailed engineering design has been carried out by various departments at Fermilab on both of the designs listed above, including detailed calculations of the magnetic field shapes, and quite detailed estimates of costs. Both designs seem feasible. We discuss the relative merits of the two designs and conclude that the superconducting design is the more cost effective solution and provides substantial space for

additions or modifications if required.

To check the reliability of the programs used in the design of the muon shield, we have calculated the background muon fluxes in the existing E-613 muon shield in the Meson Lab for a variety of conditions. We found that the agreement between the measured fluxes and the fluxes calculated by the three independent programs is quite satisfactory. These results were reported in June 1982 to the Directorate. The programs reproduce satisfactorily the detailed distributions of the muon flux measured by E-613 at the end plane of the iron shield and at the front face of the detector. The programs also permitted a calculation of a factor of  $\approx 5$  reduction in the muon flux measured with the modified version of the shield used in the spring 1982 run of E-613. In fact, this reduction factor was predicted by one of the programs before the shield was modified and the fluxes were measured. We therefore have confidence that the programs give realistic results to within a factor of two or three. In view of the safety factor of  $\approx 10$  in the design for the 15-ft. and 32-in. chambers, this seems quite satisfactory.

In Section III of this report we describe in detail the three Monte Carlo programs used in these calculations. In Section IV we give the details of the flux calculations for the E-613 shield and the comparisons with the observed fluxes with various configurations of that shield. In Section V we describe the designs that have been developed for the neutrino area shield. In Section VI we discuss the problem of proton beam transport losses

and the associated muon fluxes. Finally, in section VII a comparison of the two solutions is made which covers cost, effectiveness, schedule and responsiveness to future unknowns. We conclude that there are not overwhelming reasons for the choice of one design over the other. However, for a variety of secondary reasons the superconducting design offers advantages. We therefore propose the construction of the prompt neutrino facility with the superconducting magnet design.

### III. Description of the Monte Carlo Programs

The difficulties and uncertainties in predicting the background muon rate leaking through an active muon shield for a beam dump experiment are by now well known. In order to increase confidence in the design of a Tevatron beam dump facility each experimental group with approval for the area as well as the design group within Fermilab have developed a program for this calculation. The three programs have been written quite independently, though discussions between the groups have frequently contributed to the understanding of the effects involved.

The following sections will discuss the various effects included in the three programs. Detailed equations will be included in an appendix.

Each of the three programs takes a different approach to the calculation of muon production by protons incident on a heavy target. The Columbia and Fermilab programs treat muon production in two stages: pion production and either pion decay or direct muon production expressed as a fraction of pion production. The MIT program directly expresses muon production from all sources.

The pion production formulas used in the Columbia and Fermilab programs derive from the radial scaling fits to pion production data from many  $p \rightarrow \pi^\pm X$  experiments at various energies up to 400 GeV. These fits extend to a  $p_\perp$  of 6 GeV/c for  $\pi^+$  and somewhat lower for  $\pi^-$ . In the Fermilab program a correction is made to give agreement with ISR data at still larger  $p_\perp$ , out to 10 GeV/c. Since radial scaling gives excellent fits to data over a wide range of incident proton energies, it is expected that the interpolation to 1 TeV will be satisfactory.

The calculation of pion decay to muons in a material of given interaction length is straight forward. The ratio of direct muon production to pion production has been measured in several experiments at Fermilab. The general result is that the  $\mu/\pi$  ratio is independent of  $P_{\perp}$  at small  $x$  and falls with  $x$  as a power of  $(1-x)$ . The Columbia <sup>formula</sup> uses  $(1-x)^3$  and the Fermilab program  $(1-x)^2$ . Either form gives a reasonable fit to the measurements.

The product of pion production and either the pion decay probability or the  $\mu/\pi$  ratio gives the rate of muon production by the primary proton beam. In a thick target such as the beam dump re-interaction of produced pions and protons are an important contribution to the total. The Columbia program carries out a shower Monte Carlo for each production interaction. In this calculation secondary pions are allowed to interact and produce either more pions or direct muons. The Fermilab program uses an enhancement factor as a function of  $p_{\pi}/p_{\text{beam}}$  that is derived from a separate shower Monte Carlo calculation.

This calculation allows secondary pions to interact as in the Columbia program, but in addition one forward secondary nucleon is generated and allowed to interact. This calculation follows the shower to a depth of 3 in the pions and 6 in the nucleons.

Finally, both the Columbia and Fermilab calculations must correct from production in pp collisions to that in pA collisions where A may be Be, Fe, Cu, or W. For this purpose an approximate A dependence of the pion invariant cross sections as given by L. Voyvodic is applied. In addition, the  $\mu/\pi$  ratio should increase as  $A^2$  since pion production rises more slowly than direct muon production.

The MIT program does not attempt to determine muon production from a stepwise calculation but relies instead upon a fit to total muon production from a W target as generated by W. Buza. That formula includes both direct and decay muons from all generations of the shower in a thick target.

All three of the programs under discussion make use of standard techniques to follow the central trajectory of a produced muon from the target through the absorbers and magnets of a particular shield design. The Columbia and Fermilab programs generate initial muon momenta and directions randomly and weight according to the production spectrum discussed above. The MIT program proceeds more systematically, stepping in  $p_{\perp}$  and  $p$  until all of phase space is covered. Comparisons of trajectories for particular initial conditions have indicated good agreement among the programs in the calculation of magnetic bending.

A muon that would not strike the detectors if it were not deflected may nonetheless produce a hit if it undergoes one of a number of processes along its path. The first such process considered in the programs is multiple Coulomb scattering. In the Columbia and MIT programs Coulomb scattering is normally treated by calculating the undeflected ray and determining where it would strike the plane of a detector. The total Coulomb scattering angle is calculated and the probability of a hit by this central ray is determined by an integration of the 2-dimensional scattering probability distribution over the area of the detector. In contrast, the Fermilab program changes the direction of a muon according to the Coulomb scattering distribution appropriate to the thickness of material traversed in one step of the path integration.

An important observation is that for large thickness, such as the entire dump, a Gaussian distribution is an excellent approximation to the true Coulomb distribution. For small steps the Molière tails must be taken into account. The Fermilab program does this in a way that crudely accounts for the nuclear form factor but includes the effects of large angle plural scattering.

A second effect that can cause an otherwise "safe" muon trajectory to strike a detector is inelastic muon scattering in the material of the dump. The Fermilab program determines the effect of inelastic muon scattering by producing a scatter at a random point along the trajectory and then following the deviated path. Scatters are generated uniformly in and within chosen limits. This is to ensure that all regions of the scattering distribution are sampled adequately. The scattering probability<sup>is</sup> converted to a weight and multiplies the production weight of the muon to give the final weight added to the total to give the number of hits on a detector.

In the MIT program inelastic scattering is taken account of by an integration over  $q^2$  and  $\nu$  carried out at many points along the path of a muon. The range in  $\nu$  is determined taking into account the stopping power of the portion of the dump remaining between the scattering point and the detector. The integral accumulates the scattering probability for that portion of the kinematic space that leads to a hit on the detector.

A third process that can contribute to the background is electromagnetic trident production. This effect is particularly dangerous since it can lead to an effective change of sign of the muon and thus to a cancellation of the magnetic deflection achieved before

the interaction. The spectrum is relatively hard, dropping as  $1/p$ , so it is difficult to defeat this process by range. All three programs calculate the effects of trident formation by treating it as a special kind of inelastic scattering, but allowing for the possible sign change.

The Columbia and MIT programs both treat energy loss of the muons as they travel through the dump as a continuous process. The Columbia program allows for the energy dependence of  $dE/dx$  in iron but treats loss in dirt as a constant. The MIT program uses an equation that fits the calculated loss rate in iron as a function of energy and scales that formula to give the correct minimum loss rate for dirt. In the Fermilab program a table is constructed that includes the exact restricted energy loss calculation for each relevant process-ionization, electron pair production and Bremstrahlung. This table contains  $dE/dx$  for each material at intervals of 1 GeV/c momentum up to 1 TeV/c. Only losses due to collisions in which less than 10% of the energy is lost are included in this table. A separate calculation randomly generates an occasional large stochastic energy loss from the range 10% to 100% of the incident energy.

In the Columbia and MIT programs the magnetic fields in active elements of the dump are always entered in the form of detailed field maps. These maps have been derived from various sources, sometimes by hand calculation and sometimes by detailed calculation with programs such as POISSON. The Fermilab Monte Carlo has the capability to accept detailed field maps, but has usually been applied in a mode in which it is given the field in a series of regions on the midplane of a magnet and then calculates the vertical and horizontal return fields by applying flux conservation. This

calculation gives the uniform field that would return the central flux. If the iron of the return yoke is saturated a uniform field is a good approximation. For unsaturated return yokes a linear variation is added to give agreement with detailed calculations.

14  
Appendix

This appendix gives details of the equations used in the three beam dump Monte Carlo programs. For each class of formula the equations in each program will be detailed.

## 1 Energy Loss

### 1.1 Columbia

In Fe the Columbia program uses an energy dependent rate of energy loss given by:

$$\frac{dp}{dx} = \begin{matrix} 1.327 + 2.418 \times 10^{-2} p + 3.8342 \times 10^{-4} p^2 & p < 30 \text{ GeV/c} \\ 1.592 + 5.169 \times 10^{-3} p + 6.971 \times 10^{-7} p^2 & p > 30 \text{ GeV/c} \end{matrix}$$

in GeV/c /m

In concrete a constant value is used:

$$\frac{dp}{dx} = .5 \text{ GeV/c /m}$$

### 1.2 Fermilab

A calculated rate of restricted  $dE/dx$  for  $dE/E < .1$  is used in the Fermilab program. The values are shown in Figure A-1. Larger stochastic losses are randomly produced.

### 1.3 MIT

$$\left. \frac{dp}{dx} \right|_{\text{Fe}} = 1.16 + .13 \log p + 7.1 \times 10^{-6} (\log p)^7 \quad \text{GeV/c /m}$$

$$\left. \frac{dp}{dx} \right|_{\text{conc}} = \frac{.45}{1.16} \left. \frac{dp}{dx} \right|_{\text{Fe}}$$

15

The energy loss rates used in the three programs are compared in Figure A-1.

## 2 Pion Production

## 2.1 Columbia

$$E \frac{d^3\sigma}{dp^3} = A \frac{1}{(1 + P_L^2/M^2)^4} (1 - x_R)^n$$

$$x_R = E^*/E_{\max}^*$$

$$\pi^+ \quad \frac{A}{30.2} \quad \frac{M^2}{.66} \quad \frac{n}{3.2}$$

$$\pi^- \quad 17.4 \quad .74 \quad 3.9$$

## 2.2 Fermilab

$$E \frac{d^3\sigma}{dp^3} \Big|_{\pi^+}^{A=1} = 70 e^{-7x_R} \frac{1}{(1 + P_L^2/M^2)^9}$$

$$m^2 = .1 + 3.2 x_R - 1.3 x_R^2 \quad q^2 = 3.5 + (8x_R - 4x_R^2 - 5) \left( \frac{.35}{1 + e^{(P_L^2 - 9.6)/1.8}} + .65 \right)$$

$$\pi^-/\pi^+ = 1 / (1.7 + 2.2 x_L^2 + 9.1 x_F^2)$$

$$\frac{d^3\sigma}{dp^3} \Big|_A / \frac{d^3\sigma}{dp^3} \Big|_1 = A^{.8 - .3x_F + .15 P_L}$$

## 2.3 MIT

The MIT program does not separate muon production into pion production and subsequent decay or proportional direct muon production. The following equation is thus for muon production:

$$\frac{dN}{dE dp_x dp_y} = \alpha \frac{(1 - E/E_0 - P_L^2/2E)^4 (1 - E/E_0)}{E/E_0 (1 + P_L^2/.74)^{3.5}}$$

$$\mu^- \quad \frac{\alpha}{10^6/10^{12} p}$$

$$\mu^+ \quad 1.5 \times 10^6/10^{12} p$$

AT 400 GeV  $E_0$

### 3 Muon-pion Ratio

#### 3.1 Columbia

$$\left. \frac{\mu}{\pi} \right|_{DIR} = 10^{-4} (1-x_F)^3$$

#### SHOWER MONTE CARLO

#### 3.2 Fermilab

$$\left. \frac{\mu}{\pi^+} \right|_{DIR} = 10^{-4} (-1.91 + .88 \log E_{CM}) (A/56)^{0.2} (1-x_F)^2 \quad E_{CM} > 15.4 \text{ GeV}$$

$$R_{DIR}^{SHOWER} = 1 + (.115 / (E/E_{BEAM}))^{1.5} \quad R_{DECAY}^{SHOWER} = 1 + (.175 / (E/E_{BEAM}))^{1.81}$$

#### 3.3 MIT

See remarks above under pion production.

The production of muons from an Fe target as measured by Bodek et al. and as calculated by the Columbia and Fermilab programs is shown in Figure A-2a. Figure A-2b compares the same data scaled to W with the values from the MIT program.

## 4 Coulomb Scattering

### 4.1 Columbia

The Columbia program uses standard Gaussian multiple scattering with:

$$\theta_{1/2} = \frac{.021}{P\beta} \sqrt{L/L_R}$$

### 4.2 Fermilab

The Fermilab program uses a modification of the Moliere scattering formalism that takes into account the form factor of the iron nucleus. Figure A-3 gives the shapes of the scattering angle distributions used.

### 4.3 MIT

Standard multiple scattering:

$$\theta_{1/2} = \frac{.02}{E} \sqrt{L/L_R}$$

## 5 Inelastic Muon Scattering

## 5.1 Columbia

SIMILAR TO FERMI LAB

## 5.2 Fermilab

$$\frac{d^2\sigma}{dq^2 d\nu} = \frac{2\pi\alpha^2}{p^2 q^4} \frac{F_2(q^2, \nu)}{\nu} \left[ 2EE' - \frac{q^2}{2} + \frac{(q^2 - 2M\mu)(1 + \nu^2/q^2)}{1+R} \right]$$

$$F_2(q^2, \nu) = A(2+\epsilon_0)x(1-x)^{1+\epsilon_0} + B \frac{14(4+\epsilon_1)}{9(5+\epsilon_1)}(1-x)^{3+\epsilon_1} \frac{q^2}{q^2+m_0^2}$$

$$\epsilon_0 = G_{00} + \epsilon \quad \epsilon_1 = G_{10} + \epsilon$$

$$\epsilon = \kappa \log \left[ \frac{(q^2+m_0^2)}{m_0^2} \right]$$

$$A = .661 \quad B = .357 \quad \kappa = .33 \quad G_{00} = 1.69 \quad G_{10} = 7.2 \quad m_0^2 = .573$$

$$R = .44$$

## 5.3 MIT

$$\frac{d^2\sigma}{dE'_2 d\Omega} = \frac{4\alpha^2 E'_2}{q^4} W_2(q^2, x) \left[ \frac{\sin^2 \theta/2}{G(\nu, q^2) M} + \frac{x \cos^2 \theta/2}{\nu} \right]$$

Figure A-4 compares calculations by the three programs with data from the EMC on the scattering of 280 GeV/c muons from 2.3 m of Fe.

### 6 Muon Trident Formation

All of the programs treat muon trident formation as a special kind of deep inelastic scattering, including a possible sign change of the produced muon.

#### 6.1 Columbia

Uses the real photon process for muon pair production multiplied by a factor (a la Jack Smith) to take the virtual photon process (which is larger) into account.

#### 6.2 Fermilab

$$\sigma(E) = \frac{\alpha}{2\pi} \left(\frac{Z}{6}\right)^2 \left[ \log \frac{E}{6.7m_\mu} \left( \log \frac{E}{6.7m_\mu} - \frac{3}{2} \right) \ln 3 \right] 1.52 \mu b$$

$$\frac{dN}{d\nu dM_{\mu\mu}} \propto \frac{1}{\nu} e^{-2M_{\mu\mu}}$$

#### 6.3 MIT

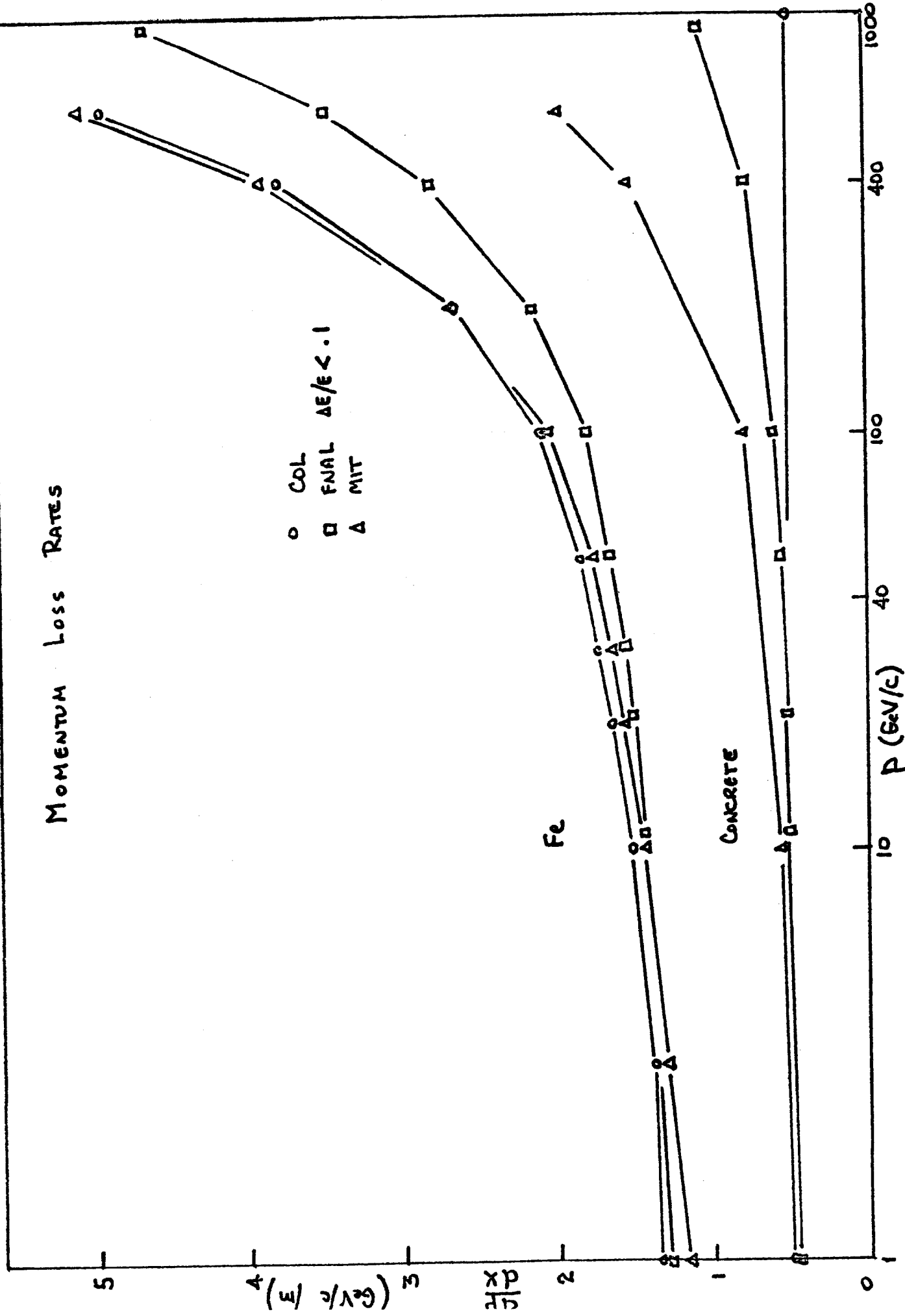
$$\frac{d\sigma}{d\nu dQ^2} = \frac{\alpha}{\pi} \frac{1}{Q^2} \frac{1}{\sqrt{Q^2+\nu^2}} \left(\frac{Z}{6}\right)^2 1.52 \mu b \frac{m_\mu^2}{m_\mu^2+Q^2} \left[ (1-\nu/E)(1-Q_{min}^2/Q^2) + \frac{\nu^2}{2E^2} + \frac{Q^2}{4E^2} \right] \log \frac{\nu}{6.2m_\mu^2}$$

FLAT  $\nu$  DIST  
COLLINEAR PRODUCTION

A-1

# MOMENTUM LOSS RATES

- COL
- FNAL  $\Delta E/E < .1$
- △ MIT



MUON PRODUCTION  
 BY  
 400 GeV/c PROTONS  
 ON  
 Fe

$\mu^+$

$\mu^-$

50  
 40  
 30  
 20  
 10  
 0

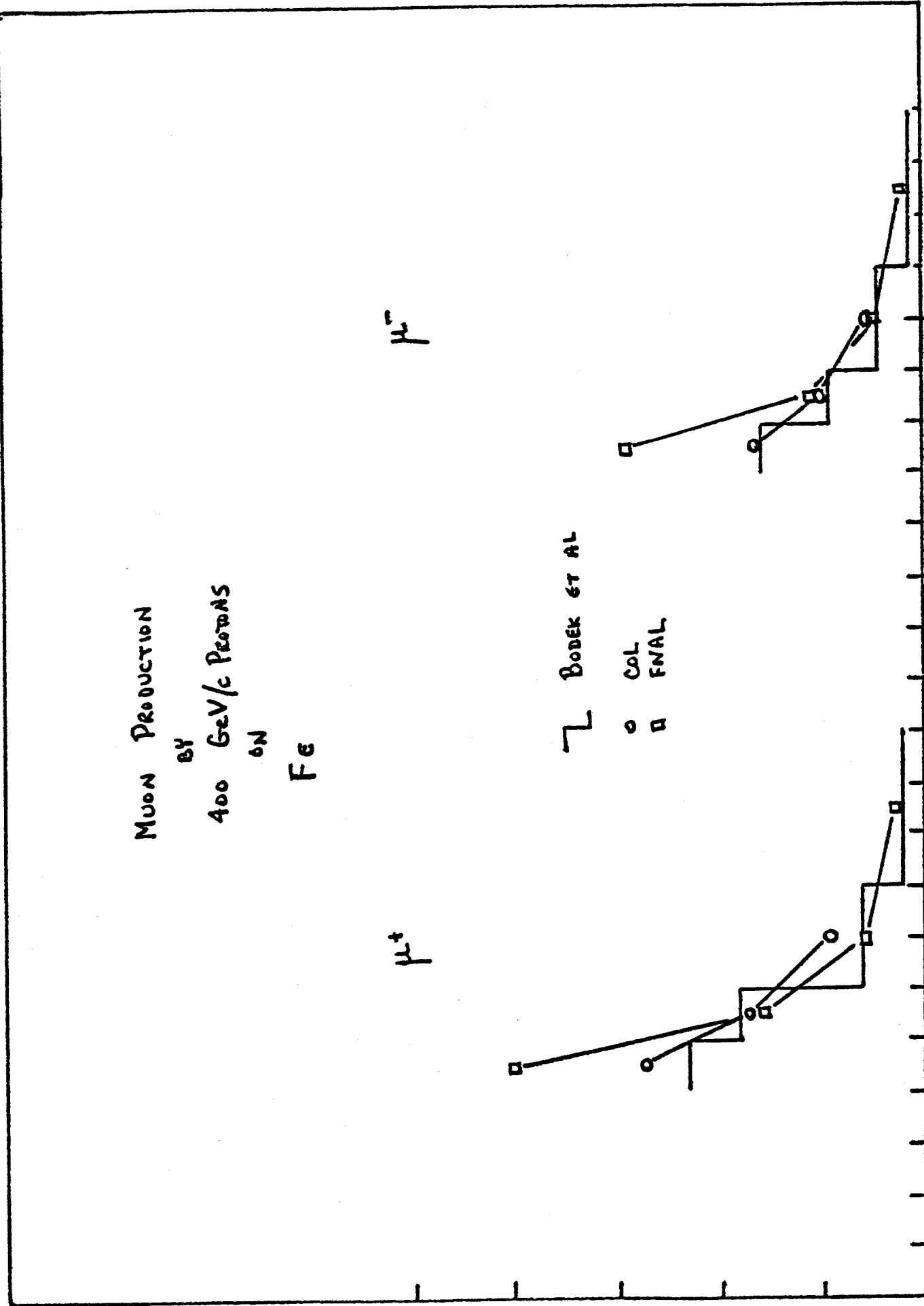
$\mu/10^6 P / 10 \text{ GeV/c}$

BODEK ET AL

○ COL  
 □ FNAL

0 20 40 60 80 100

$P_\mu \text{ (GeV/c)}$



MUON PRODUCTION  
 BY  
 400 GeV/c PROTONS  
 ON  
 W

$\mu^-$

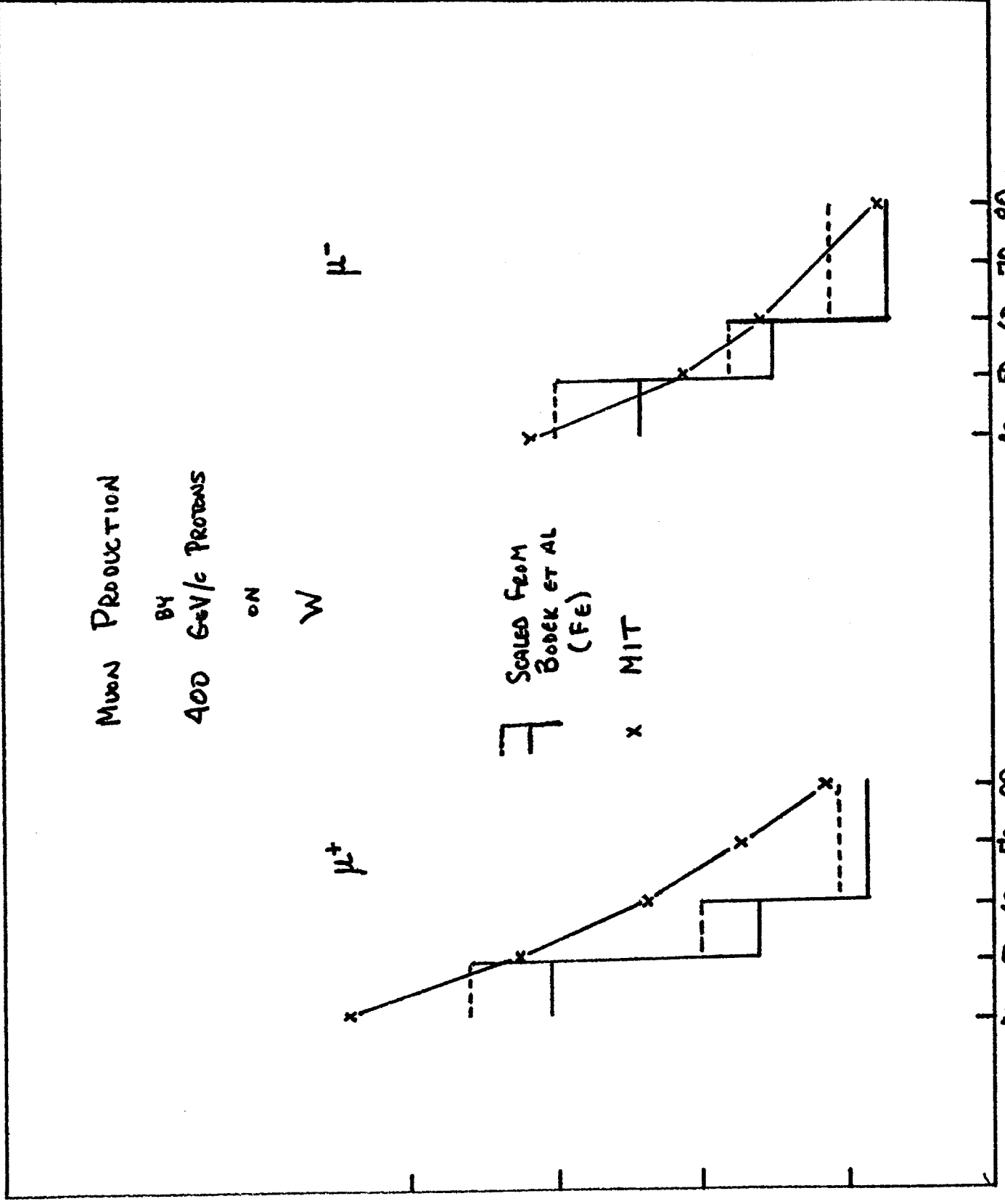
$\mu^+$

SCALED FROM  
 BONEK ET AL  
 (FE)

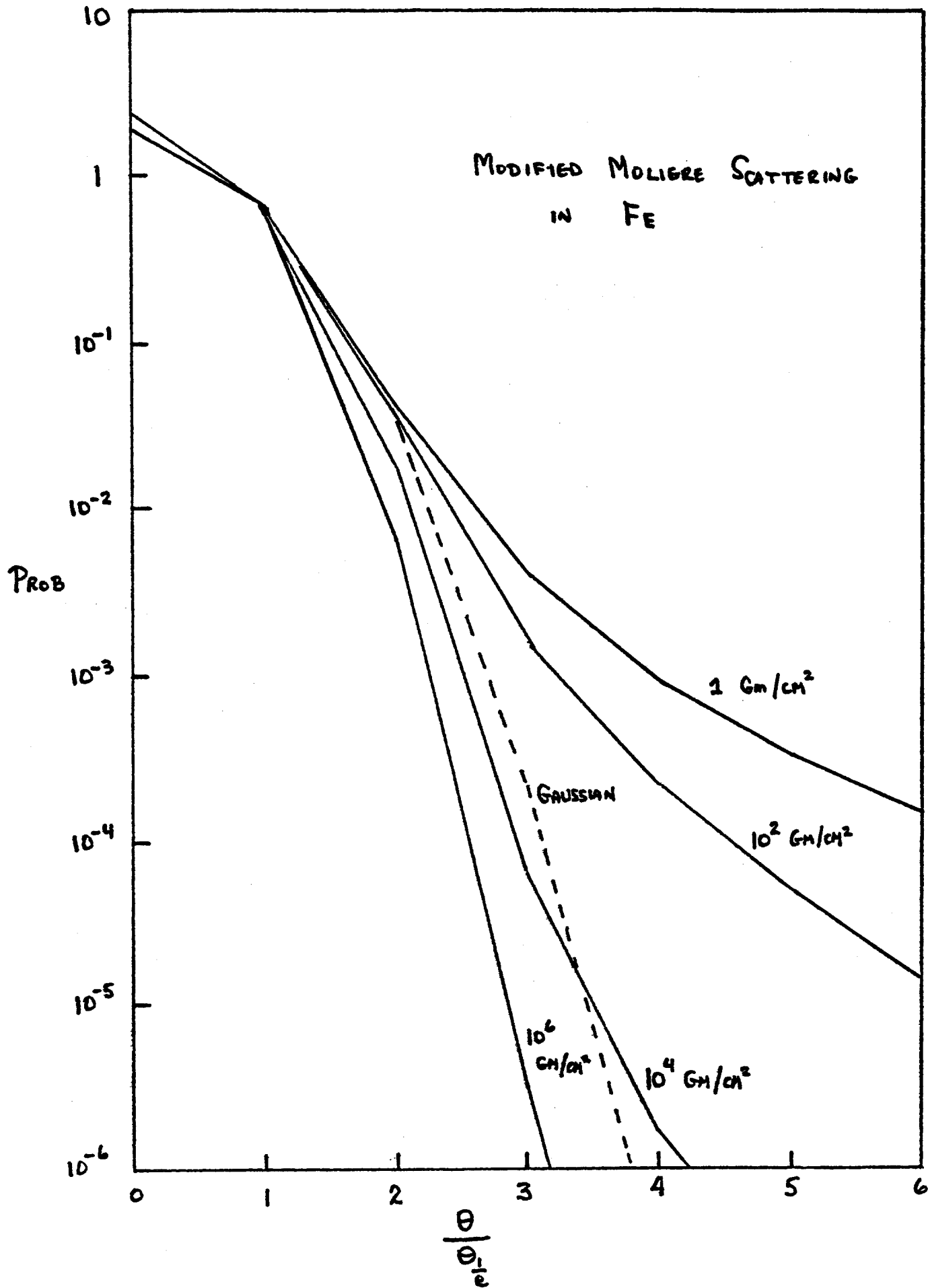
x MIT

$\mu/10^6 P/10 \text{ GeV/c}$

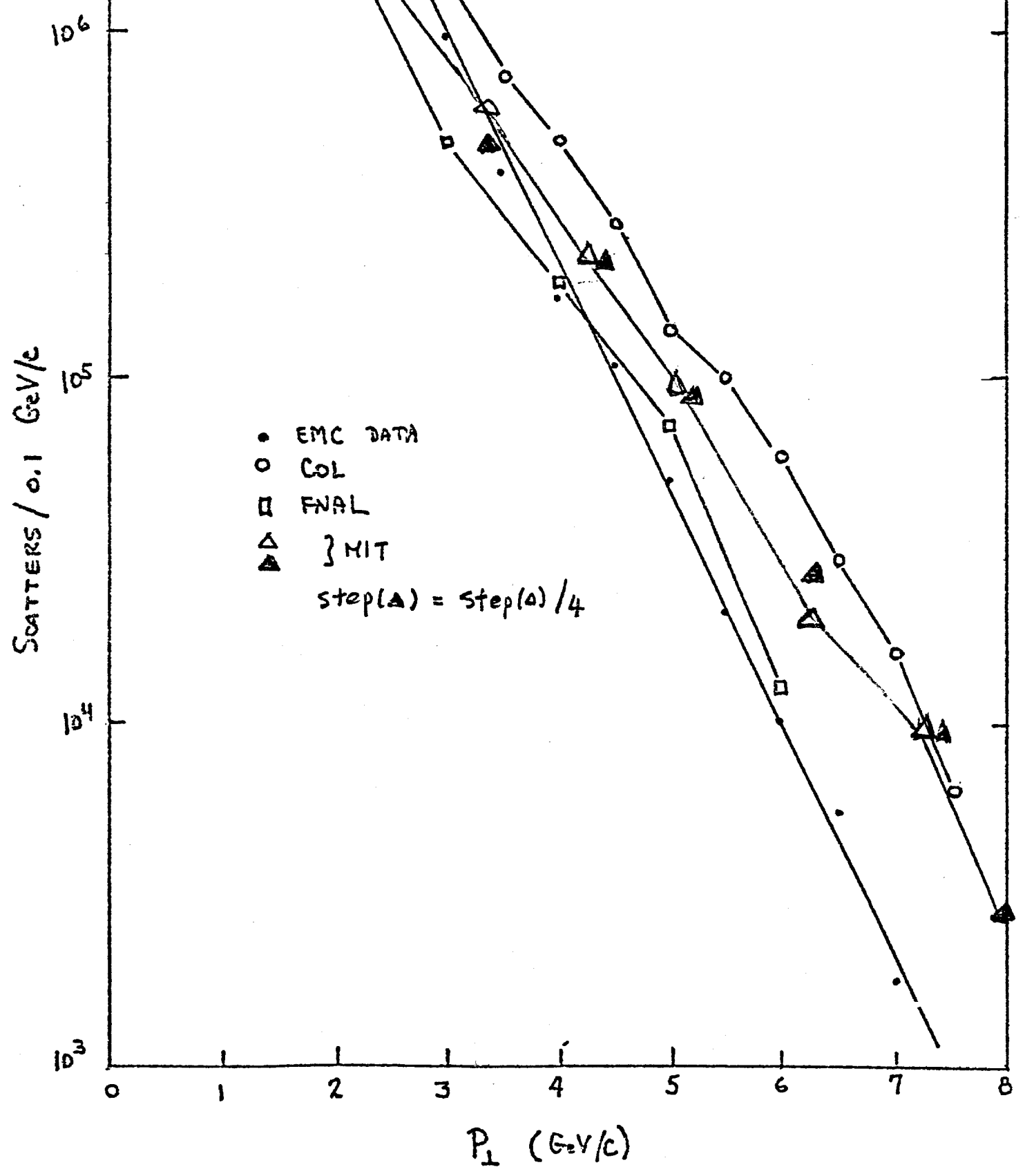
$P_\mu \text{ (GeV/c)}$



### MODIFIED MOLIGRE SCATTERING IN FE



# MUON INELASTIC SCATTERING



#### **IV.** The E-613 Shield

The magnetized muon shield built for the beam dump experiment E-613 in the meson lab has some similarities to the shield we are designing for the prompt neutrino beam in the neutrino area. We felt that it would be a significant test of our programs to calculate the background muon fluxes in the E-613 shield and compare these to the actually measured muon fluxes. Such calculations have therefore been carried out using all three of the programs used in the neutrino area design for a variety of configurations of the E-613 shield. The agreement between the calculations and the measured fluxes is satisfactory for all three programs. In this section we describe these comparisons in some detail.

We have considered two different versions of this shield - the "Old Shield" used in the Spring 1981 run, and the "New Shield" used in the Spring 1982 run. In both versions the shield consisted of a magnetized iron front end followed by a passive iron shield. (See Figs. **IV**-1 and **IV**-2 for a sketch of these two versions). The magnetized part was the same for both versions and consisted of three magnets M1, M2, and the Hyperon magnet (10.4 meters total length) followed by two off axis "spoiler" magnets. The passive part was approx. 13 meters long in the 1981 shield and about 18 meters long in the 1982 shield. Between the passive shield and the detector there was another 3 m long but narrower piece of passive iron (called

the AVIS magnet) and 1.4 meters of concrete. Some parameters of these shields are summarized below

	<u>1981 Shield</u>	<u>1982 Shield</u>
Length of magnetized iron <sup>a</sup>	10.4 m	10.4 m
Total B x L	223 kgm	223 kgm
Total bending $\Delta P_t$	6.7 Gev/c	6.7 Gev/c
Total length of iron <sup>b</sup>	24 m	29 m
Minimum energy loss in shield	35 Gev	42 Gev
Multiple scatt. ( $\Delta P_t$ ) rms proj.	0.56 Gev/c	0.62 Gev/c

a) Excluding spoiler magnets.    b) Excluding spoiler magnets and AVIS iron

The muon flux measurements carried out with this shield are given in the May 4, 1982 note by S. Childress and B. Roe and a December 8, 1981 note by G.K. Fanourakis. The available data fall into four categories:

1. The muon anticounters (MUANTI) at the front face of the detector. They cover a total of 5 feet x 5 feet, consisting of five horizontal strips labeled A, B, C, D, E which are 5 feet wide by 1 foot high each. These give the total muon flux hitting the detector.

2. A probe counter (P counter) which is about 7" x 10" in size at the end of the passive iron shield ( $\sim$ 31 meters from target in 1981,  $\sim$ 36 meters from target in 1982) counting in coincidence with the MUANTI counters (called P, MUANTI).

The P counter was moved up and down at the end of the shield, but was always centered horizontally on the beam axis. The P. MUANTI coincidence gives the vertical distribution at the end of the passive iron for muons that hit the detector.

(See Figs. IV.3-6)

3. The singles counting rate with the P counters both at the end of the passive iron and in the plane of the front face of the detectors. In regions of very high counting rate these counts are probably related to the total muon flux. However in regions of low muon flux they may have substantial backgrounds, or may even be dominated by, hadronic or electromagnetic junk (they are singles counts in a 7" x 10" counter).

4. Muons seen in the E-613 detector in the time gate of a neutrino event trigger (called "stale muons"). These muons must have at least 1.1 Gev to be detected, and about 5 Gev to traverse the whole detector. Thus the muon flux between 1.1 and 5 Gev and the flux above 5 Gev in the detector are available.

Due to an error in stacking at the time when the 1981 shield was modified to the new 1982 configuration, too much iron (by 6 blocks) was placed on top of the passive iron shield. In this position the extra 6 blocks intercepted the very high flux of deflected muons, multiple scattered some of them into the detector, and thus increased the flux of muons in the detector. These blocks were then removed when the error was discovered, and the muon flux decreased by the expected factor of five or so.

The fluxes were measured with all 6 blocks on, 4 of these blocks off, and finally with all six blocks off. In addition, the muon fluxes were measured by the E-613 group with the incident proton beam pitched upward by 4 milliradians ("PITCH ON" data), which was their usual running condition, and also with the incident protons at 0 milliradian (i.e. "PITCH OFF" data). Thus there exists a large amount of measured muon flux data under a large variety of conditions, i.e. the original 1981 configuration, the final 1982 configuration (with all 6 blocks off), and the two intermediate configurations (with all 6 blocks on, and with 4 blocks off, 2 on), each of these with the proton beam at 0 mrad and 4 mrad. We have calculated the expected muon fluxes for each of these configurations with each of the three programs (i.e. Columbia, Fermilab, and MIT) independently. The large variety of different conditions provided a fairly thorough check of the calculations.

The results of the calculations for the total muon fluxes (sum of  $\mu^+$  and  $\mu^-$ ) are compared with the E-613 measurements in Table ~~IM~~-1. The first column of the Table gives the measured fluxes, and columns 2, 3, and 4 give the fluxes calculated by the three programs. We see that the calculations are within a factor of two of each other and the measurements for all of the various conditions for which measurements are available. We consider this very satisfactory agreement.

The calculations of the vertical distribution of the muon flux at the end of the passive iron (for muons that also hit the detector) are compared with the P. MUANTI coincidence counts in Figures ~~IM~~ - 3 to ~~IM~~ - 6. Finally, the calculations for the vertical and horizontal distribution of the total muon

flux in the plane of the front face of the detector are compared with the corresponding P singles measurements in Fig ~~IV~~ - 7 and ~~IV~~ - 8. The agreement between the calculations and the measurements is within a factor of 3 or so even in these detailed distributions, which we consider quite satisfactory.

However, a few comments about the precision of the agreement that can be expected might be useful.

a) The precision of the measured fluxes can be estimated by looking at the internal consistency of the measurements.

For example, consider the "PITCH OFF" data with the incident protons at 0 mrad to the horizontal. Since the 613 detector is vertically centered 30 cm above the horizontal axis, with the incident protons at 0 mrad the high energy end of the muons (300 to 400 Gev) clip the upper edge of the detectors. From the simple geometry of the situation we see that these muons pass the end plane of the passive iron shield (at 36 meters from the target) in a narrow region around 6 feet above the floor (see Fig. ~~IV~~ - 9). Such a peak is indeed observed and can be seen in Figs. ~~IV~~ - 4, 5, 6. However both the magnitude and the position of this peak at 6 feet should be independent of the number of steel blocks above 9 feet on top of the shield. But the measured peak in Figs III - 4 to 6 (Figures 9, 10, and 11 of the May 4, 1982 note by Childress and Roe) vary by a factor of two in magnitude and 6" in position. We thus conclude that the precision (normalization, position, etc.) of the P. MUANTI measurements are no better than a factor of two in magnitude and 6" in position.

Another example worth looking at is the horizontal distribution of the muons above the detector (Fig. III - 8, or Fig. 13 of the May 4, 1982 report by Childress and Roe) which shows a sharp peak about 20" off center. However, all of the relevant components of the beam and shield are claimed to be centered horizontally, so therefore our programs calculate a peak of magnitude comparable to the observed peak but centered horizontally. This indicates that either the placement of some of the shield or beam components or the position accuracy of the E-613 flux measurement are off by as much as 20".

b) In a detailed comparison of the inner workings of the three muon flux programs, we tried to separate the effects of the initial muon production rates in the dump from the calculation of the transmission of the shield. We define the transmission ratio at a particular set of initial values of the total momentum  $P$  and the transverse momentum  $P_t$  as the fraction of muons (produced in the dump at that  $P$  and  $P_t$ ) that end up in the detector. This ratio is clearly independent of the number of muons produced at that  $P$  and  $P_t$ . Figs. ~~III~~ - 10 and ~~III~~ - 11 show the comparisons of the three programs at a few values of  $P$  and  $P_t$ . The agreement is well within a factor of two.

The three programs use different parametrizations of the pion production rates and of the  $\mu/\pi$  ratios in the dump, as discussed in section II of this report. The agreement between these parametrizations is not better than a factor of two. We therefore believe that the differences between the fluxes cal-

culated by the three programs are mainly due to the muon production formulas and not because of differences in calculating what muons do in the shield.

In view of the above comments about the precision of the muon flux measurements, the positioning of the elements of the shield, and the uncertainties of the muon production formulas, we believe that the agreement between our calculations and the actually observed muon fluxes are quite satisfactory, both in the total fluxes and the detailed flux distributions.

In last years' progress report we stated that our program calculated a muon flux a factor of 8 lower than the rate observed in the Spring 1981 run. After some study the lower estimate was traced to two factors. One was the fact that the return field of the hypron magnet was entered incorrectly in the program. When this error was corrected the calculated flux increased by a factor of two. The remaining factor was due to the fact that the muon production formula used at that time neglected A dependent effects and the increased muon production due to the hadronic cascade in the beam dump target. Improved estimates of these two effects led to the present flux predictions.

Another point worth noting is that the factor of 5 decrease in the muon background flux in the E-613 detector due to the additional 5 meters of passive iron (the main change from the 1981 shield to the final 1982 shield configuration) was predicted

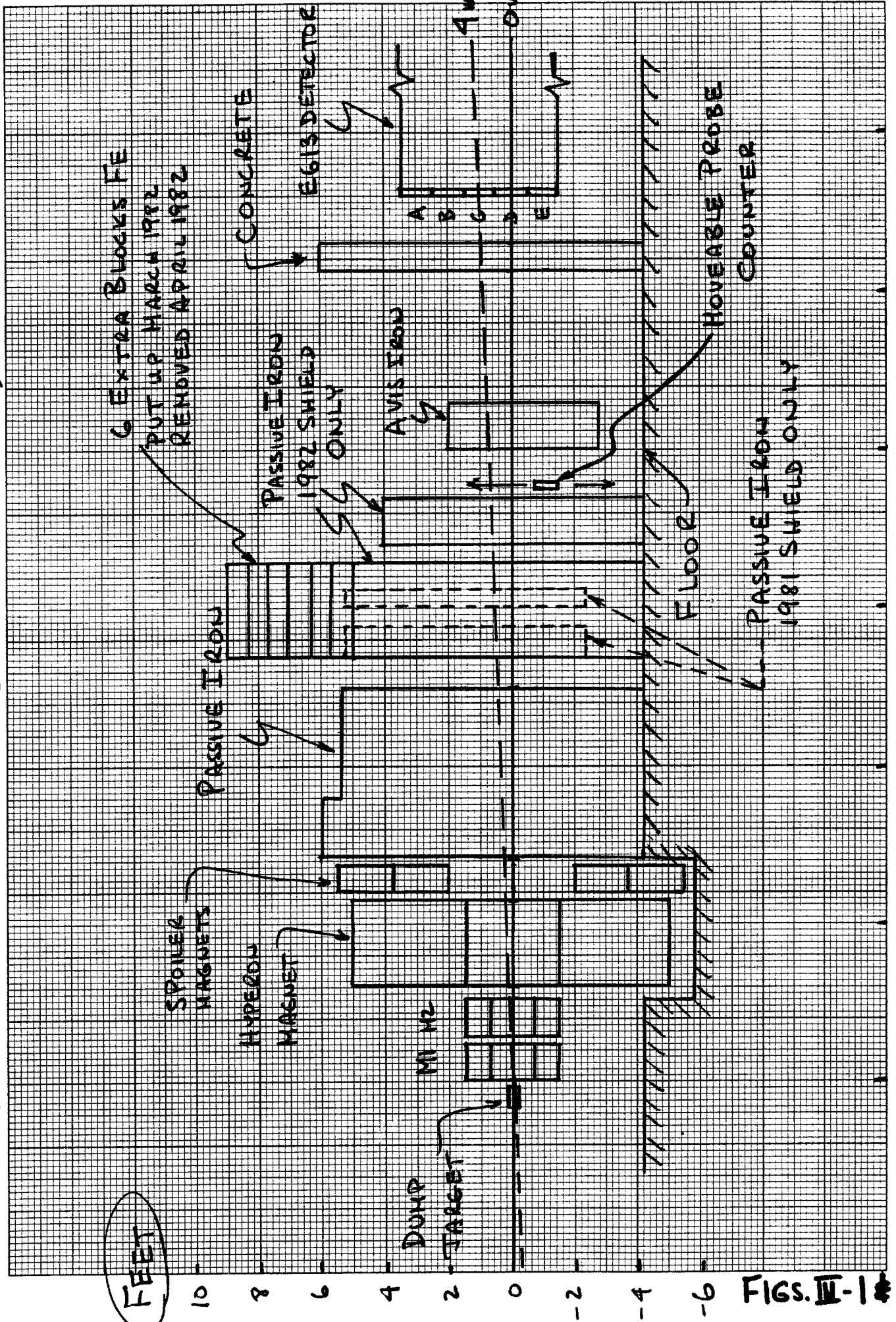
by one of our programs before the shield was restacked and the reduced flux was measured. It gives us more confidence in our programs that they are not only able to explain fluxes after the observed rates are known but they can predict what will happen in some new configuration before the flux measurements are made. In addition, the set of muon measurements with full density tungsten target and the final shielding configuration was made after our muon flux predictions were made available for that configuration. The agreement is again satisfactory.

TABLE I - 1

E-613 Shield Muon Flux Comparisons

	<u>Observed Flux</u>	<u>Columbia Program</u>	<u>Fermilab Program</u>	<u>MIT Program</u>
1. <u>Old Shield (1981)</u>				
Total MUANTI	47,500	56,000	40,000	58,500
$P_{\mu} \geq 1.1 \text{ GeV/c}$	25,000	34,000		
Counter A	15,053	19,500	10,300	18,000
B	11,048	1,200	5,200	12,500
C	9,171	10,600	6,500	9,500
D	7,035	11,500	10,300	9,000
E	7,336	13,800	7,700	9,500
2. <u>New Shield (1982)</u>				
6 Blocks ON	58,000		48,000	53,000
4 Blocks OFF, 2 ON	29,000			20,000
Final (All 6 Blocks OFF)	10,400	6,200	5,400	8,000

# EG13 SHIELD - OLD (1981) AND NEW (1982) VERSIONS



FIGS. IV-1 & 2

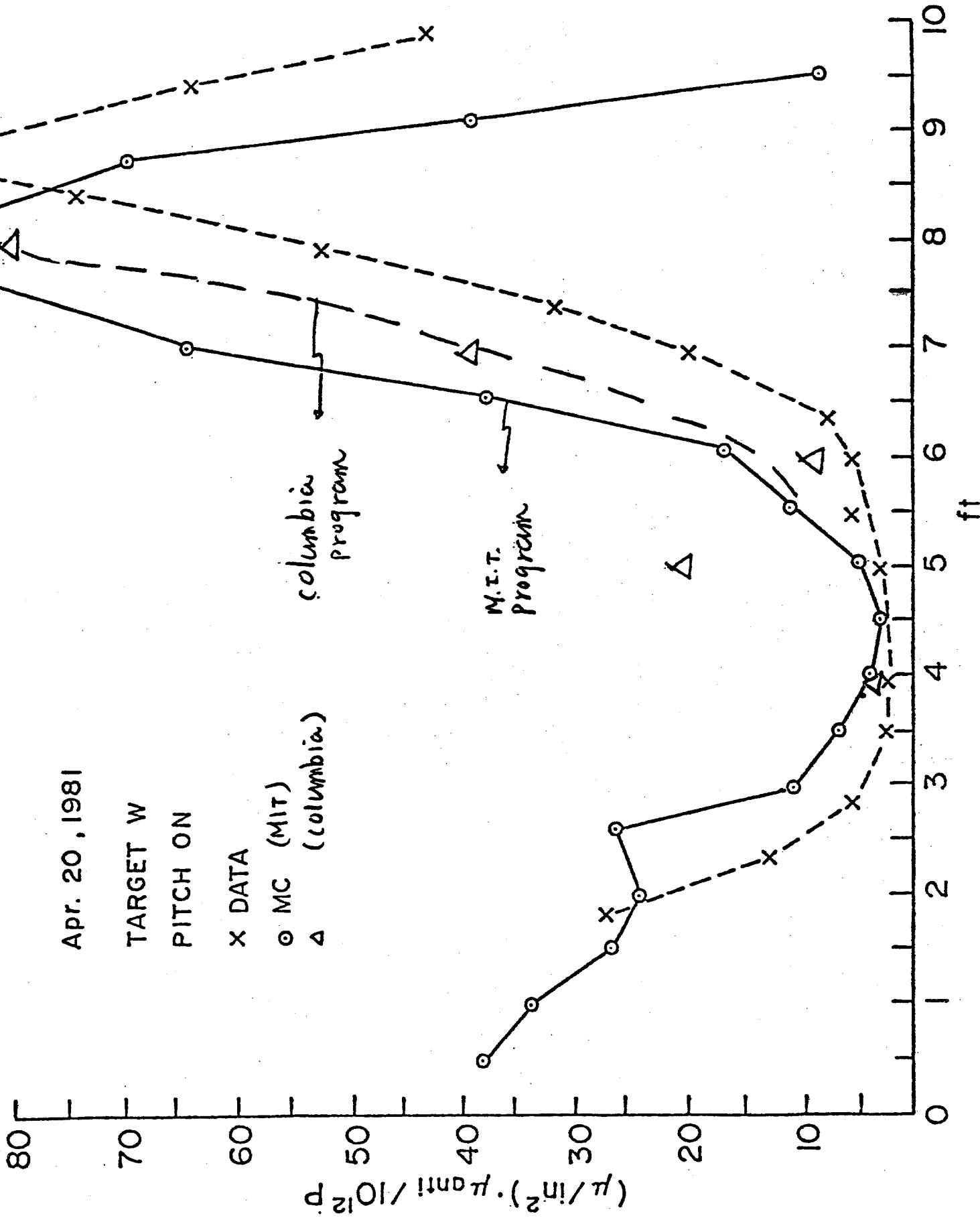


Fig. IV-3

S. ORA (M.I.T)

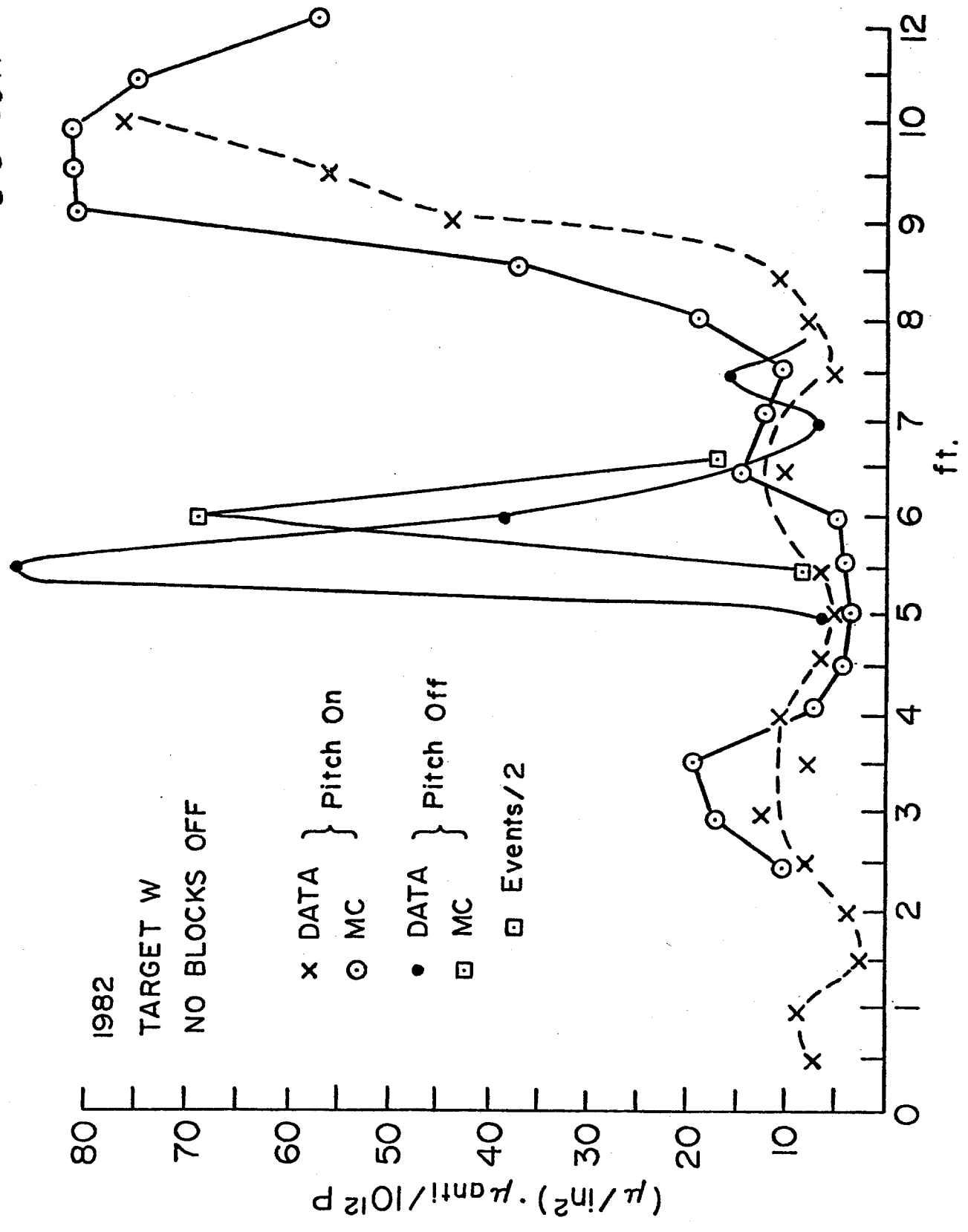


Fig. IV-4



Seog Oh (MIT)

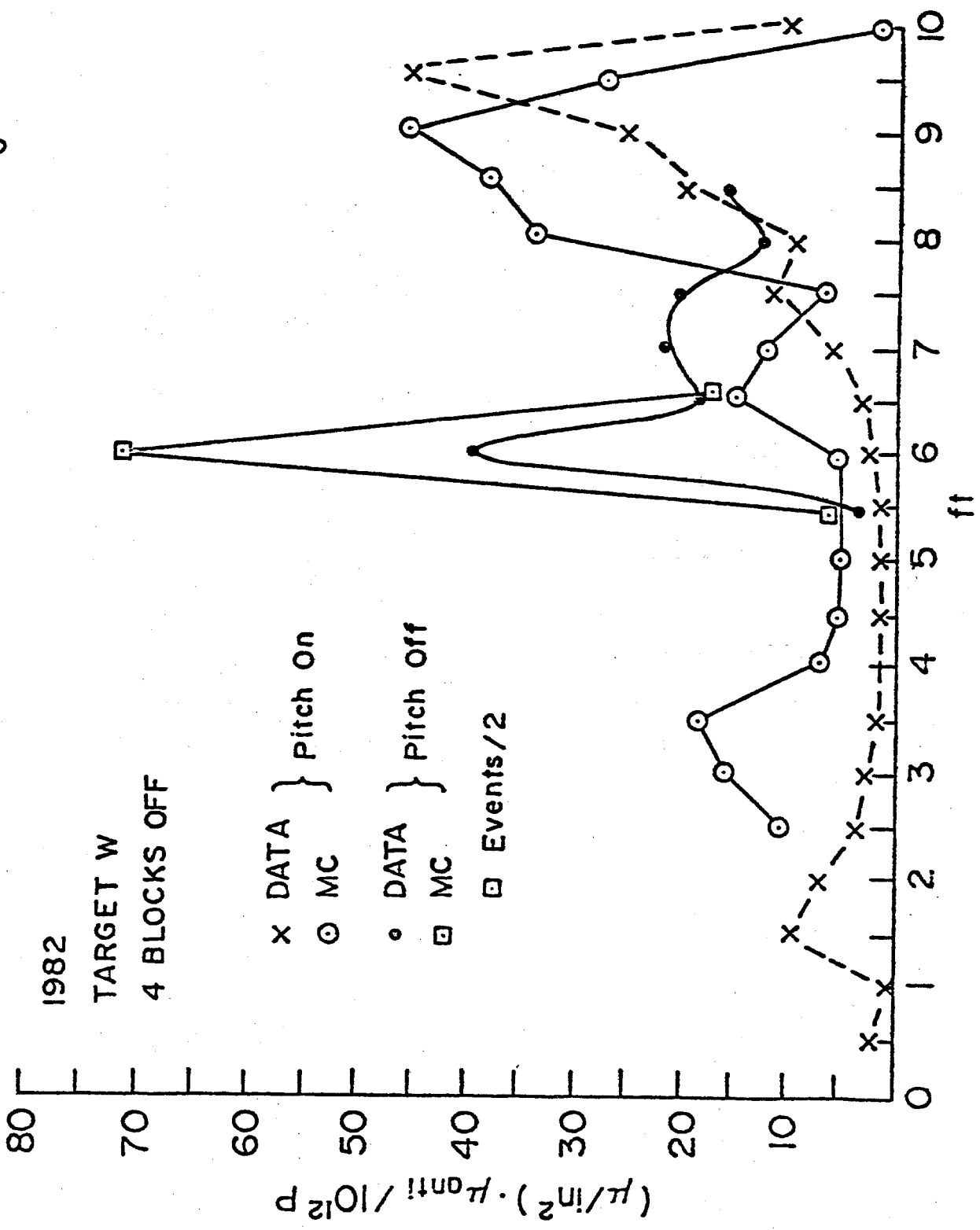


Fig IV-5

1982

TARGET W  
G Blocks off

- \* DATA ) pitch on
- MC
- DATA ) pitch off
- MC
- Events/2

$(M/in^2) \cdot (M_{ANTI}) / 10^{12} P$

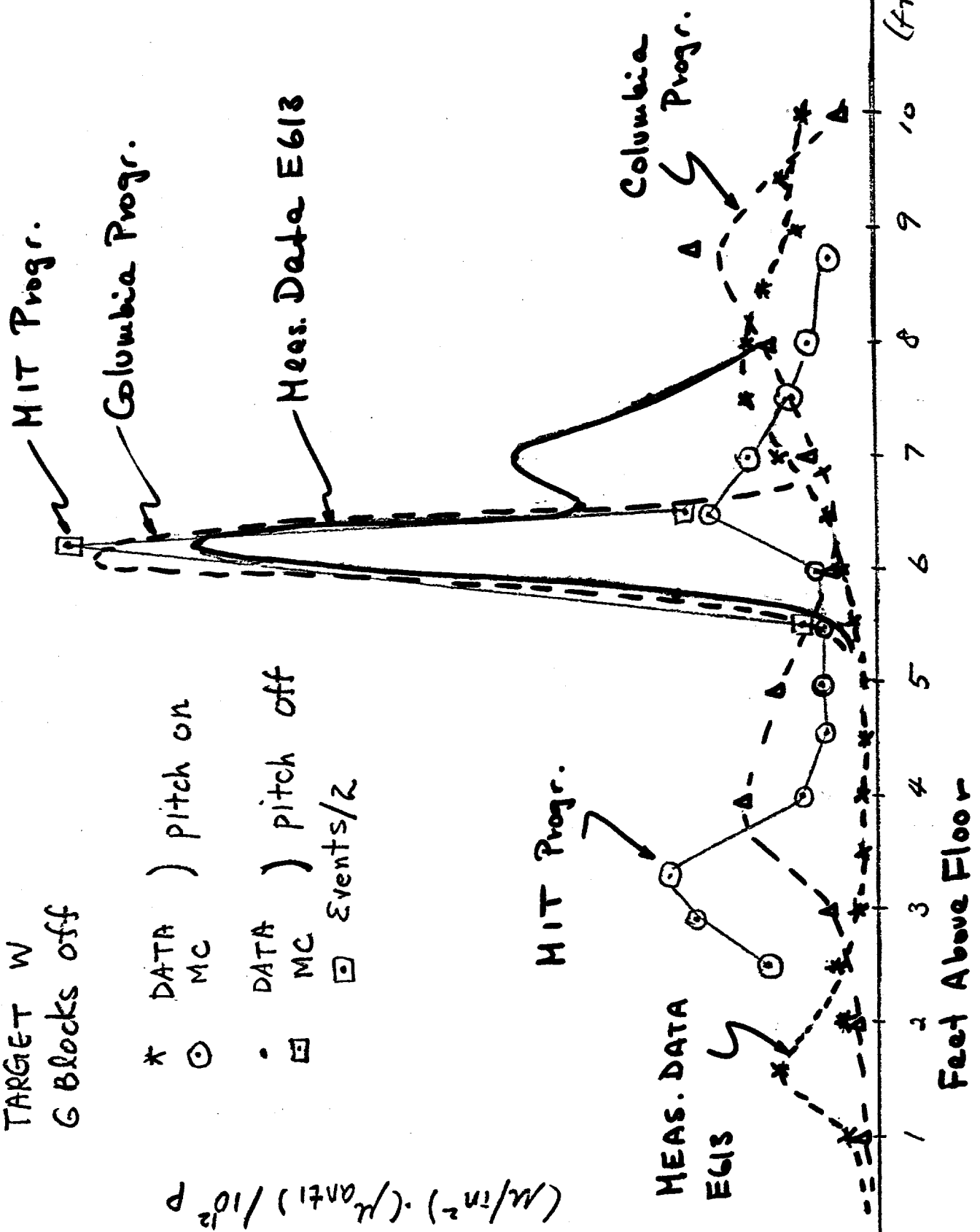


FIG. III - 6

μp SINGLES 40

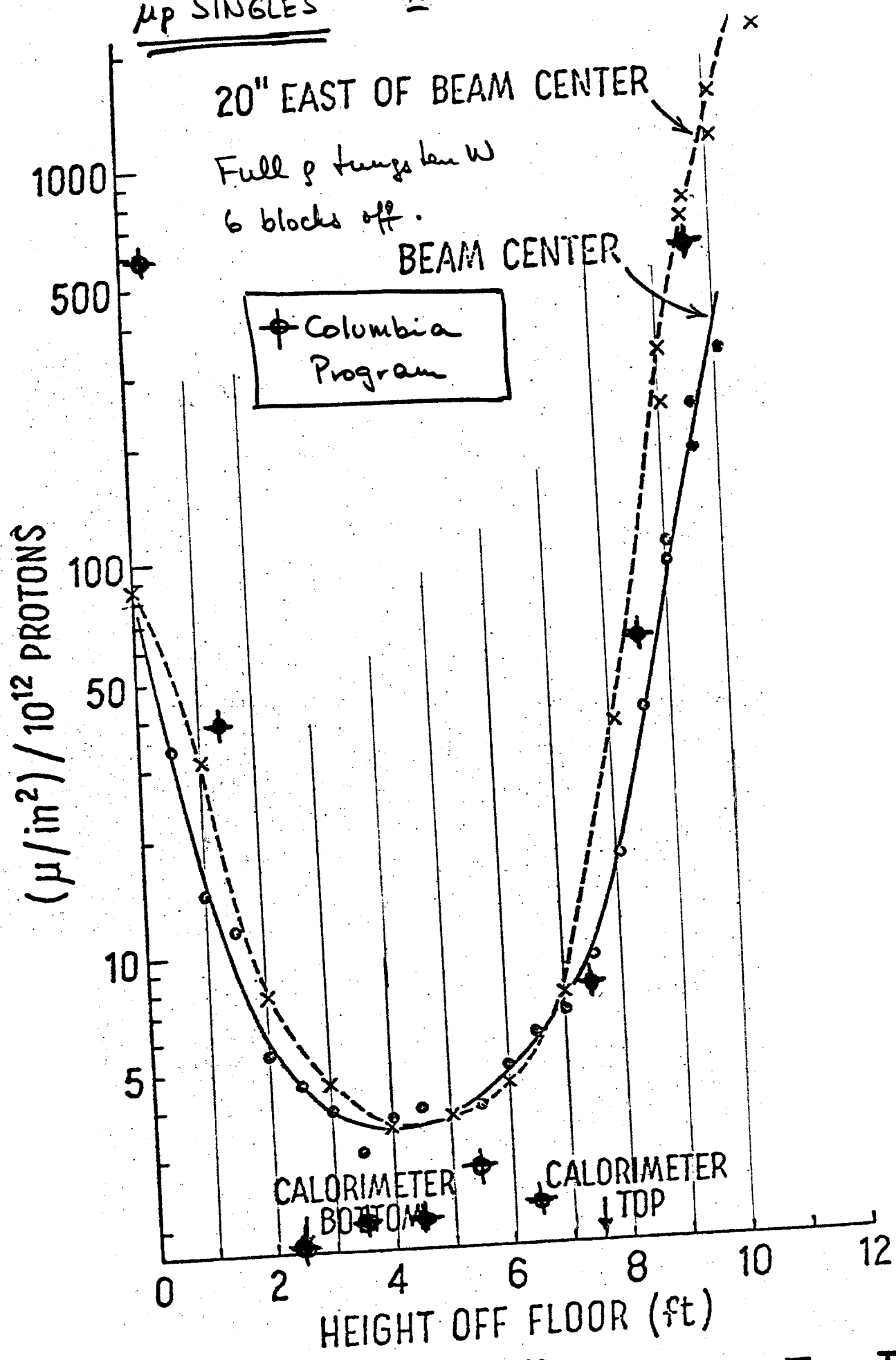


Figure 12

FIG. IV-7

Seeg Oh(MIT)

<sup>41</sup>  $\mu p$  SINGLES AT FRONT DETECTOR FACE

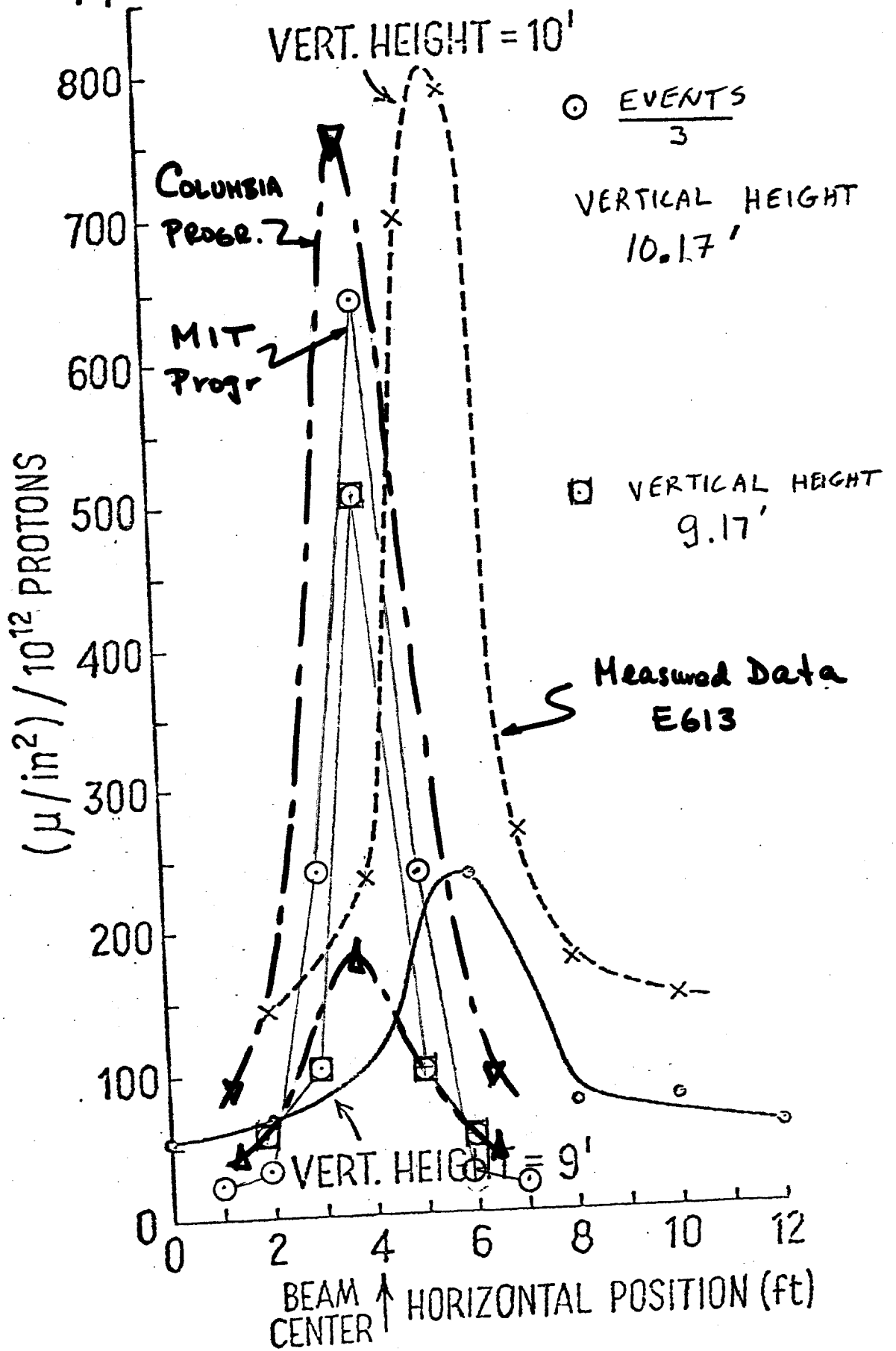


Figure 13

FIG. IV - 8

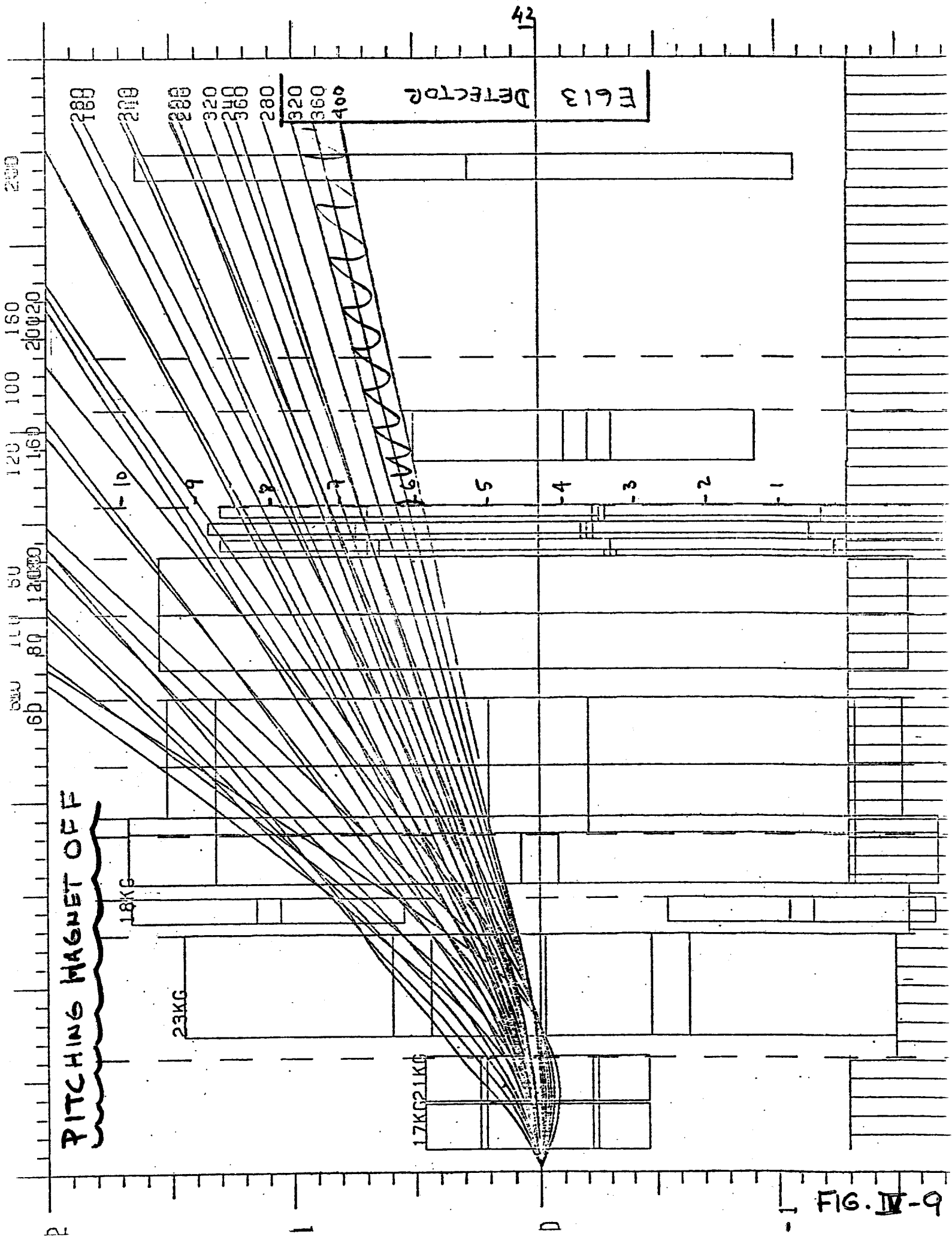


FIG. IV-9

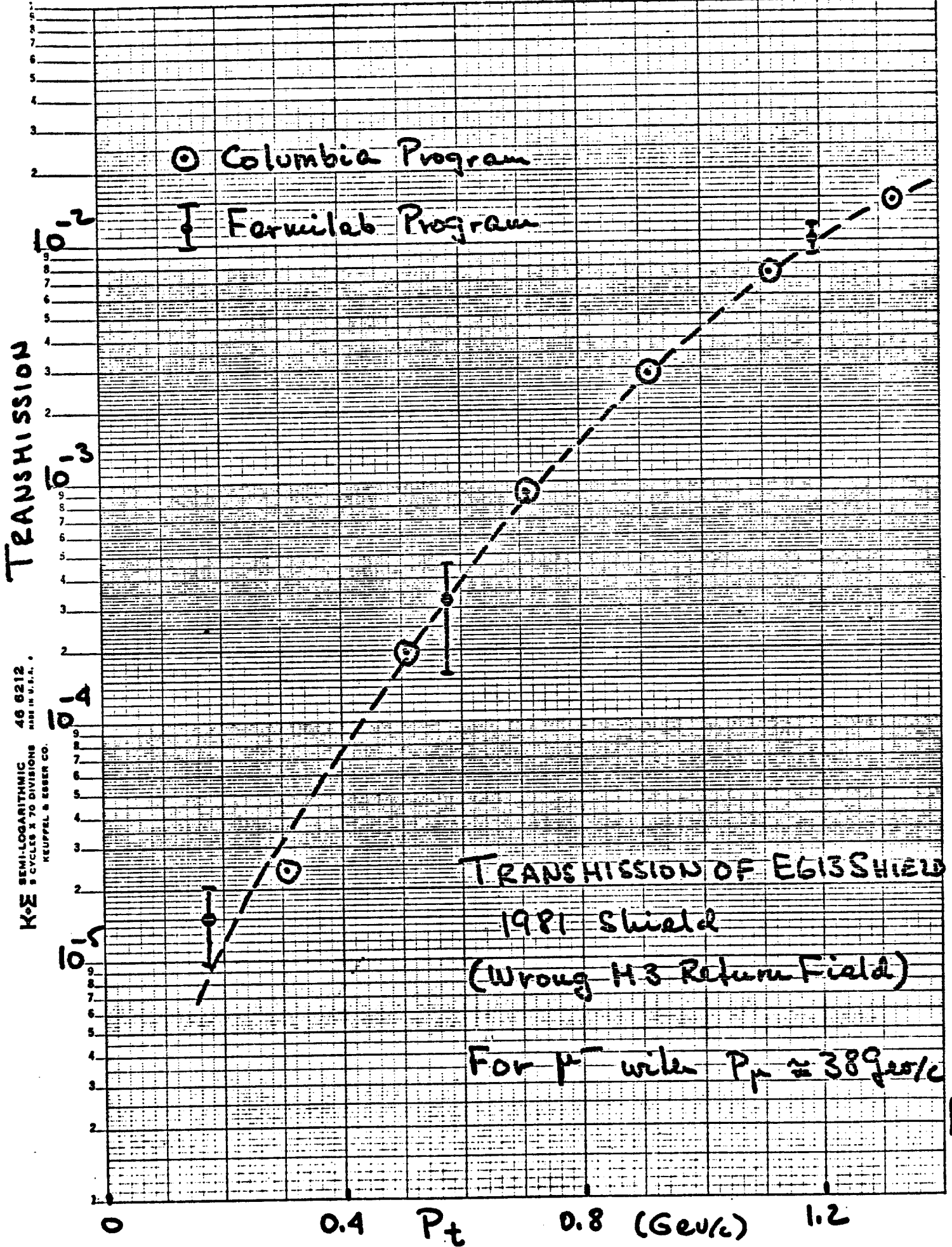


FIG. IV - 10

K&E SEMI-LOGARITHMIC 46 6212  
5 CYCLES X 70 DIVISIONS MADE IN U.S.A.  
KEUFFEL & ESSER CO.

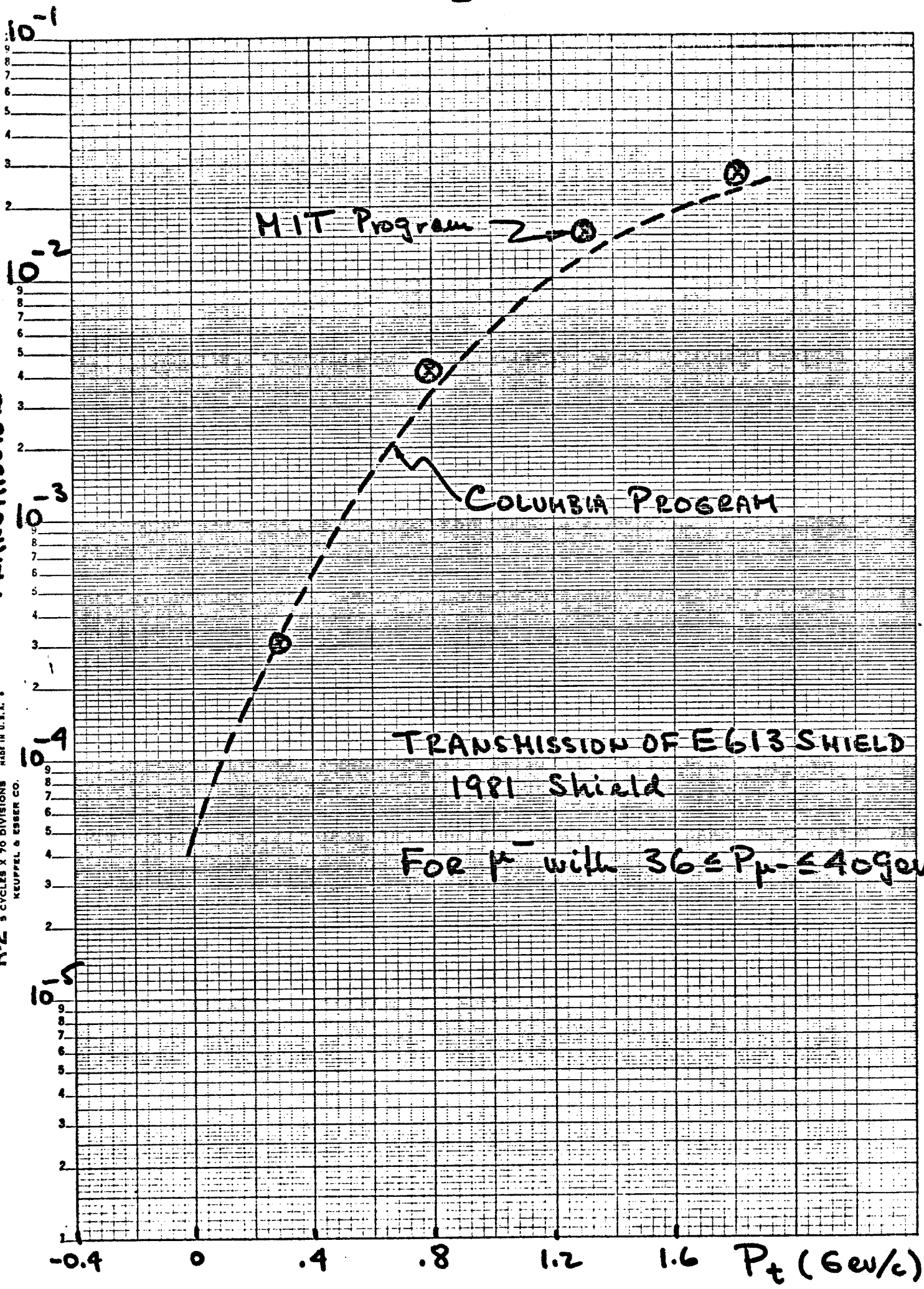


FIG. IV-11

AppendixMuon Production Formulae

## 1. The Muon Flux Formulae

a. The Columbia program started with the  $\pi^+$  production formula obtained from a fit to the low  $P_{\perp}$  data by Taylor and Walker:

$$E \frac{d\sigma}{d^3p} = C \frac{(1-x_R)^n}{(1+P_{\perp}^2/m^2)^4} \text{ mbarns/GeV/c}^2/\text{nucleon}$$

where  $x_R \cong (1-x-P_{\perp}^2/2P_{\parallel})$

and

	<u>c</u>	<u>m<sup>2</sup></u>	<u>n</u>
$\pi^+$	30.2	0.66	3.2
$\pi^-$	17.4	0.74	3.9

To obtain numbers of particles produced per interacting proton we correct for the fact that the total cross section goes like  $A^{0.7}$  while high  $P_{\perp}$  and large  $x$   $\pi$  and  $\mu$  production goes more like  $A^{1.0}$

$$dn/dxd^2P_{\perp} = C \times \frac{A^{0.3}}{40 \text{ mb}} \frac{1}{x} \left( E \frac{d\sigma}{d^3p} \right)$$

These formulae were then multiplied by the  $\mu/\pi$  ratios to obtain the  $\mu$  fluxes. This ratio came from two processes:

i) Prompt muon production in the first collision of the proton (we call these direct  $1 \mu$ 's). A fit to the experimental data (see Fig. A1) gives

$$\mu/\pi|_{\text{prompt}} = (1.0 \times 10^{-4}) (1-x)^3$$

ii) In a thick target we get additional muons from  $\pi$  and K decays in the hadronic cascade as well as additional prompt muons produced in the interactions of the pions in the hadronic cascade. These fluxes were calculated by a Monte Carlo program in which the hadronic cascade was followed and the muon flux from both prompt and decay sources were calculated. The resulting muon fluxes were then fitted to give (see Fig A1b)

$$\frac{\mu}{\pi} \Big|_{\substack{\text{Decays \& prompt} \\ \mu\text{'s in hadronic} \\ \text{cascade}}} = \left(\frac{350}{E_{\text{prot}}}\right) [(1.0 \times 10^{-4})(1-x)^3 + (8.0 \times 10^{-4})e^{-23x}].$$

Combining these we get

$$\frac{dn\mu^+}{dx d^2p_{\perp}} = \frac{30.2 A^{0.3}}{40} \frac{1}{x} \frac{(1-x_R)^{3.2}}{(1+p_{\perp}^2/0.66)^4} \times \left\{ [1.0 \times 10^{-4}(1-x)^3] + \left(\frac{350}{E_{\text{prot}}}\right) [1.0 \times 10^{-4}(1-x)^3 + 8.0 \times 10^{-4}e^{-23x}] \right\}$$

and similarly for  $\pi^-$ . We see that once we get to  $x \geq 0.1$  or so where the  $e^{-23x}$  is unimportant we have dependences like

$$\sim \frac{(1-x)^{6.2}}{(1+p_{\perp}^2/m^2)^4} \quad \text{for } \mu^+$$

$$\sim \frac{(1-x)^{6.9}}{(1+p_{\perp}^2/m^2)^4} \quad \text{for } \mu^- .$$

b. The Fermilab program used the  $\pi^{\pm}$  production formula

$$E \frac{d\sigma(\pi^+)}{d^3p} = 70 \frac{e^{-7x_R}}{(1+p_{\perp}^2/m^2)^n}$$

where

$$m^2 = 0.1 + 3.2 x_R - 1.3 x_R^2$$

$$n = 3.5 + (8x_R - 4x_R^2 - 0.5) \left( \frac{0.35}{(p_{\perp}^2 - 9.6)/1.8} + 0.65 \right)$$

$$\pi^-/\pi^+ = 1/(1.7 + 2.2 x_{\perp}^2 + 9.1 x_F^2)$$

$$\left. \frac{d\sigma}{d^3p} \right|_A = (A^{0.8 - 0.3x_F + 0.15p_{\perp}}) \left. \frac{d\sigma}{d^3p} \right|_{A=1}$$

The  $\mu/\pi$  ratio was fitted to existing data (for the prompt part) and  $\pi$  and K decay contributions were calculated by a Monte Carlo program and then fitted, to yield

$$\left. \frac{\mu}{\pi} \right|_{\text{prompt}} = 10^{-4} (-1.91 + 0.88 \log E_{\text{cm}}) \left( \frac{A}{56} \right)^{0.2} (1 - x_F)^2$$

The contributions from the hadronic cascade were expressed as

$$\left. \frac{\mu}{\pi} \right|_{\text{hadronic shower}} = (R_{\text{decay}} + R_{\text{direct}}) \left. \frac{\mu}{\pi} \right|_{\text{prompt}}$$

$$R_{\text{direct}} = 1 + (0.115 / (E/E_{\text{beam}}))^{1.5}$$

$$R_{\text{decay}} = 1 + (0.175 / (E/E_{\text{beam}}))^{1.81}$$

c. The MIT program used a formula for muon production directly, based on a fit to the muon production data by W. Busza.

$$E \frac{dn\mu}{d^3p} = A(1-x) \frac{(1-x-P_{\perp}^2/2P_{\parallel})^4}{(1+P_{\perp}^2/0.74)^{3.5}}$$

where  $A = 6 \times 10^{-4} \mu$ 's/proton/GeV/c<sup>2</sup> for  $\pi^+$  at 1000 GeV/c

$A = 4 \times 10^{-4} \mu$ 's/proton/GeV/c<sup>2</sup> for  $\pi^-$  at 1000 GeV/c

From calculating the E613 shield we found that this formula overestimated the  $\mu$  flux at large  $x$  as well as at large  $P_{\perp}$ .

The formula was therefore modified to

$$E \frac{dn\mu}{d^3p} = A \frac{(1-x_R)^6}{(1+P_{\perp}^2/0.74)^4} \quad \text{for } P_{\perp} < 3 \text{ GeV/c}$$

$$= A \frac{(1-x_R)^7}{(1+P_{\perp}^2/0.74)^4} \quad \text{for } P_{\perp} \geq 3 \text{ GeV/c}$$

MIT  
The formula ~~are~~ <sup>is</sup> intended to be valid for thick targets (dumps).

The predictions of the 3 formulae at 1000 GeV are compared in Fig. A7.

## 2. Comparison of the Muon Production Formulae

with Measured Data.

a. The most relevant data for the total muon production is the data of Bodek, Ritchie et al. In this experiment, the total  $\mu^{\pm}$  production rate was measured with 350 GeV protons in an iron beam dump. Jack Ritchie was very kind to supply us with this data before corrections were subtracted for  $\pi, K$  decays, etc. These numbers then can be directly compared to the total muon rates from our formulae, which is the quantity that is relevant to us. His numbers were for  $6.038 \times 10^8$  protons interacting in the dump. He thought that the data were reliable for the region  $P_{\mu} \geq 50$  GeV and  $P_{\perp} \geq 0.6$  GeV/c.

The comparison for the  $x$  dependence is shown in Fig. A2a,b and the  $P_{\perp}$  dependence in Fig. A3a,b. We see that the agreement is not bad, with the Columbia formulae overestimating by a factor of typically 1.5, and the MIT formula by  $\sim 2$ . *But, note the data is for iron and the MIT prediction is for tungsten.* Since the formulae predict more than the data, our calculations using these formulae will be conservative since we will calculate more background than we should actually have.

b. The comparison with the Bodek, Ritchie et al data is very reassuring. It covers a fairly large range in  $x$ , out to  $x = 0.63$ . However, it is limited to  $P_{\perp} \leq 2.2$  GeV/c. To check the high  $P_{\perp}$  fluxes, we compared with the CERN ISR data on  $\pi^0$  production in the CCOR experiment out to  $P_{\perp} \sim 14$  GeV/c. The comparison of these data with the Taylor-Walker formula for  $\pi$  production used in the Columbia *and the Fermilab* program is shown in Figs. A4 and A5. The agreement is quite good at low  $P_{\perp}$  (as it should be) but at  $P_{\perp} \sim 10$  GeV/c, which is the highest  $P_{\perp}$  that may be relevant in the muon shield calculations, the formula overestimates the measured cross sections by a factor of 5 or so (at  $\sqrt{s} = 53$ , which is similar to the Tevatron). Again, the calculations using this formula are then conservative since they overestimate the background. *The formula used in the Fermilab program agree well with the data.*

c. The highest  $P_{\perp}$  muon production data that we could find was that of Cronin et al. This was for inclusive  $\mu^+$  production by 300 GeV protons. The data available is for the prompt  $\mu^+$  production in a thin nuclear target, corrected

for  $\mu$ 's from  $\pi$  and K decay. The comparison with the prompt  $\mu$  cross section from the formula used in the Columbia program is shown in Fig. A6. The agreement is good at low  $P_{\perp}$  but the formula overestimates the measured cross section by almost an order of magnitude at  $P_{\perp} \sim 6$  GeV/c. The MIT formula for the total  $\mu^+$  cross section is also shown (the prompt and the decay contributions cannot be separated in this formula) and is larger than the measured data.

Thus the calculations based on these formulae can be expected to be conservative at high  $P_{\perp}$ . The formula used in the Fermilab program agrees very well in shape but the normalization is slightly low (but within a factor of two or so of the data).

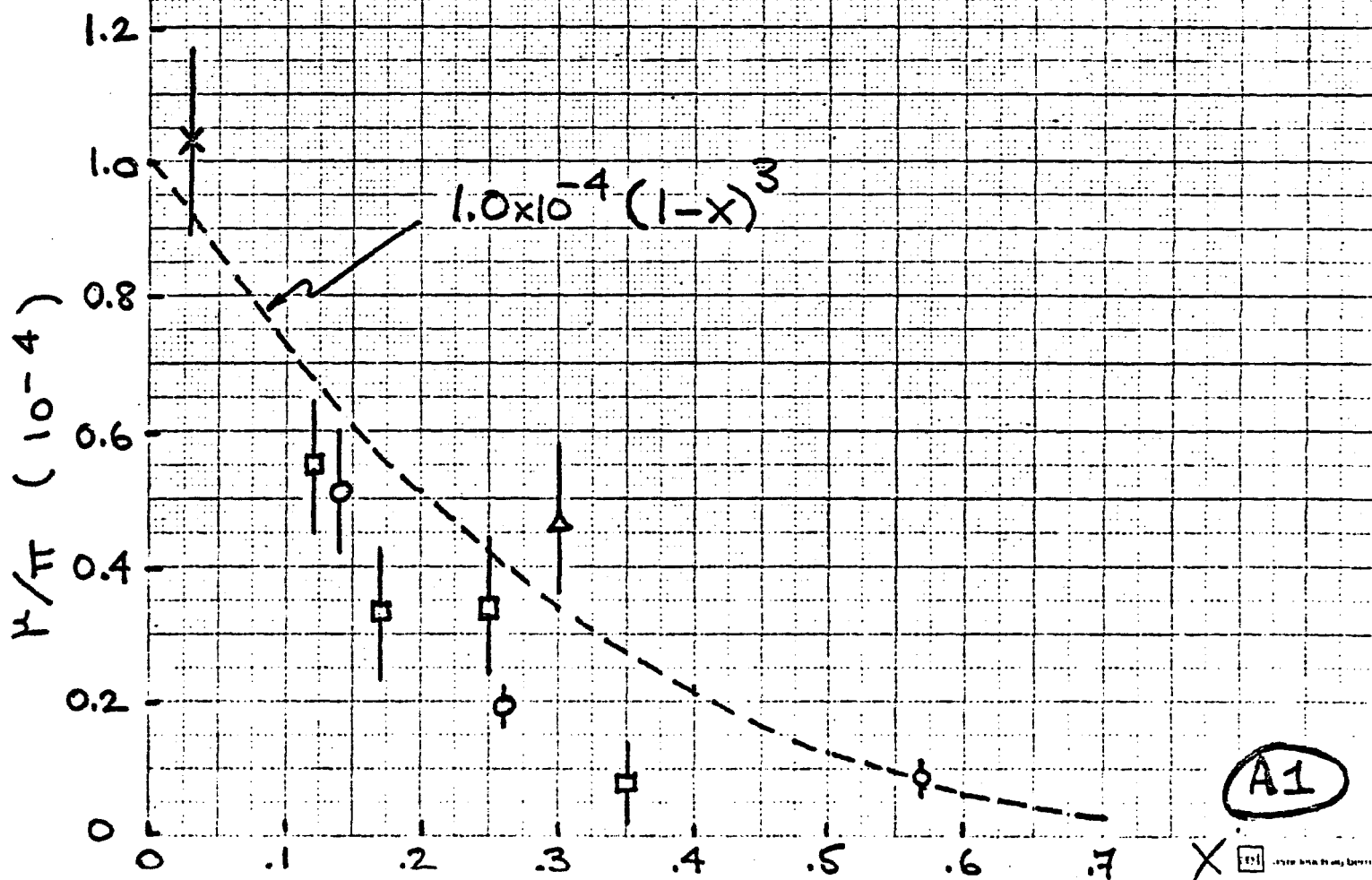
# EXPTL. MEASUREMENTS OF THE $\mu/\pi$ RATIO

○ ADAIR ET AL

□ PILCHER ET AL

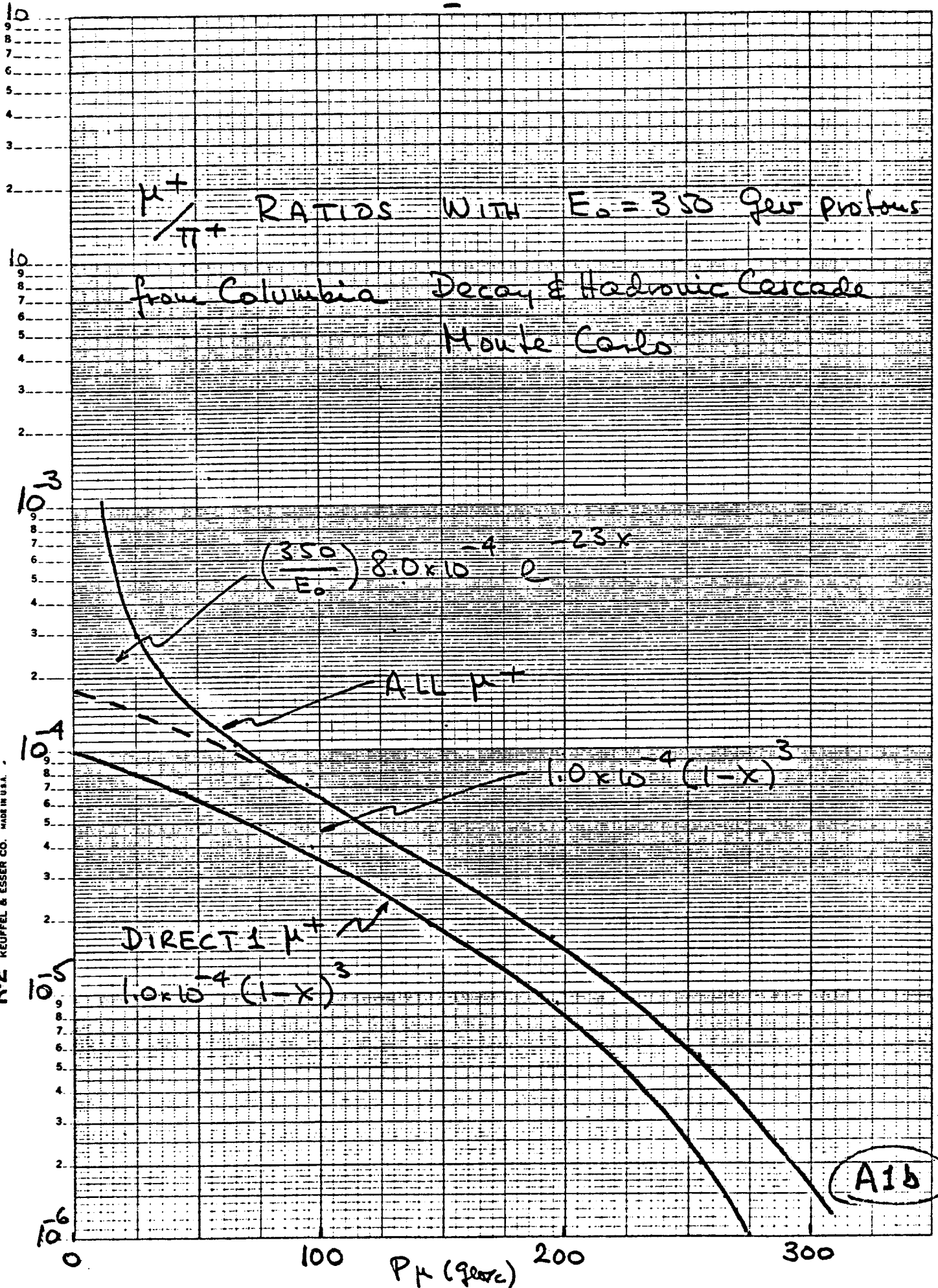
\* BODEK ET AL

△ BUCHHOLZ ET AL



46 6210

K&E SEMI-LOGARITHMIC 5 CYCLES X 70 DIVISIONS  
KEUFFEL & ESSER CO. MADE IN U.S.A.



No. of  $\mu$ 's 46 6210

K&E SEMI-LOGARITHMIC 5 CYCLES X 70 DIVISIONS KEUFFEL & ESSER CO. MADE IN U.S.A.

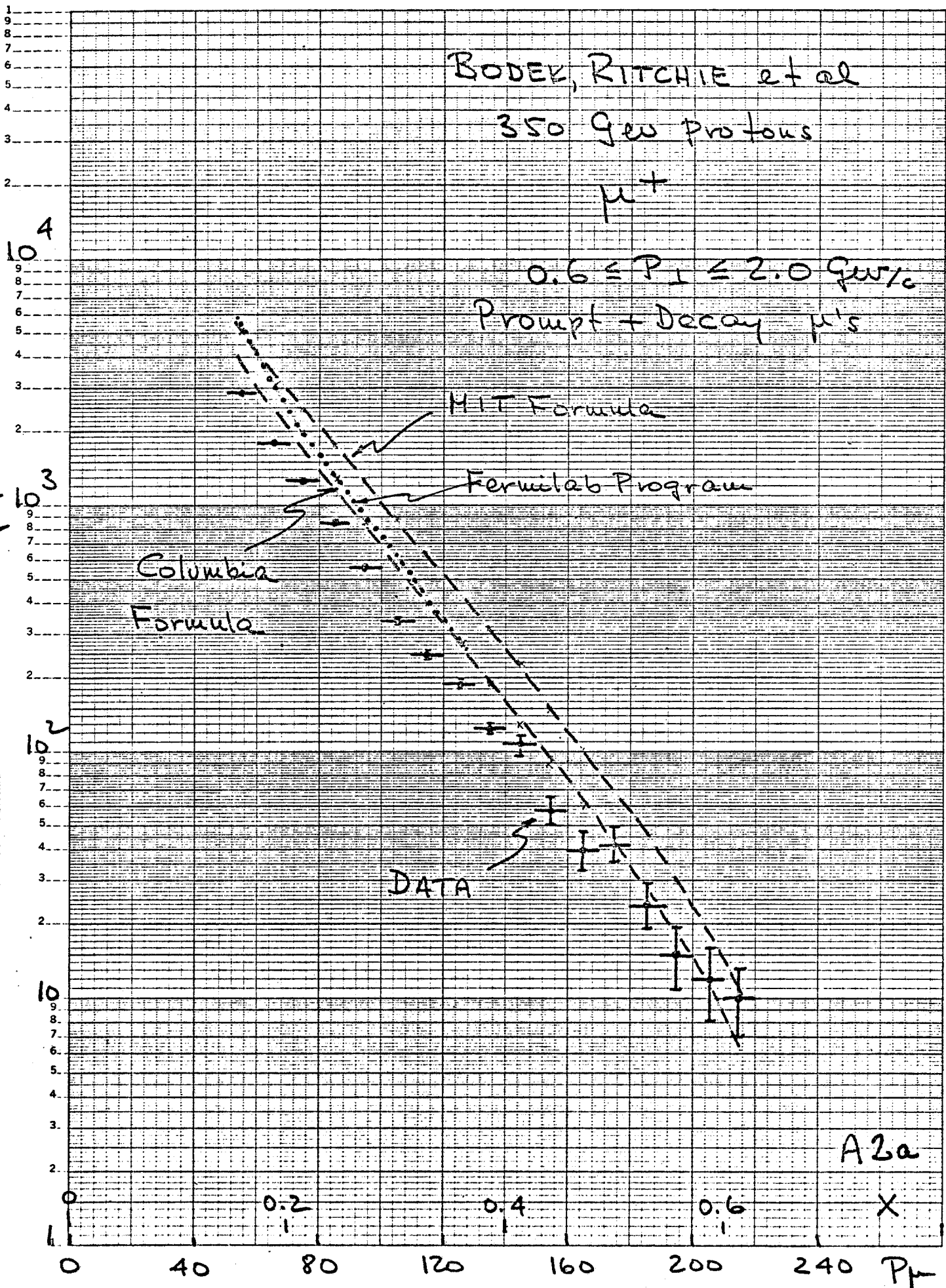
BODEK, RITCHIE et al

350 Gev protons

$\mu^+$

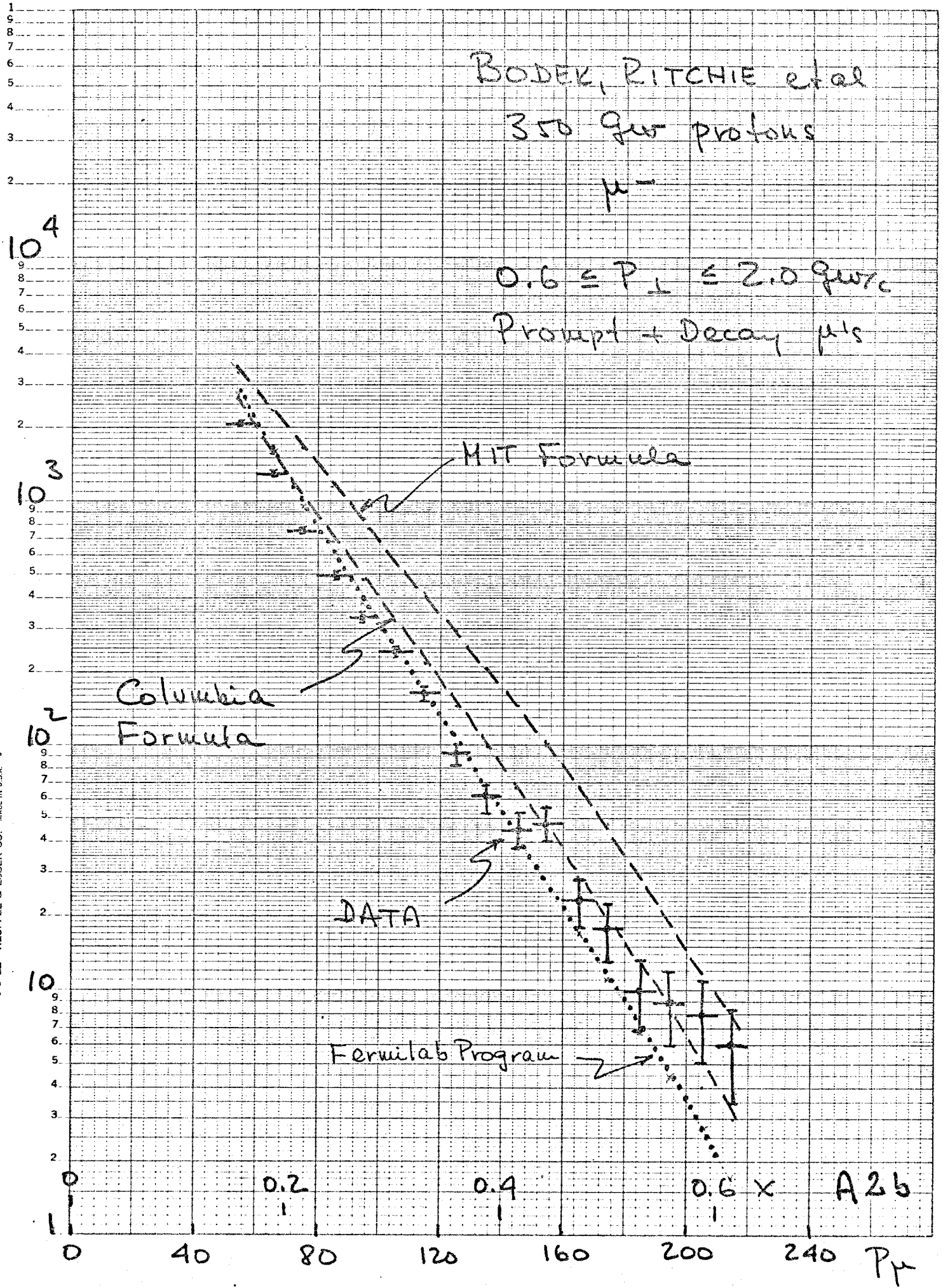
$0.6 \leq P_L \leq 2.0$  GeV/c

Prompt + Decay  $\mu$ 's



No of  $\mu$ 's 46 6210

KE SEMI-LOGARITHMIC 5 CYCLES X 70 DIVISIONS KEUFFEL & ESSER CO. MADE IN U.S.A.



BODEK, RITCHIE et al  
350 GeV Protons

$\mu^+$   $50 \leq P_{\mu} \leq 220$  GeV

Prompt + Decay  $\mu^+$ 's

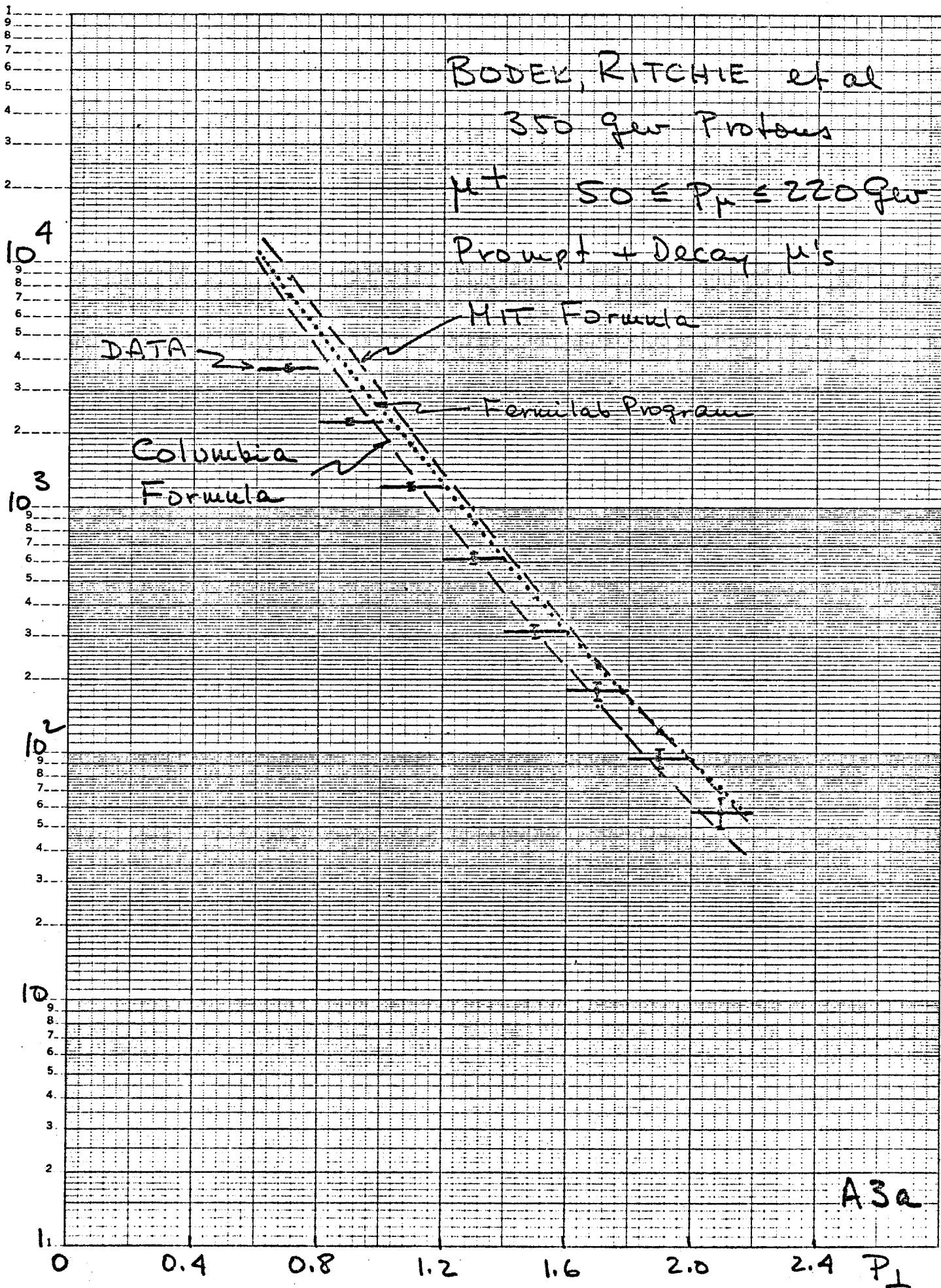
MIT Formula

Fermilab Program

DATA

Columbia  
Formula

No of  $\mu^+$ 's



BODEK, RITCHIE et al

350 GeV Protons

$\mu^-$   $50 \leq P_{\perp} \leq 220$  GeV

Prompt + Decay  $\mu$ s

No of  $\mu$ 's

1  
9  
8  
7  
6  
5  
4  
3  
2  
 $10^4$   
9  
8  
7  
6  
5  
4  
3  
2  
 $10^3$   
9  
8  
7  
6  
5  
4  
3  
2  
 $10^2$   
9  
8  
7  
6  
5  
4  
3  
2  
 $10$   
9  
8  
7  
6  
5  
4  
3  
2  
1

DATA

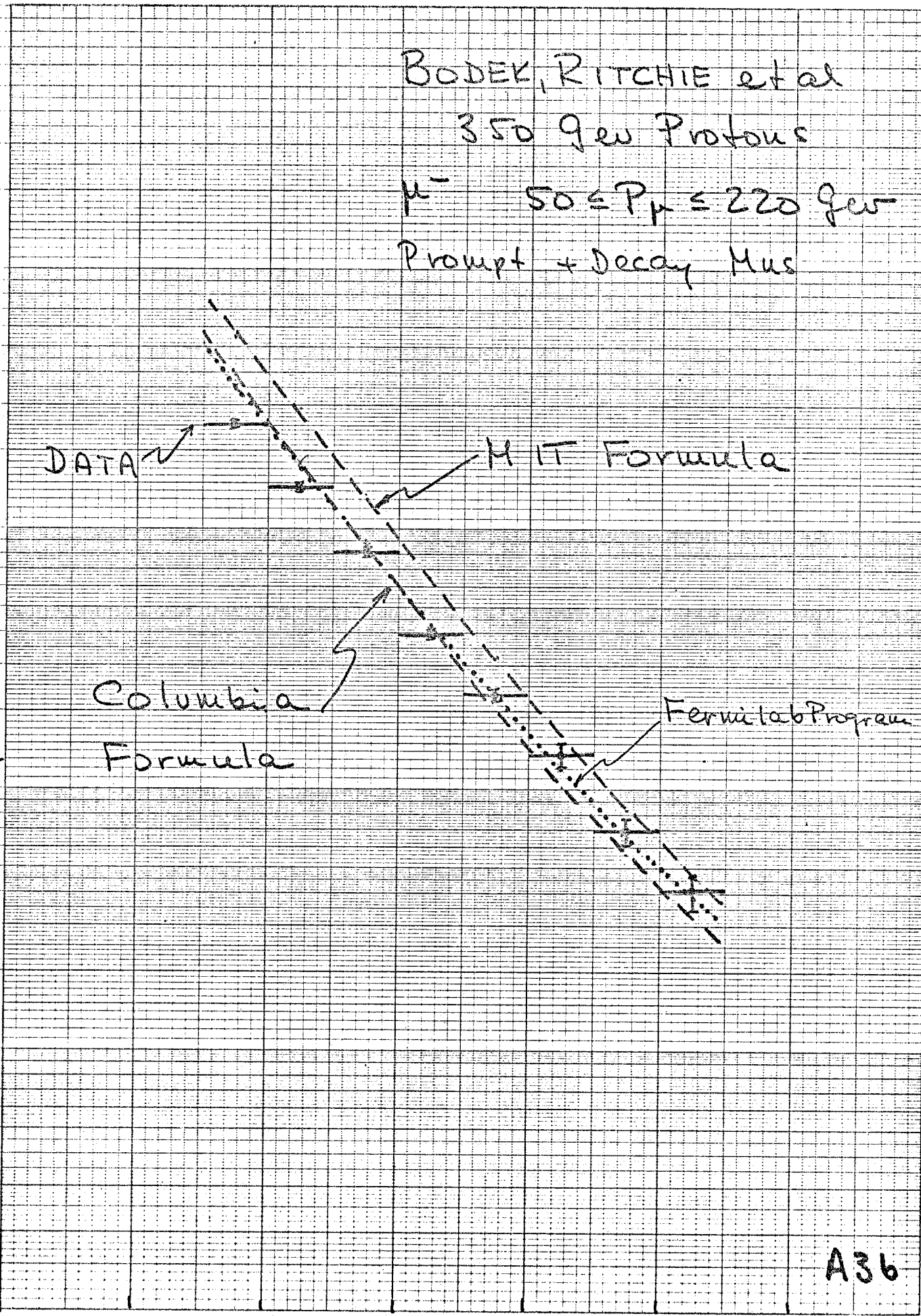
MIT Formula

Columbia Formula

Fermilab Program

0 0.4 0.8 1.2 1.6 2.0 2.4  $P_{\perp}$

A36



R806, all agree to the inclusive  $\pi^0$  yield departing from above from the distribution (9.2) which matches very well the medium  $p_t$  domain. Figure 9.8 gives the CCOR data extending up to 14 GeV/c. The discrepancy with the  $p_t^{-8}$  behaviour has by then reached almost an order of magnitude. As discussed later, part of the neutral yield, which is actually the one observed, could by then correspond to the prompt photon component. Nevertheless, as indicated by the results of R806, the actual  $\pi^0$  yield should still dominate. While it is too early to conclude, one certainly meets qualitative agreement with expectations based on QCD.

The ISR may still have too low an energy to provide a clear test. Nevertheless, granting that the observed effect (fig. 9.8) corresponds to the emergence of the  $p_t^{-4}$  component, predictions can be made for what should be observed at much higher energies, as soon as available with the SPS used as a collider, with acceleration of protons and antiprotons. Figure 9.9 gives the expected yields for jets (anything associated with the fragmentation of constituent C in fig. 8.6) as calculated by Feynman and Field according to a QCD approach matching the medium  $p_t$  data, and eventually giving a  $p_t^{-4}$

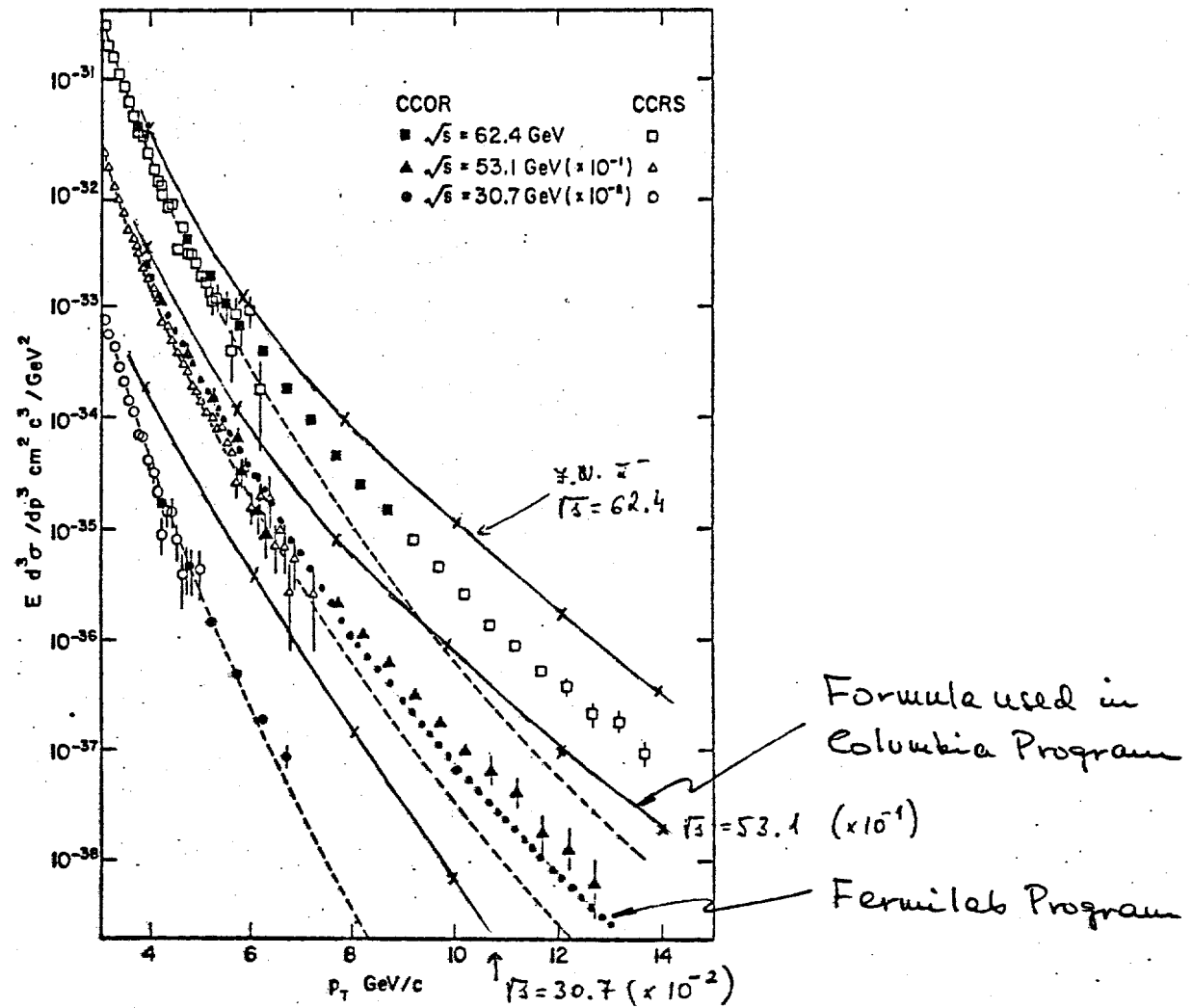


Fig. 9.8. Inclusive  $\pi^0$  yields at very large  $p_t$  (R108). The dashed curve corresponds to a successful fit to the medium  $p_t$  data with  $n = 8$ . The observed yields are far in excess of what was predicted by the simple extrapolation. It may correspond to the emergence of a new regime with  $n = 4$ .

R806, all agree to the inclusive  $\pi^0$  yield departing from above from the distribution (9.2) which matches very well the medium  $p_t$  domain. Figure 9.8 gives the CCOR data extending up to 14 GeV/c. The discrepancy with the  $p_t^{-8}$  behaviour has by then reached almost an order of magnitude. As discussed later, part of the neutral yield, which is actually the one observed, could by then correspond to the prompt photon component. Nevertheless, as indicated by the results of R806, the actual  $\pi^0$  yield should still dominate. While it is too early to conclude, one certainly meets qualitative agreement with expectations based on QCD.

The ISR may still have too low an energy to provide a clear test. Nevertheless, granting that the observed effect (fig. 9.8) corresponds to the emergence of the  $p_t^{-4}$  component, predictions can be made for what should be observed at much higher energies, as soon as available with the SPS used as a collider, with acceleration of protons and antiprotons. Figure 9.9 gives the expected yields for jets (anything associated with the fragmentation of constituent C in fig. 8.6) as calculated by Feynman and Field according to a QCD approach matching the medium  $p_t$  data, and eventually giving a  $p_t^{-4}$

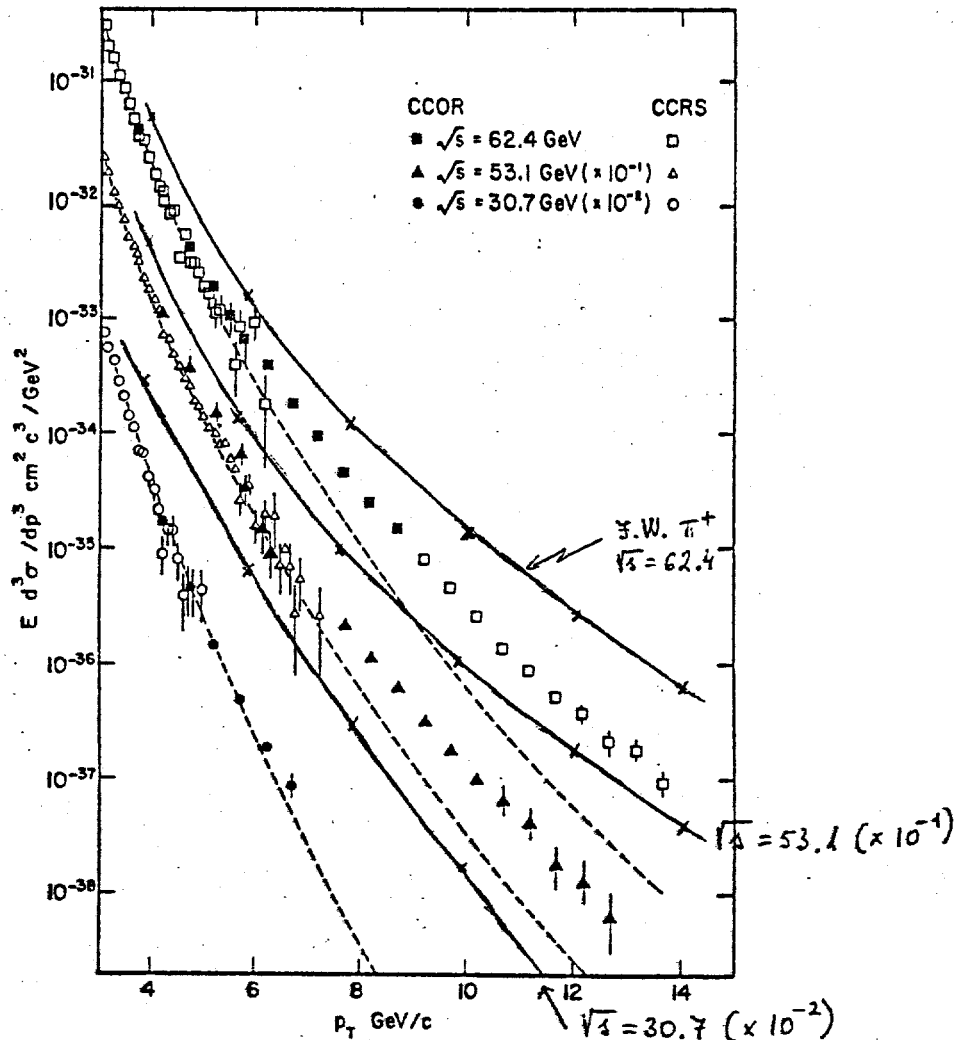
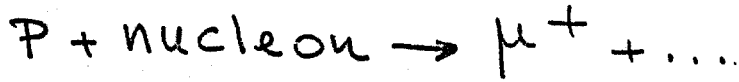
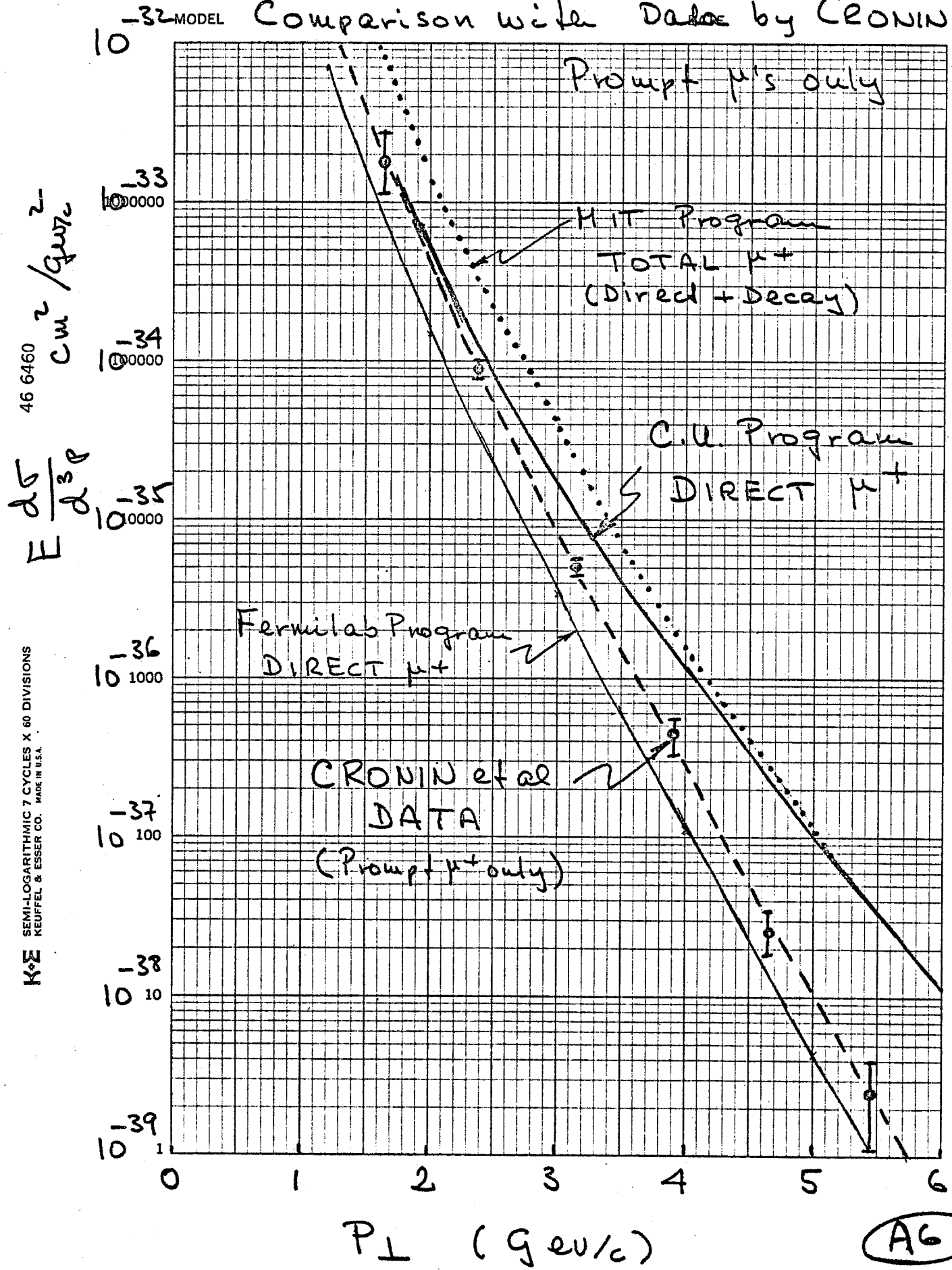


Fig. 9.8. Inclusive  $\pi^0$  yields at very large  $p_t$  (R108). The dashed curve corresponds to a successful fit to the medium  $p_t$  data with  $n = 8$ . The observed yields are far in excess of what was predicted by the simple extrapolation. It may correspond to the emergence of a new regime with  $n = 4$ .

A5



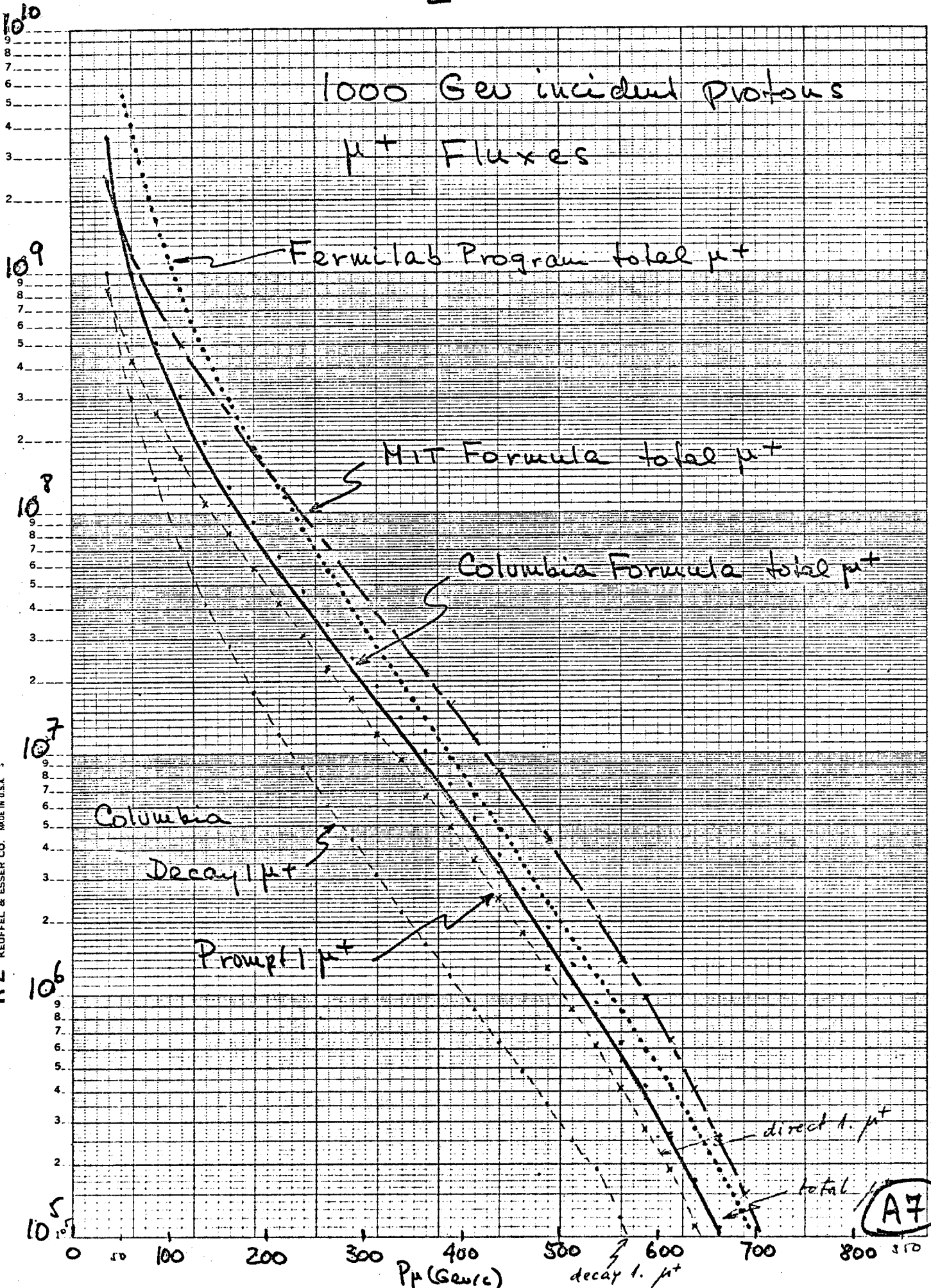
Comparison with Data by CRONIN et al



AG

$\mu^+ / 25 \text{ GeV/c} / 10^{10} \text{ protons}$   
46 6210

K-E SEMI-LOGARITHMIC 5 CYCLES X 70 DIVISIONS  
KEUFFEL & ESSER CO. MADE IN U.S.A.



A7

## V) MUON SHIELD DESIGN FOR THE PROMPT NEUTRINO FACILITY

It is desirable to have maximum prompt neutrino flux in the detectors. This requires the distance from the target to detectors to be minimized. However, unless special precautions are taken the muon flux from the target will prevent the successful operation of the detectors. As a design guideline we have required the muon flux in the 32" and 15' Bubble Chamber to be less than 5 per  $10^{13}$  interacting protons. This criterion has been satisfied with the use of large magnets to deflect the muons and locating the detectors at about 58 meters and 160 meters from the target.

### A) General Layout of Area

Figure V.1 shows a layout of the area stretching from the Target Hall to Lab C which contains the final neutrino detector in the line. The principle items downstream of the target point are listed below:

- (i) Solid iron magnet 4m long operated at 21 Kg which can be installed and removed through the target box.
- (ii) A second conventional 5m long, 20 Kg magnet. This magnet cannot be moved once it is installed and surrounded by shielding.
- (iii) Large magnet or magnets whose purpose is to deflect muons away from the detectors.

- (iv) The new 32" Bubble chamber and its associated active and passive shield.
- (v) A new experiment hall for an electronic detector.
- (vi) Lab E which exists and contains an electronic neutrino detector.
- (vii) Passive shielding for low energy background radiation.
- (viii) The 15' Bubble Chamber.
- (ix) Lab C which exists and contains an electronic detector.

Here we shall briefly review the general characteristics of the first three items. The target box magnet, in addition to bending muons limits residual activity to less than about 1 R at its downstream face where electrical and water connections are made. This imposes the length of the magnet to be not less than 4.0 m. We have chosen this length because a larger magnet would rapidly become impossible to handle through Prompt Hall. The second magnet in addition to contributing to the sweeping action on muons, attenuates the neutron flux from the dump target. At the downstream face of the magnet there is a tolerably low neutron flux such that the Bubble Chambers can operate successfully at 58m and 160m respectively.

The design of the large magnet or magnets for deflection of muons out of the detectors has demanded an exhaustive and extensive study. The number of  $\approx$  800 Gev muons produced in the target is adequately low that they may be permitted to strike the

detectors. To sweep out  $< 800$  GeV/c momenta imposes a lower limit to the integral magnetic field bending power. This corresponds to about 600 Kg meters. The transverse dimensions of the magnetic field must be such that all muons of  $\geq$  than about 40 GeV/c and  $p_{\perp} < 10$  GeV/c must also be swept out of line of the detectors otherwise the fluxes are unacceptably high. These criteria must be met by any magnetic system design.

#### B) Alternative Designs of the Magnetic Shield System

Three distinct designs have been studied. These are:

- (i) Solid iron conventional magnets
- (ii) Air gap conventional magnets
- (iii) Superconducting magnet with iron for the return magnetic flux.

The general mechanical and electrical descriptions of these systems will now be given along with general design considerations.

##### 1) Solid Iron Conventional Magnet System

This was the first design studied and a progress report was written in June 1981 and made available to the P.A.C. and subsequently this design received laboratory review in November 1981. Figure IV.2 shows a layout of the set of magnets. The five magnets have horizontal magnetic fields providing vertical bending

for the muons. Figure IV.3 shows 100 GeV/c muon trajectories for initial vertical transverse momenta in the range -6 to +6 BeV/c. Muons that reached the Bubble Chambers were found to be principally from deep inelastic scattering in the iron and more particularly from trident interactions in the iron. In the latter process a muon produced in the target at a typical momentum of 200 GeV/c would be deflected by the first two magnets and produce a muon pair in the coulomb field of an iron nucleus. The opposite charge member of that pair then would be deflected by the subsequent magnets back towards the detectors. To eliminate these muons it was found necessary to add an additional magnet with a vertical field downstream of the previous set of magnets as shown in Figure V.2. This magnet does not affect the vertical deflection given to the muons by the first set of magnets, but bends the typically less than 100 GeV/c troublesome trident muons horizontally away from the detectors. Calculated muon fluxes satisfied the initial design criteria.

Parameters:

Total iron weight =	11,000 tons
Total power consumption =	0.6MW (D.C.)
	0.2 MW (Pulsed)

Capital Cost

Cost of Coils	\$ 150K
Cost of iron at \$500/ton	\$5,500K
Manpower	\$ 250K
Power Supply	\$ 100K
Rigging and Surveying	\$ 500K
Civil Construction	\$ 300k
	<hr/>
	\$6,800K

Operating Cost (Pulsed)

0.2 MW x 25% duty cycle x \$30,000/month  
x 12 months = \$20K/year

Total 5 Year Cost = \$6,900K

This design was considered to have substantial uncertainties in the calculated muon fluxes. The background muons into the detectors came from interactions of the primary muons in the form of deep inelastic scattering, trident production and somewhat less from charm production and subsequent decay into opposite sign muons etc. Hence, the reliability of the calculations would be greatly increased if minimal material was placed in the path of

the high flux of primary muons. This consideration led to the second design.

2) Air Gap Conventional Magnet

This design was initiated in October 1981 and a preliminary report was made in November 1981 at the laboratory review mentioned previously. Figure V.4 shows a layout of the six magnets required in this design. A preliminary engineering design of this system has been made by R. Fast of Research Services and is attached as Appendix V.1. The main results are as follows. The magnetic field profiles of the magnets have been calculated and included in the programs which calculate the muon fluxes. The central fields are designed to be 2T. The D.C. power requirement is 4.1 MW. However, it has been shown that the magnets can be pulsed to match the repetition rate of the Tevatron and thereby reduce power consumption to about 1.1 MW. It will be possible to use the old 30-inch Bubble Chamber power supply for this purpose.

A summary of the cost of this system is as follows:

Capital Cost

Cost of coils	\$ 1,140K
Cost of iron at \$500/ton	\$3,308K
Manpower	\$ 250K
Power Supply	\$ 100K

Rigging and Surveying	\$ 404K
Civil Construction	\$ 400K
	<hr/>
	\$5,612K

Operating Cost

30 months continuous operation      \$1530K

The major advantage of this design is the fact that the intense muon flux is contained primarily within the gap region of the magnets. Hence, muon interactions are minimized and the reliability of the design is enhanced. Because opposite sign muon production by muons is reduced the final magnet with vertical field may be eliminated thereby reducing the weight of the overall system from 11,000 tns to 7,200 tons.

When the proton beam is targeted at non-zero angle relative to the detector axis, it is necessary to move the air gap magnets sideways to align the gap region with the region of high muon flux. Under these conditions, the muon rate into any detector for production angles in the range 0 - 40mr, is acceptably low as defined earlier.

The air gap conventional magnet design therefore has greater reliability than the original design, and in addition, will cost less. For this reason we will not discuss further the solid iron magnet design.

### 3) Superconducting Magnet

In December of 1981 we started to investigate the properties of a large superconducting magnet which would have the desired field properties described earlier. By increasing the magnetic field to 5.0 Tesla it made the effective bend point of the magnet closer to the target and hence a somewhat smaller integral magnetic field could be realized.

The superconducting magnet preliminary design has been made by E. Leung of Research Services. The details are described in

Appendix IV.2. A summary is provided here.

The 8.4 m long magnet has a horizontal dipole field and is composed of four coils wound in the form of a racetrack. The clear aperture of the magnet is 30 cm horizontally and 1.4m above and below the beam axis. The stored energy of the system is about 600 MJ. The coils are shown in Figure V.5. The use of iron around the magnet is to shield the surroundings, reduce the ampere-turns, and help range out low energy muons. The horizontal field profile as a function of height above the beam axis is shown in Figure V6. The layout of the area with the superconducting magnet is shown in Figure V 7(a) and (b).

A summary of the cost of this system is as follows:-

Capital Cost

Coils	\$1,438K
Iron at \$500 per ton	1,907K
Refrigeration, power supply, instrumentation	735K
Manpower	884K
Civil Construction	357K
Rigging and Surveying	<u>229K</u>
Total	\$5,550K

Operating Cost

For 30 months continuous use	\$225K
------------------------------	--------

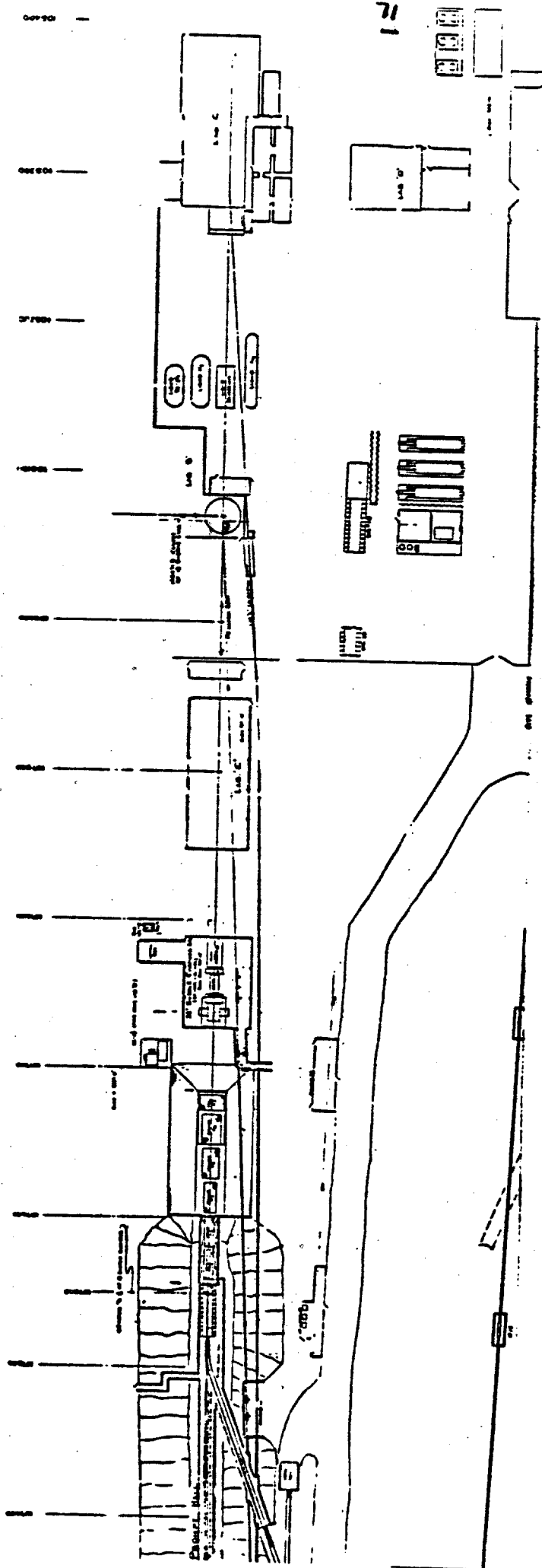
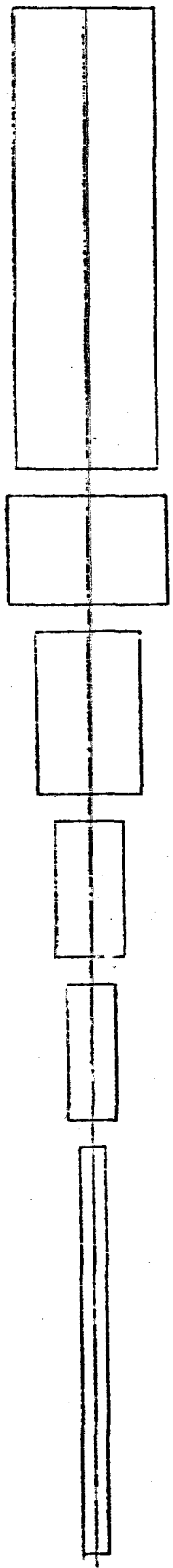
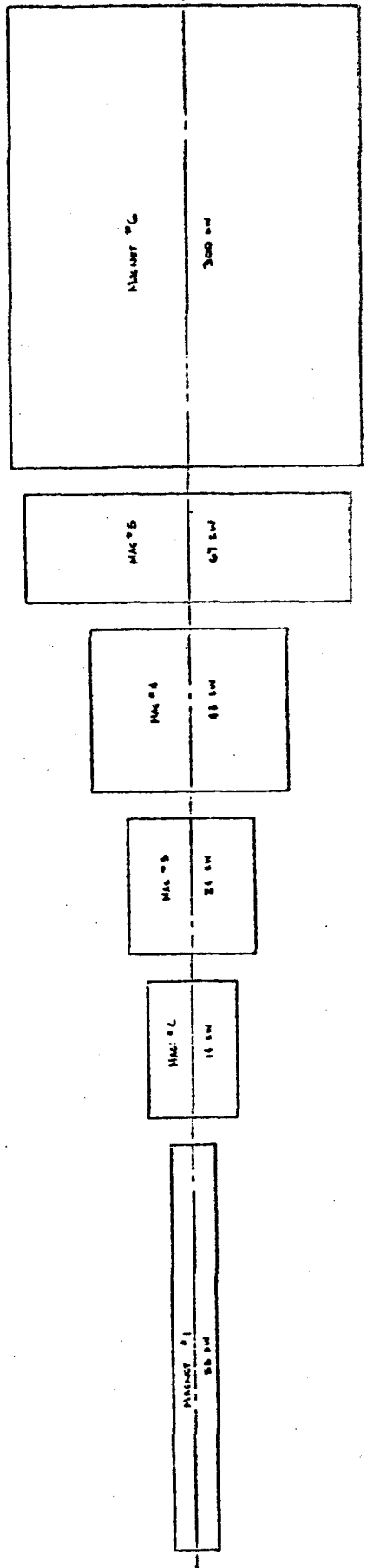


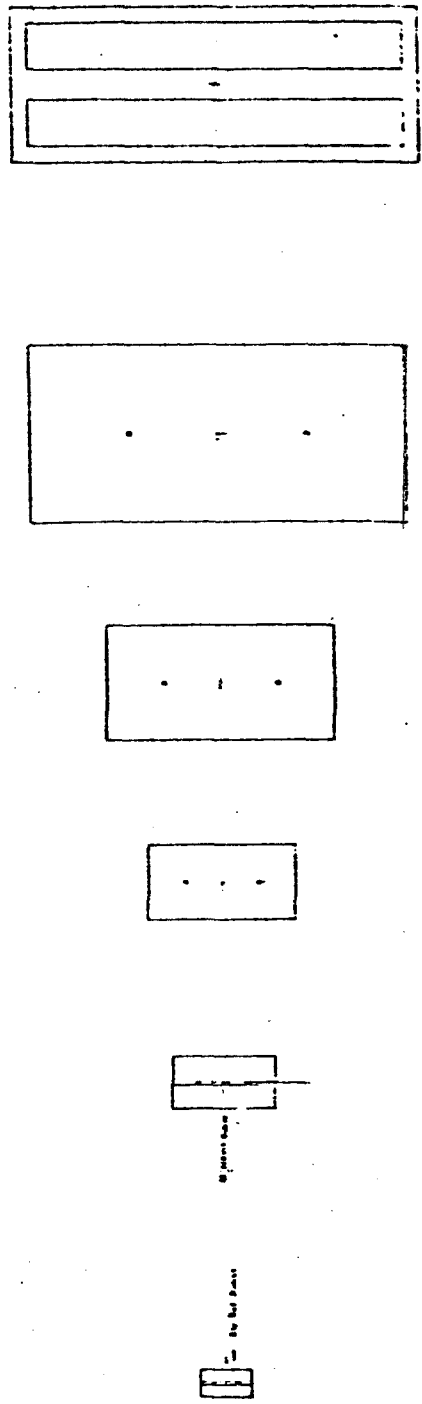
FIGURE V.1



PLAN VIEW



ELEVATION VIEW  
Scale 1/4" = 1'-0"



SCALE 1/4" = 1'-0"  
 ELEVATION VIEW  
 MANNET #C  
 MAN #6  
 MAN #5  
 MAN #4  
 MAN #3  
 MAN #2  
 MAN #1

FIGURE V.2

Design 1.2  
Diver on face of M1.

HEIGHT = 6.1 DE/DS = 1.4 PTOT = 100 GEV/c

$P_L = 0 \pm 6 \text{ GeV/c}$

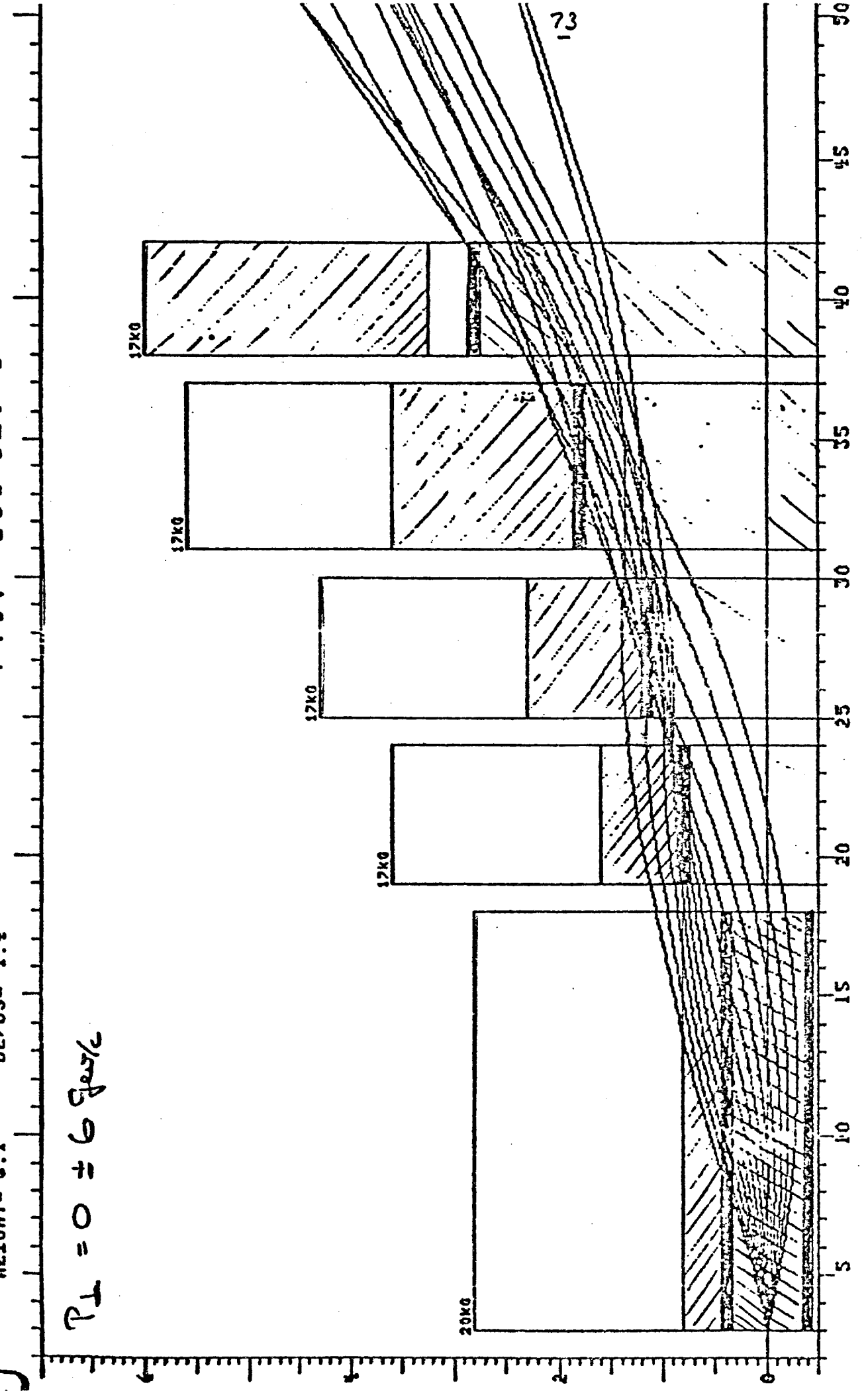


FIGURE V.3



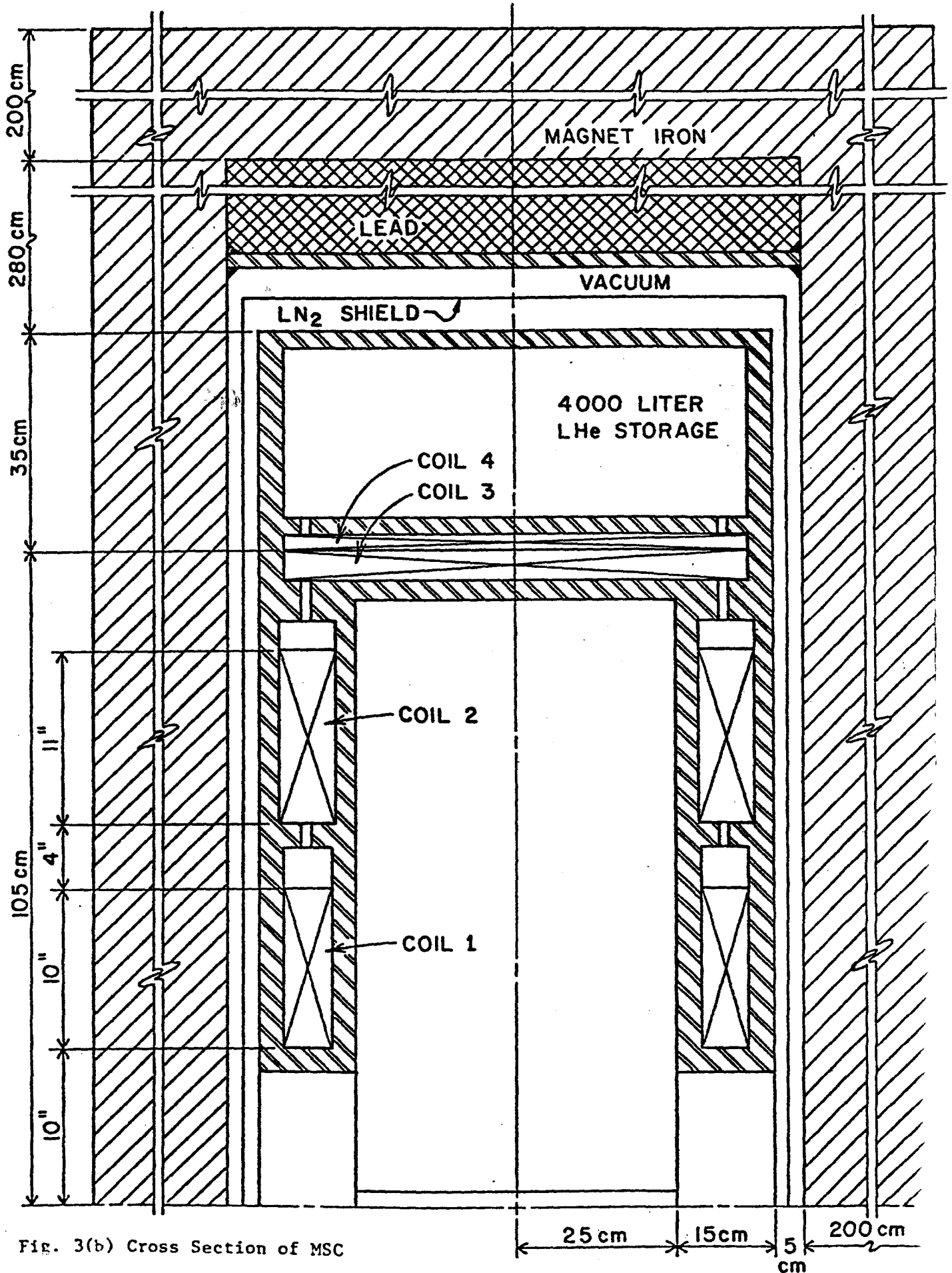
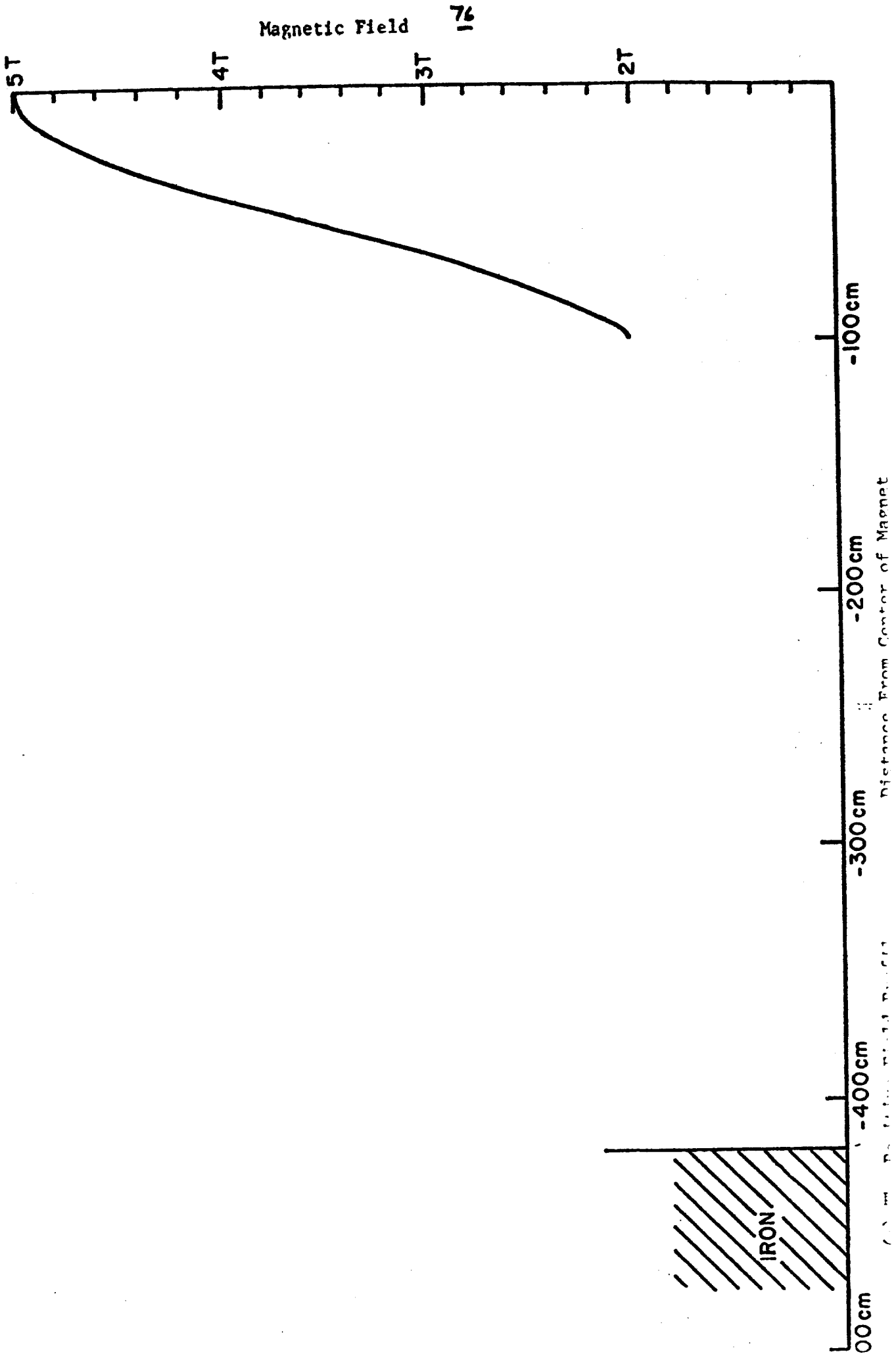


Fig. 3(b) Cross Section of MSC

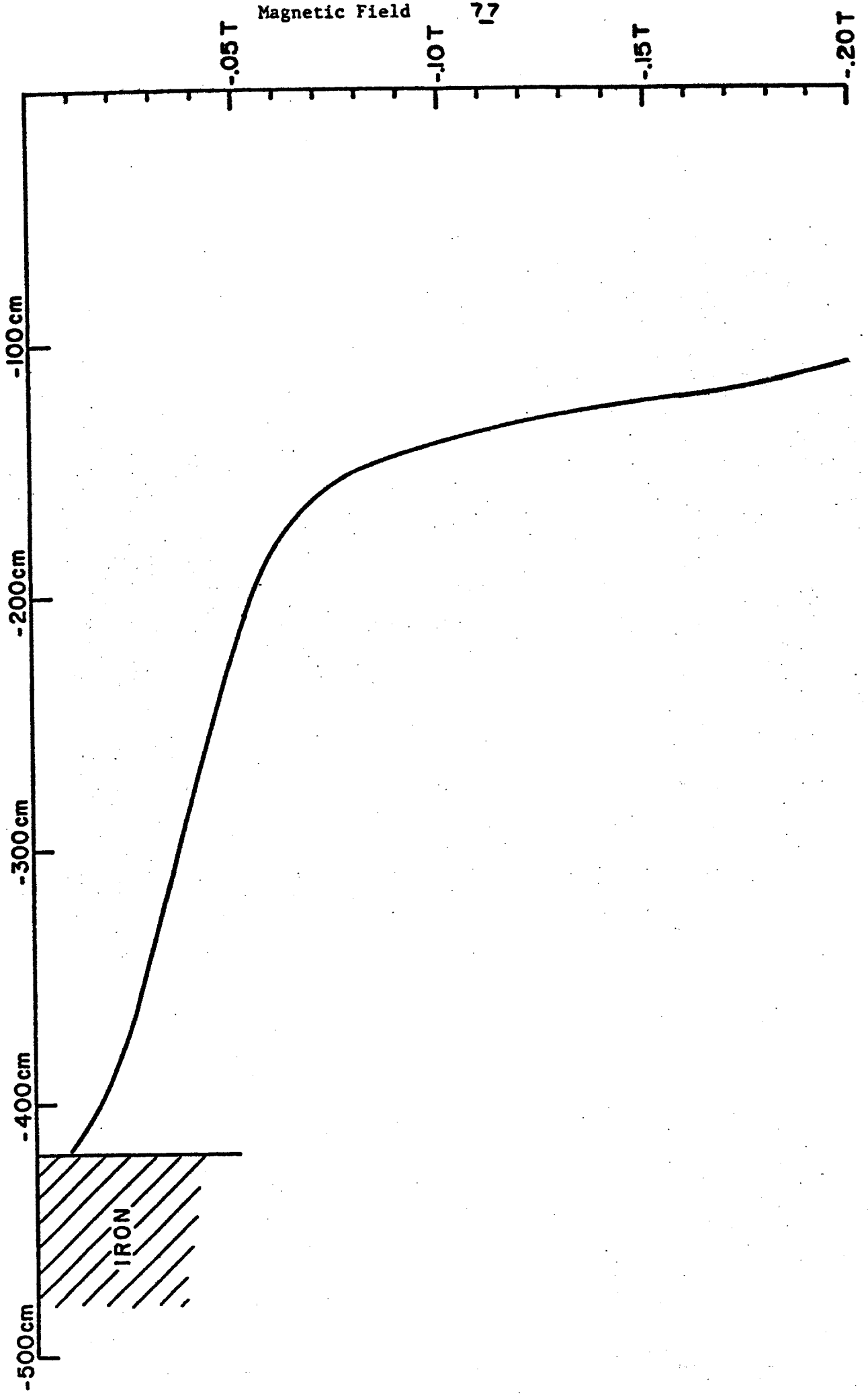
FIGURE V.5

Fig. V66) The Vertical Distribution of Horizontal Field on the Mid-Plane



(b) The Return Field Above the Coils

Distance From Center of Magnet



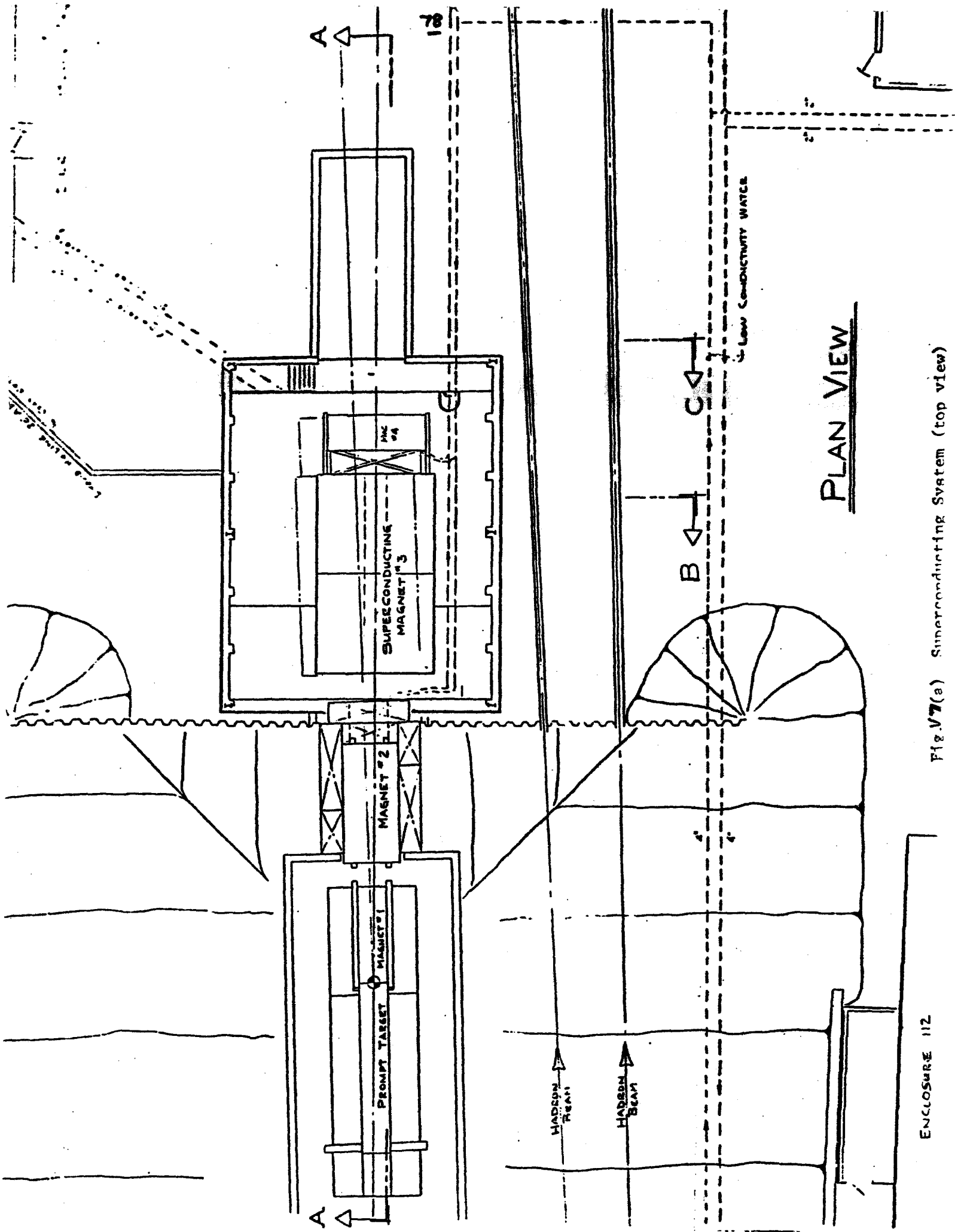


Fig. V7(a) Superconducting System (top view)

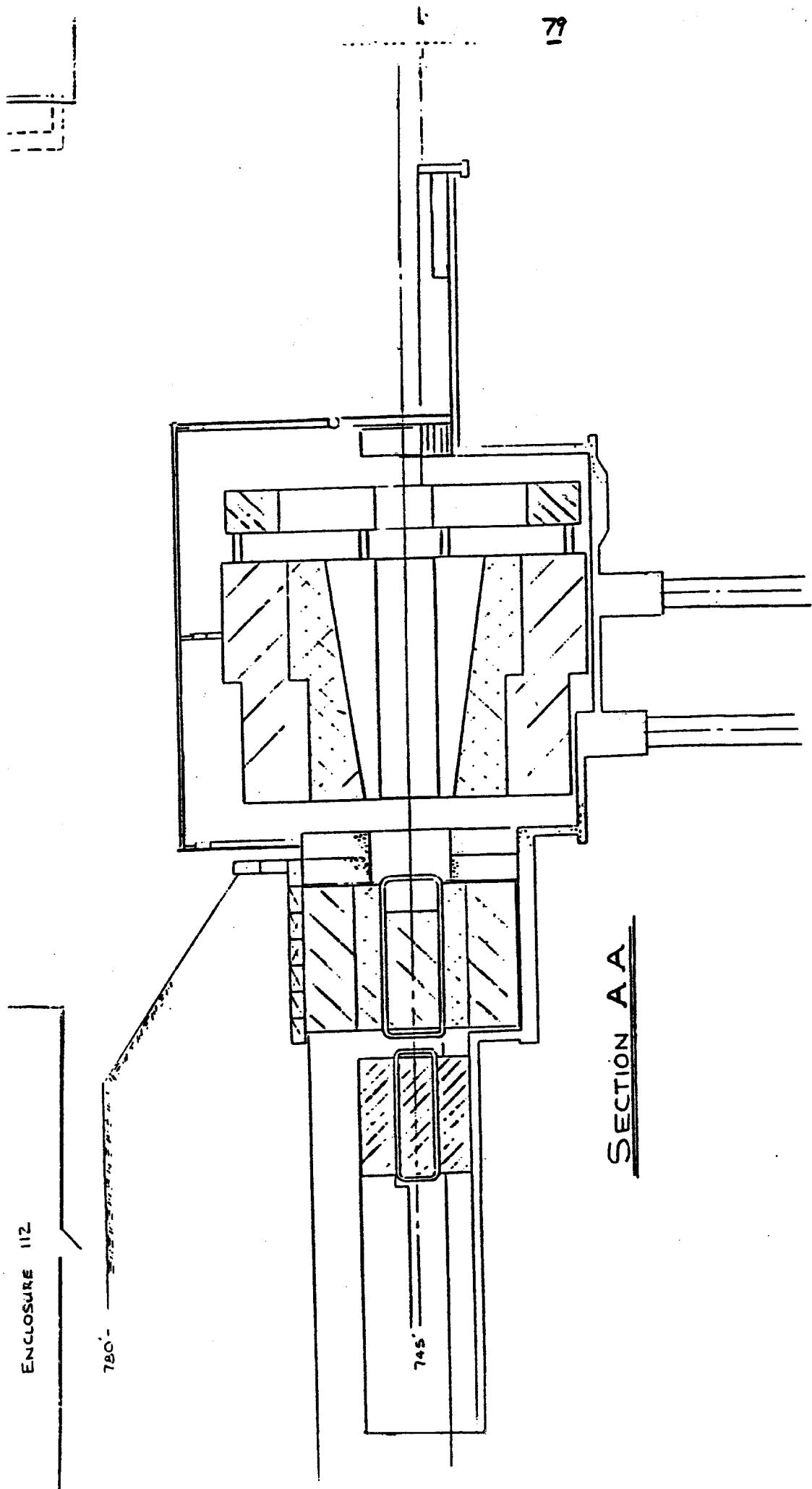


Fig. V7(b) Superconducting System (side view)

#### 4. Muon Fluxes from the Dump

Muon fluxes in the new 32" B.C. and 15' B.C. have been calculated independently by the three programs described earlier. Results are presented for both the conventional magnet and superconducting magnet designs. These fluxes are for the case of a full density tungsten target and include prompt and non-prompt muon production sources. Final results are shown in the attached table. The calculations refer to:

- I. Columbia
- II. Hawaii-Fermilab
- III. MIT

The results of the different calculations are in good agreement with each other as they were in the case of the E-613 shield calculation. It can be seen that in both the conventional and superconducting magnet designs no more than a few muons per  $10^{13}$  protons at 1 TeV are expected in either of the bubble chambers.

I. CONVENTIONAL MAGNET DESIGN

		32" B. C.			15' B. C.		
		<u>CALCULATION</u>			<u>CALCULATION</u>		
		I	II	III	I	II	III
Coulomb Scattering	$\mu^+$	0.3	0.2	0.5	<0.1	<0.1	<0.1
	$\mu^-$	0.3	0.5	0.5	<0.1	<0.1	<0.1
Deep Inelastic Scattering	$\mu^+$	0.2	<0.1	<0.1	<0.1	<0.1	<0.1
	$\mu^-$	<0.1	<0.1	0.5	0.1	0.1	1.0
Trident Production	$\mu^+$	0.5	0.1	1.5	<0.1	0.7	0.2
	$\mu^-$	0.2	0.1	0.5	0.5	0.2	0.5

II. SUPERCONDUCTING MAGNET DESIGN

		32" B. C.			15' B. C.		
		<u>CALCULATION</u>			<u>CALCULATION</u>		
		I	II	III	I	II	III
Coulomb Scattering	$\mu^+$	0.4	0.6	0.5	<0.1	0.2	<0.1
	$\mu^-$	0.2	0.8	0.5	0.1	0.9	<0.1
Deep Inelastic Scattering	$\mu^+$	<0.1	<0.1	0.5	<0.1	<0.1	0.2
	$\mu^-$	0.25	0.6	1.5	0.5	0.1	0.5
Trident Production	$\mu^+$	0.7	<0.1	0.7	<0.1	0.1	0.5
	$\mu^-$	0.1	0.2	0.3	0.1	0.2	1.0

Some general comments on muons from the various sources is of interest.

i. Columb Contribution

a. Muons in the band pass energy.

This source may be the most serious if the design is not done properly because of the potentially very high intensity. In the present designs, the band pass energy is around 20 GeV which is sufficiently low so that the muons can be absorbed in the passive shield inside the magnets. There is no resulting muon contribution from this source.

b. Muons with Threshold Energy

Other than the muons in the band pass, there are muons which barely escape out of the dump with energy around and less than 1 GeV. These low energy muons may scatter with a very large angle and hit the chambers. Although the muons can be absorbed in the passive shield in front of the chambers, it is safer not to have them in the first place. To eliminate the problem, a small magnet (called spoiler) with low field is placed so that it kicks away the low energy muons that just emerge from the absorber in the magnet. There is also no resulting muon background contribution from this source.

c. Muons get caught in the fringe field.

As shown in the Appendix, the field of the C-magnets extends beyond the coil unlike a solid iron magnet, in which there is a sharp cut off of magnetic field. Because the field around the coil is neither strong nor weak, there are muons with energy of around 40 GeV and vertical  $p_{\perp}$  of around  $\pm 5$  GeV which get caught and bent back toward the detectors. The muon background to the 32" B.C. by this process is small ( $\leq 0.5$ ) for the design with the superconducting magnet and  $\sim < 2$  for the design with C-magnets. There is no contribution to the 15' B.C. by this process.

ii. Muons Scattered Deep Inelastically.

Since both systems are designed so that high energy muons with high intensity do not pass through much material in the dump, neither designs have serious problems from this source. However, there is some contribution from the dirt. This problem is limited to the design with superconducting magnet because:

- a. the length of the magnet is short, i.e., there is more dirt between the dump and detectors,
  - b. the bending power of the design with the superconducting magnet is about 15% less than the design with c-magnets.
- For these two reasons, the superconducting magnet design gives about one muon to both chambers from this source.

Also, the muons can scatter off the superconducting coil and this contributes about 0.5 muons in the 32" bubble chamber.

iii. Trident Production.

Any trident produced inside a magnet field is potentially dangerous. As mentioned earlier, this is the reason for air-gap magnets. The major source of tridents for both designs is the pole face of the magnets which are hit by high  $P_1$  muons. There is one muon background with the superconducting magnet design and two muons in the other design in the 32" chamber.

A source of tridents for the 15' B.C. is the magnet of the 32" chamber. One sign of muon produced in the magnet bends toward the 15' B.C. and this gives about 5 muons as background. Modification of the 32" B.C. magnet has been initiated. A slot in the magnet is made so that high intensity muons do not interact. With the slot the background gets better by a factor of 6 so that there is less than one muon in the 15' B.C. Another reason for the slot is to reduce the background in the downstream detectors of the 32" bubble chamber. It is found that without the slot there are about 20 muons in CRISIS from tridents produced in the magnet. With this slot the number drops by about a factor of 5.

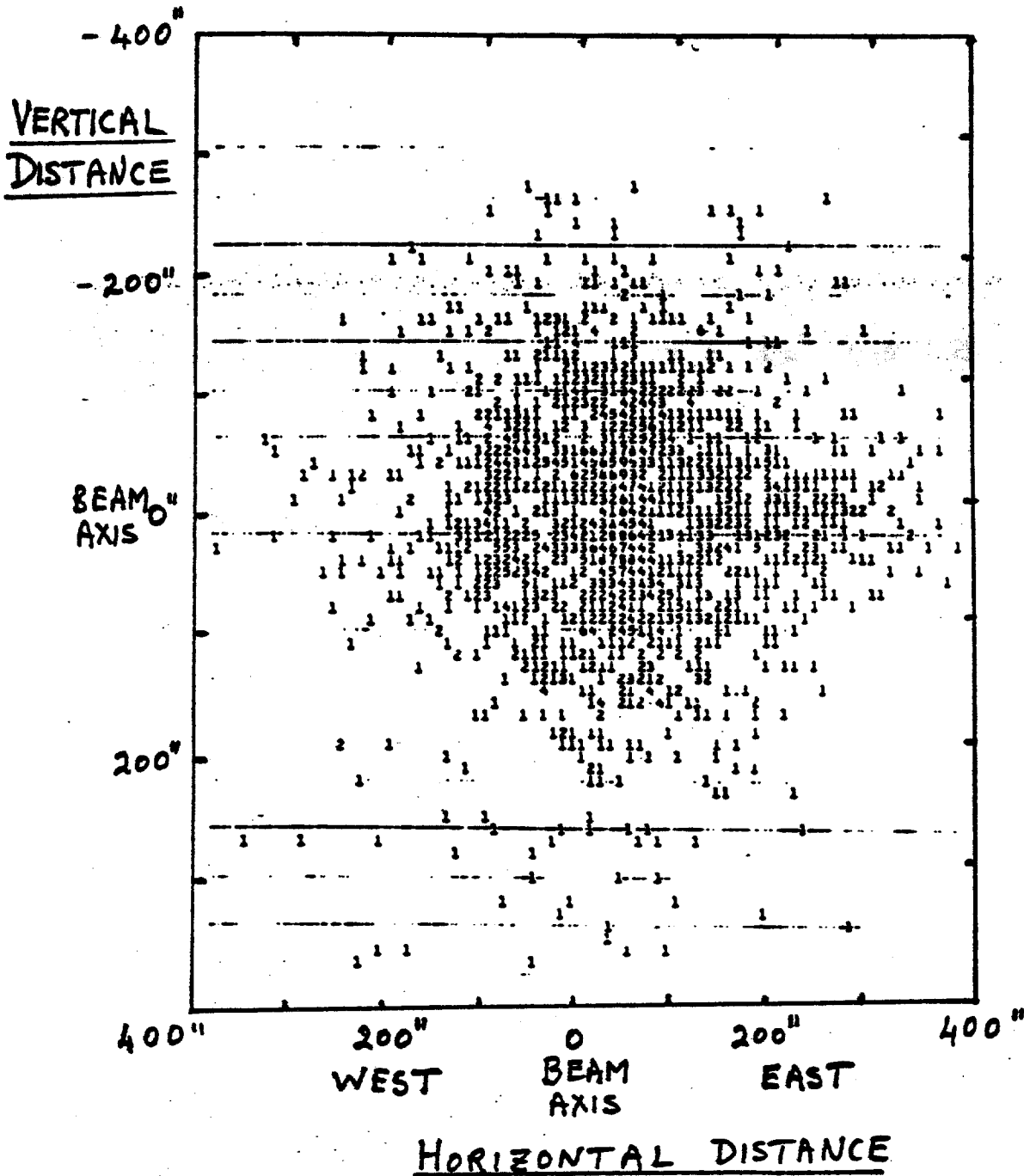
## VI. Muon Fluxes Associated with the Proton Beam Transport

### 1. Beam Gas Interactions

We have examined the effects of proton beam interactions with the residual air of the vacuum system in the transport system. Pions and kaons produced in the air can decay to muons which traverse magnets and earth berm and reach the bubble chambers. The program HALO has been used to study this problem.

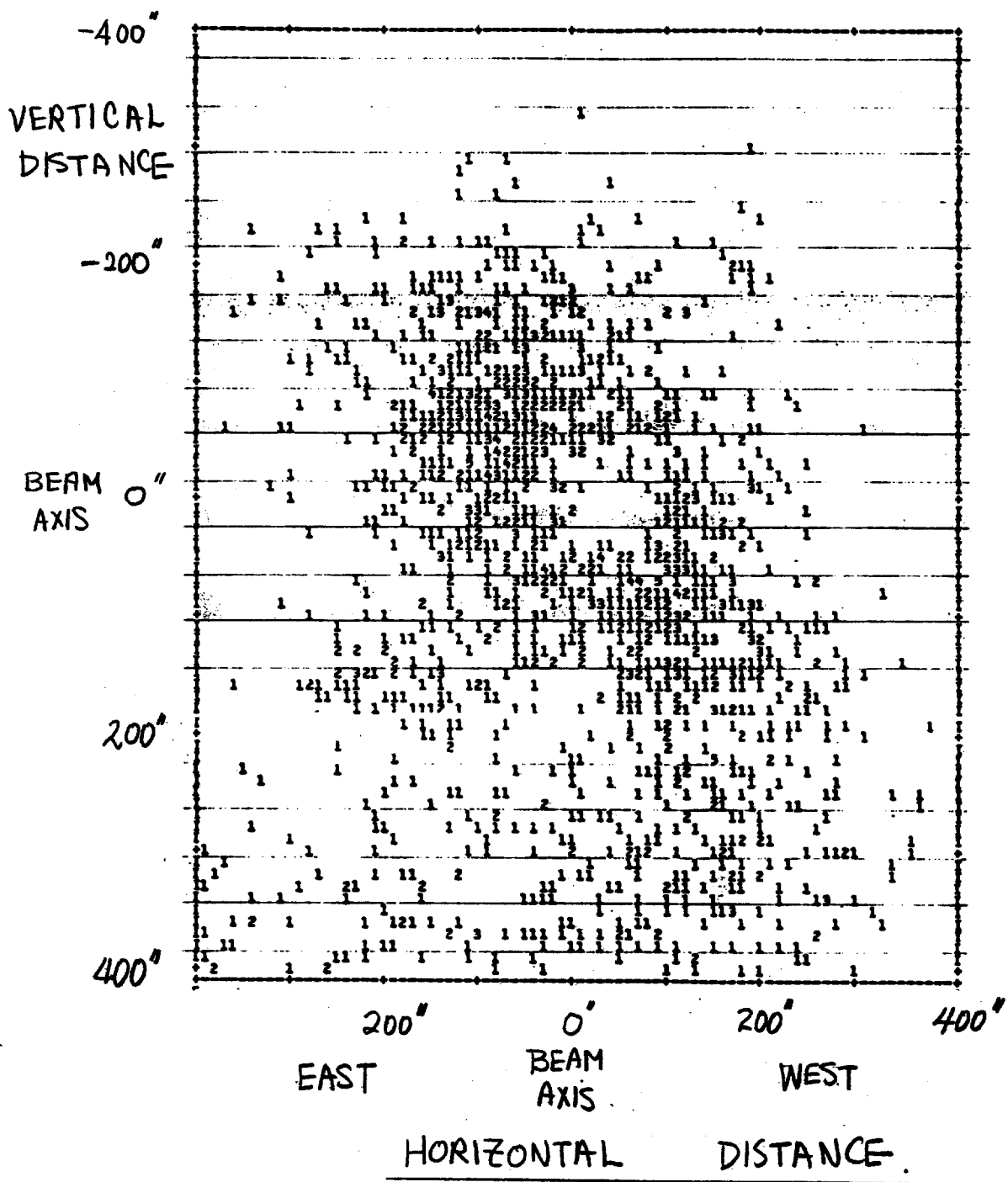
Proton-residual gas interactions were simulated by considering segments of 300' long to be lumped at the centre of that particular segment. All dipoles and quadrupoles together with tunnel dimensions and external earth shielding were simulated in the calculation. The spatial and correlated angle and momentum distribution of muons arriving at a plane transverse to the beam at the location of the tungsten target is shown in Figure VI.1. This result is for interactions at the front of the Wonder Building. Similar distributions for other source locations are shown. These distributions of muons were then entered as input to the standard Monte Carlo program used for calculating muon fluxes from the tungsten dump. The output of that program gave muon fluxes in the detectors.

The results of the calculation are shown in the attached Table for the case of the superconducting magnet design. For pressures of  $\leq 0.3 \mu$  upstream of E-103 and  $\leq 0.1 \mu$  throughout E-103 and down to the target the resulting muon fluxes are tolerable.



Negative muon spatial distribution in a plane transverse to the beam direction at the location of the tungsten target in Prompt Hall. The muons are produced by the interaction of  $5 \times 10^6$  protons at the front of the Wonder Building.

FIGURE VI. 1



Positive muon spatial distribution in a plane transverse to the beam direction at the location of the tungsten target in Prompt Hall.

The muons are procured by the interaction of  $2.5 \times 10^7 p$  at the front of Enc. 103.

FIGURE VI.2

## 2. Beam Collimation

It can be seen from the previous discussion that fractional beam losses of  $\leq 10^{-7}$  in E-103 are acceptable and somewhat less than this downstream of E-103. Beam losses  $< 10^{-6}$  have been achieved in the proton transports for E-613 in the Meson Lab and prompt neutrino experiments at CERN. Due to the fact that the bubble chambers at CERN were protected by a full 400 GeV muon range shield they experienced no difficulties. In the present case the situation is more difficult and great care must be exercised in minimizing beam losses. Our work in this area has begun and we can only give a progress report.

To ensure low beam losses we must collimate the beam and eliminate halo at some point upstream of E-103. We have examined two possibilities; E-100 and the downstream end of E-99. The results look rather encouraging although the statistics must be improved. It appears that we can interact halos of  $\geq 10^9$  protons per pulse at both E-100 and the downstream end of E-99 with acceptably low muon fluxes in the detectors. We would like to push our knowledge of these limits further by more extended computer runs. In addition, we have to explore the possibility of collimation at the upstream end of Front Hall where the situation should be even more favorable.

Much more work remains to be done on the final choice of locations of collimators, decisions on magnet apertures, i.e. 6x3x120 versus B2 magnets, and the optimum approach to achieving the required vacuum in the transport system. However, it appears

there are no insurmountable problems in the design of an adequately clean proton transport for the prompt neutrino facility.

One important fact has emerged from this study with direct relevance to the choice of design of active muon shield. The conventional magnet and superconducting magnet designs are about equal in their response to the transmission of the diffuse muon distributions associated with losses in the proton beam transport system. Thus shielding from the muon halo cannot be used as a distinguishing feature in the choice of optimum design of the active muon shield.

	<u>VACUUM</u>	<u>μ BACKGROUND</u>	
		Muons/Pulse	
	Microns Pressure	32"	15'
E99-E100	0.3	0.2	0.6
E100-E103	0.3	0.2	0.6
E103-E204	0.1	0.0	0.2
E204-E206	0.1	0.0	0.5
E206-Prompt Hall	0.1	0.1	0.2
Prompt Hall-Target	0.1	0.2	0.1
	<b>TOTAL</b>	<b>1.3</b>	<b>4.6</b>

It should be noted that these calculations were performed assuming there were magnetized iron toroids (18kg) with length 3' and radius 1' located every 30' between enclosure 206 and Prompt Hall. Without the toroids being present the requirements on the vacuum system are about one order of magnitude more stringent than given in the Table. The final choice of whether to use toroids or not will depend upon vacuum tests which will permit a cost analysis of the two approaches.

VII. Comparison of Designs and Conclusions

The conventional and superconducting magnet designs perform equally well in reducing muon fluxes into both bubble chambers. This refers to muons coming from the dump target and also halo muons associated with losses in the proton transport system. In terms of effectiveness of the objective of the design there is no clear basis for choosing one design over the other.

The cost and construction schedule for building either of the two systems are also identical within the uncertainties of the estimates. Again, there is no impetus for choosing one design over the other.

We have studied the relative sensitivity of the two designs to effects such as a 20% loss of magnetic field, an error in our formulation of ionization loss of energy by muons in the absorber in the magnets, etc. and find that the two designs respond in a similar way.

The operational reliability of the two types of magnet is expected to be similar.

Hence, we can see no major reason for preferring one solution over the other.

There is, however, some secondary advantages of the superconducting magnet design. Its short length provides an additional sixteen meters distance between the magnet and the 32" bubble chamber. The extra distance provides the opportunity to respond to an unexpectedly high muon flux in the detectors. The response could be in the form of additional magnets or passive

shielding.

Also, muon trajectories are simpler in the superconducting design with a much smaller fraction of muons going through regions of fringe field. This may enhance the reliability of the calculated fluxes in the superconducting design. Another consequence of simpler muon trajectories is that if it becomes desirable to measure muons in coincidence with, or independently of, neutrinos from the dump then the tracking will be more straightforward. If coincidence measurements were found to be desirable, then a good duty cycle would be essential. A 20 second flat top at full field would add greatly to the power costs of the conventional magnet solution. Of course, this is not the case in the superconducting design.

For neutrino production at non-zero angles only one magnet need be moved rather than four, hence alignment problems are substantially reduced in the superconducting solution.

There is a possible advantage to the conventional magnet design. There are four air gap magnets with no obstructions in the gaps and they could therefore be useful for a variety of future purposes. The superconducting design has an "air" gap in the form of a vacuum box which contains the coils and mechanical supports traversing the gap. Hence future uses of the superconducting magnet would be substantially more limited.

Consideration of all of the above factors lead us to the conclusion that because the superconducting design offers somewhat greater calculational reliability, reaction capability to

unforeseen problems, long duty cycle use and ease in alignment it will be advantageous to choose this design.

Conventional Magnets for Prompt Neutrino Facility  
Magnets M3, 4, 5, 6

R. Fast\*  
October 14, 1982

Scope

This report will discuss some of the conventional (water-cooled) magnets for the muon shield in the prompt beam. Preliminary field calculations have been done and a satisfactory iron/coil geometry obtained. Estimates of the coil and iron capital costs and DC and pulsed power requirements given.

Requirements

$B_0$  = central field = 2.0 T

$\int B_d L = 48$  T-m (1575 kG-ft)

$(-B_x)_{\max}$  = maximum value of reversed horizontal field component outside aperture

< 500 - 600 G

$B_x(y)$  should drop quickly outside the aperture

A C-magnet style with racetrack coils was chosen to avoid tall, narrow magnets. The iron/coil geometries for the magnets are given in Figs. 1-4. In order to reduce the power requirements, a pulsed current design was considered.

Calculations

The magnetostatic problem was solved in two dimensions, the x-y plane, using the program LINDA. The program calculates

\* Research Services Department

horizontal and vertical field components as a function of position in the x,y plane of longitudinal symmetry,  $B_x(x,y,0)$  and  $B_y(x,y,0)$ . The value of the horizontal component on the mid-plane,  $B_x(0,y,0)$ , for each of the four magnets is given in Table I.

Calculations in the y,z plane, giving  $B_y(0,y,z)$  and  $B_z(0,y,z)$ , will be done as part of the final design.

In the calculations the coils were sized such that the current density was approximately 2500 A/in<sup>2</sup> (390 A/cm<sup>2</sup>), a value consistent with pulsing CCM conductor (2" square x 1.125  $\phi$ ) to 10 kA. At current densities much higher than this power requirements become large and pulsing more difficult. Lower current densities, with larger coils, result in the field dropping too slowly outside the aperture.

The coil inductances were calculated from  $L = N\phi/I =$  flux linkages per amp. The DC power was obtained from  $PDC = \rho J^2 V$  ( $\rho =$  resistivity,  $V =$  volume of copper in coil) and the resistance  $R = PDC/I^2$ .

#### Coil and Iron Parameters

The parameters of magnets which were found by S. Oh to be satisfactory are given in Table II.

#### Pulsing the Magnets

The magnets must be pulsed to reduce the AC power requirements. We propose to renovate the existing 30" bubble chamber power supply, split it into two 10 kA/275 V units and power two magnets with each unit. The detailed coil design must

yield coil circuit resistances and inductances which match the capabilities of the power supply units. It is hoped that the magnets can be ramped from some low current, a few hundred amperes, to 10 kA and back down once per one minute Tevatron beam pulse.

The appendix contains an evaluation of the proposal to rennovate and remodel the 30" power supply.

Preliminary calculations, using the parameters of Table II, show that the two-magnet circuits can be charged and discharged in one minute, reducing the power dissipation to about one third of the DC value.

#### Preliminary Cost Estimate

In order to estimate the cost of the coils and iron yokes, we have used the cost per pound of these two items. The cost of coils for the large analysis magnets fabricated in the past three years, either at the Fermilab Magnet Facility or in industry, have averaged \$2.00 per pound for conductor and \$4.00 per pound for fabrication. Some copper CCM conductor is available for the coils, we use \$0.50 per pound as the cost of preparing it for coil winding.

We have assumed that the iron yokes will be made of 8" low-carbon, scrap steel. This material has been used successfully for many magnets at Fermilab. A material cost of \$200 per pound and a fabrication cost of \$300 per pound is used.

The cost of each magnet and the cost of power supply, cooling water system, excavation and rigging is given in Table III. The excavation costs were calculated by N. Bosek (Experimental Areas Dept). The estimated capital cost, including 20% escalation and contingency, of this four-magnet system is  $\$6.7 \times 10^6$ . The 30-month operating cost is  $\$1.5 \times 10^6$ .

#### Schedule

At this point we can say only that the conventional magnet system can probably be built in the 2 - 2-1/2 years available.

M3  
5m LONG

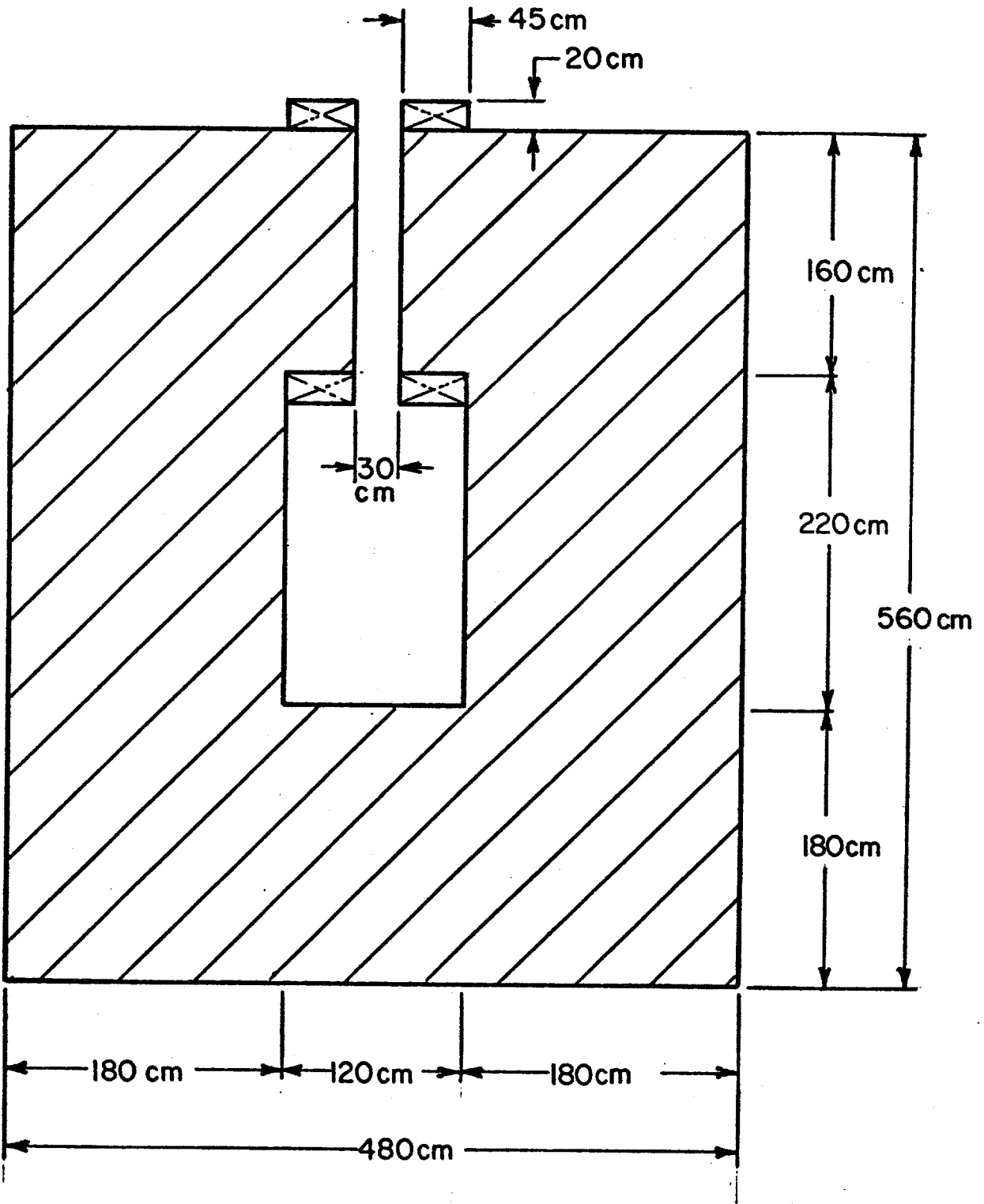


Fig. 1.

M4  
7m LONG

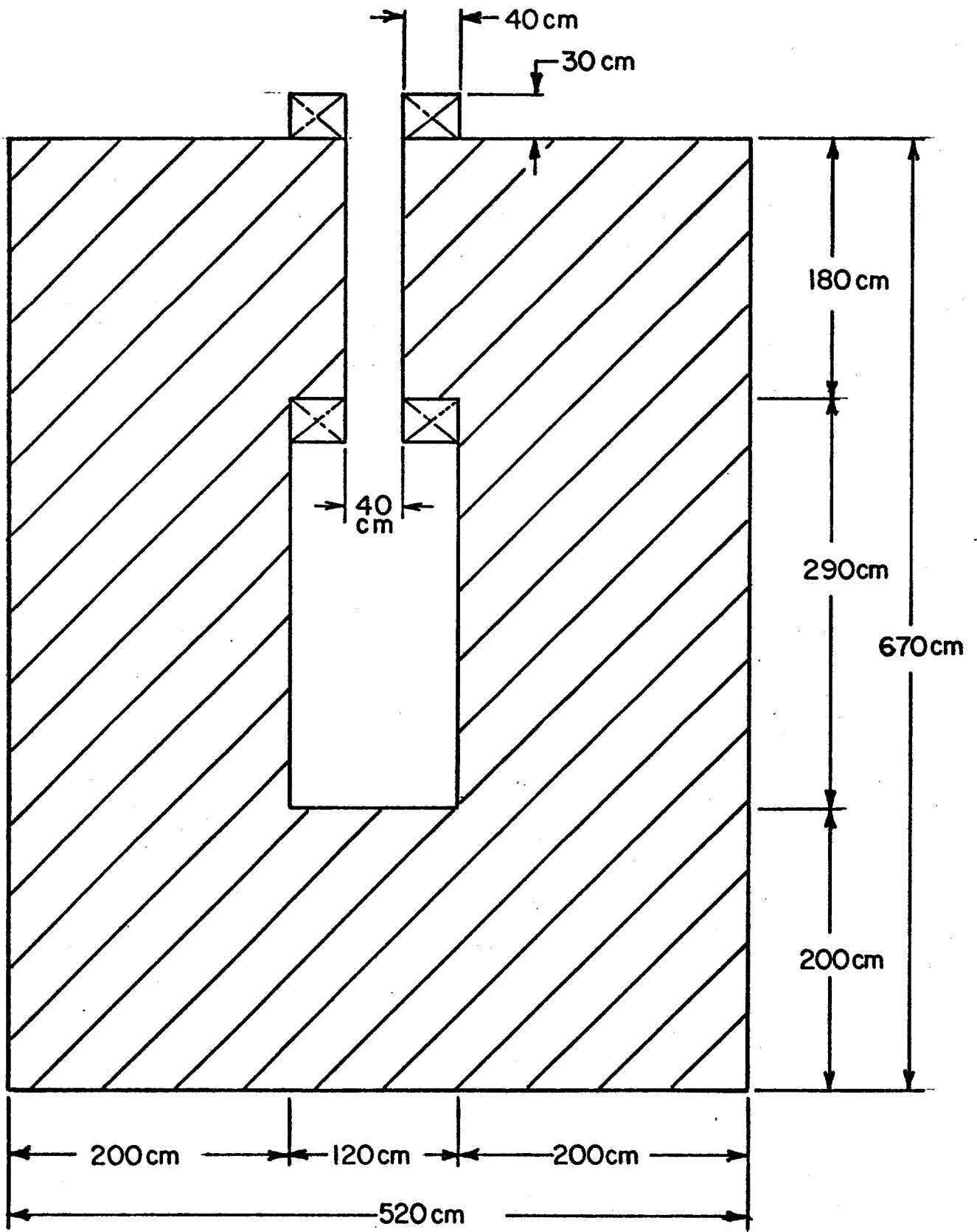


Fig. 2.

M5  
6m LONG

99

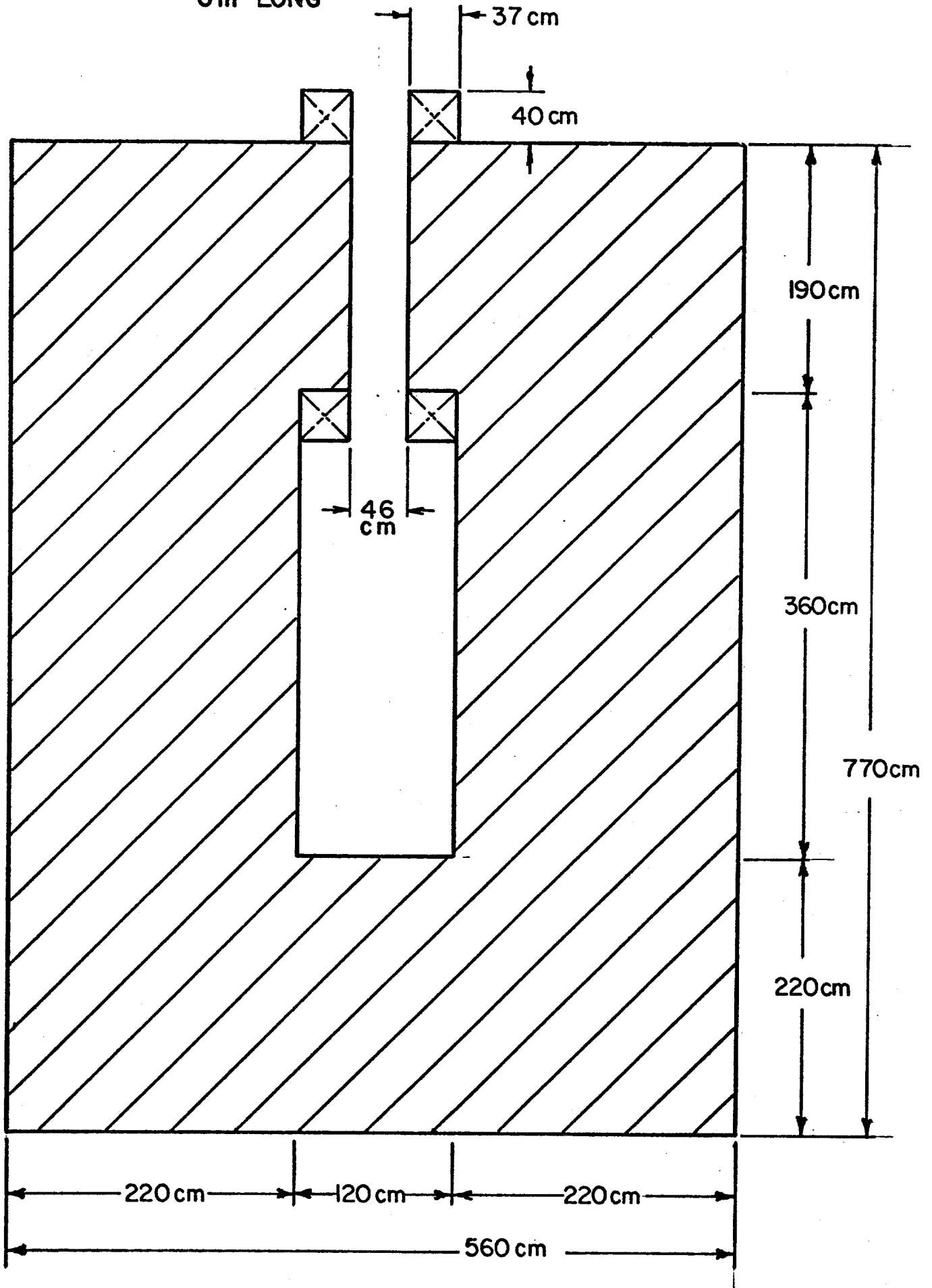


Fig. 3.

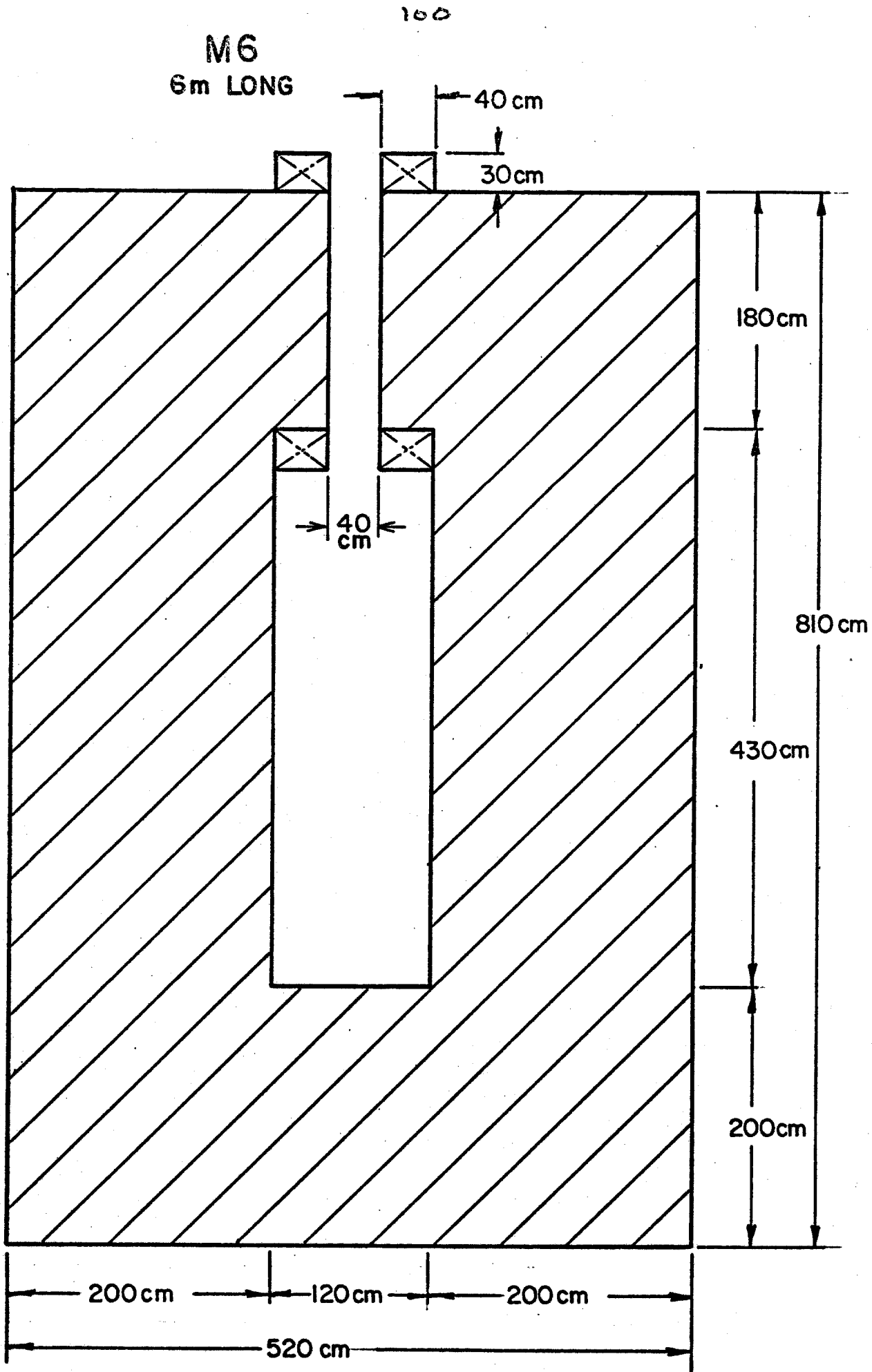


Fig. 4.

Table I - Mid Plane Field Distribution

Vertical Position (cm)	$B_x$ in tesla for magnets			
	M3	M4	M5	M6
400	-0.007	-0.010	-0.010	-0.012
350	-0.009	-0.013	-0.013	-0.015
300	-0.012	-0.018	-0.017	-0.020
250	-0.016	-0.023	-0.022	-0.026
200	-0.020	-0.027	-0.022	-0.030
150	-0.003	-0.026	-0.085	-0.021
100	0.440	0.961	1.209	0.958
50	1.927	1.944	1.951	1.944
0	2.000	2.000	2.000	2.000
-50	1.928	1.947	1.944	1.947
-100	0.425	0.953	1.214	0.947
-150	-0.038	-0.018	0.050	-0.032
-200	-0.051	-0.075	-0.072	-0.092
-250	-0.039	-0.066	-0.069	-0.082
-300	Iron	-0.052	-0.058	-0.069
-350	Iron	-0.034	-0.048	-0.058
-400	Iron	Iron	-0.036	-0.048
-450	Iron	Iron	-0.015	-0.037
-500	Iron	Iron	Iron	-0.022

Table II - Coil Parameters

Magnet	M3	M4	M5	M6	Total
kNI per half	348	445	488	450	
Coil size (cm - horiz x cm - vert)	45 x 20	40 x 30	37 x 40	40 x 30	
N per half	36	46	52	48	
I peak (A)	9667	9667	9375	9375	
L (H)	0.067	0.133	0.134	0.122	
R ( $\Omega$ )	0.0125	0.0152	0.0121	0.0148	
$\tau = L/R$ (s)	5.36	8.75	11.07	8.24	
$J_{\text{cond}}$ ( $A/cm^2$ )	515	492	440	500	
PDC (kw)	1170	1419	1065	1300	
Pulsed power (kW)	←----- 876.5 ←-----→ 788.3 ←-----→				
Stored energy (MJ)	3.1	6.2	5.8	5.4	
Conductor weight (short tons)	23.0	30.7	34.0	27.2	

Table III - Preliminary Cost Estimate

Magnet	M3	M4	M5	M6	Total
Iron weight (tons)	1010	1823	1933	1848	6614 tons
Iron cost (k\$) @ \$500 per ton	505	912	967	924	\$3308
Conductor weight (tons)	23.0	30.7	34.0	27.3	115 tons
Conductor cost (k\$) copper @ \$4000 per ton and 10% extra	100	0	0	120	\$220
Cost fabrication cost (k\$) @ \$8000 per ton	184	246	272	218	\$920
Manpower engineering and design of coils and iron (k\$)	--	--	--	--	\$250
Power supply renovation and remodeling	--	--	--	--	\$100
Cooling water system	--	--	--	--	\$10
Rigging iron and coils, at \$60 per ton	--	--	--	--	\$404
Conventional construction	--	--	--	--	\$400
<hr/>					
Capital cost					\$5612 k
Escalation and contingency (20%)					1122 k
<hr/>					
Total capital cost					\$6734 k
Operating cost for 30 months					1530 k
<hr/>					
Total cost - capital & operating					\$8264 k

## APPENDIX

TO: JIM WALKER

FROM: BOB TRENDLER

SUBJECT: 30" BC POWER SUPPLY

AT YOUR REQUEST, THE 30" BC. POWER SUPPLY WAS EXAMINED TO DETERMINE ITS VIABILITY AS A POWER SUPPLY FOR THE PROMPT BEAM DUMP CONVENTIONAL MAGNETS. A GROUP CONSISTING OF AGE VISSER, STAN ORR, LEON BEVERLY, BILL WILLIAMS, WALT JASKIERNY, BOB INNES, JIM KILMER, AND MYSELF EXAMINED THE POWER SUPPLY AND THE SCHEMATICS.

IN SUMMARY, WE BELIEVE THE POWER SUPPLY CAN BE EASILY SPLIT INTO TWO  $6\phi$  275 VOLT 10 KA UNITS. FURTHERMORE, THE UPGRADE WOULD REQUIRE NEW SCR ASSEMBLIES, IMPROVED FIRING CIRCUITS, IMPROVED FREEWHEELING DIODE CONNECTIONS, IMPROVED REGULATORS, AND SOME REWIRING. THE POWER SUPPLY WILL BE CAPABLE OF RAMPING. THE LOAD WILL, HOWEVER, WILL HAVE HAVE RESISTANCE AND INDUCTANCE PARAMETERS APPROPRIATE FOR THE 275 VOLT MAXIMUM OUTPUT AND THE RAMPING PERIOD.

WE WILL CONTINUE TO REVIEW THE UPGRADE REQUIREMENTS IN AN EFFORT TO PROVIDE A BETTER COST ESTIMATE. THE \$100K ORIGINALLY ESTIMATED SHOULD BE MORE THAN ADEQUATE.

O.C. KEN STANFIELD

RON FAST

Cost Analysis of the 5T 8.4 m long Superconducting Version  
of the Prompt Neutrino Magnet System

Eddie Leung\*

October 11, 1982

\* Research Services Department

Preface

The revised cost analysis is based on 5T, 8.4 m long superconducting version of the Prompt Neutrino Magnet System. This represents a workable design with more engineering calculations performed on it and where possible, quotations from possible vendors have been solicited; therefore the numbers presented here are accurate to  $\pm 15\%$  easily. The cryostat itself (instead of across the gap tension links) is used as the major support for the body forces because of possible adverse effects introduced to physics from the latter approach. The positive magnetic field profile provides a slightly higher overall Integral B-dl while the increase in length from 7 m to 8.4 m escalates the capital cost from \$5.1 M to \$5.55 M.

## Introduction

The Prompt Neutrino Magnet System calls for a bending power of 60→70 Tm for the removal of unwanted muons. A 5 T, 8.4 m superconducting magnet MSC is provided as an alternative to the conventional magnets M3C→M6C. The first two magnets, M1C and M2C, are the same for both the conventional and superconducting cases and they are designed to shield off most of the nuclear radiation from subsequent magnets. A preliminary design and cost analysis of this superconducting magnet is presented in this report. Figure 1 and 2 depict the arrangement of the magnets in the conventional and superconducting beamlines while Fig. 3(a) and (b) show sections of MSC. A cost comparison to the conventional case is also included.

## Magnetic Field Calculation and Coil Design

Physics requirement calls for a special magnetic field profile. The magnetostatic parameters for this four-coil design were calculated using the computer code LINDA. The vertical distribution of the horizontal field on the mid plane is given in Fig. 4. This 81 MJ magnet will have a total of 6 coils (both halves), each race-track in configuration and cryogenically stable in design. Since the different coils lie in different field regions, the optimized current density is different in each coil. These are selected in accordance with the Stekly criterion for fully cryostable magnets. Calculated coil parameters are presented in Table I.

TABLE I COIL PARAMETERS

<u>Items</u>	<u>Coil #1</u>	<u>Coil #2</u>	<u>Coil #3</u>	<u>Coil #4</u>	<u>Units</u>	<u>Remarks</u>
By (AVG)	4.34	2.39	0.41	-1.08	T	
Bx (AVG)	- .13	-0.27	- .26	- .19	T	
B (Max)	6.1	4.30	1.5	1.20	T	
NI	0.941	1.076	1.210	-0.538	$10^6$ A-turns	$3.197 \times 10^6$
$I_{op}$ , max. operating current	2000	2000	2000	2000	A	
$I_R$ , fully recovery current	2382	2459	2583	2783	A	
Coil dimensions	7.2 x 0.8	7.2 x 1.4	7.2 x 2.8	7.2 x 3.0	m x m	
Coil length	16.0 (52.5)	17.2 (56.4)	20 (65.6)	20.4 (66.9)	m (ft)	
Conductor volume	10.82	12.79	7.45	5.06	ft <sup>3</sup>	
Total (both halves) Conductor volume			72.24		ft <sup>3</sup>	
Total weight			39732		lbs	Using 550 lbs/ft <sup>3</sup>
Cost (at \$8/lb)			318		K\$	



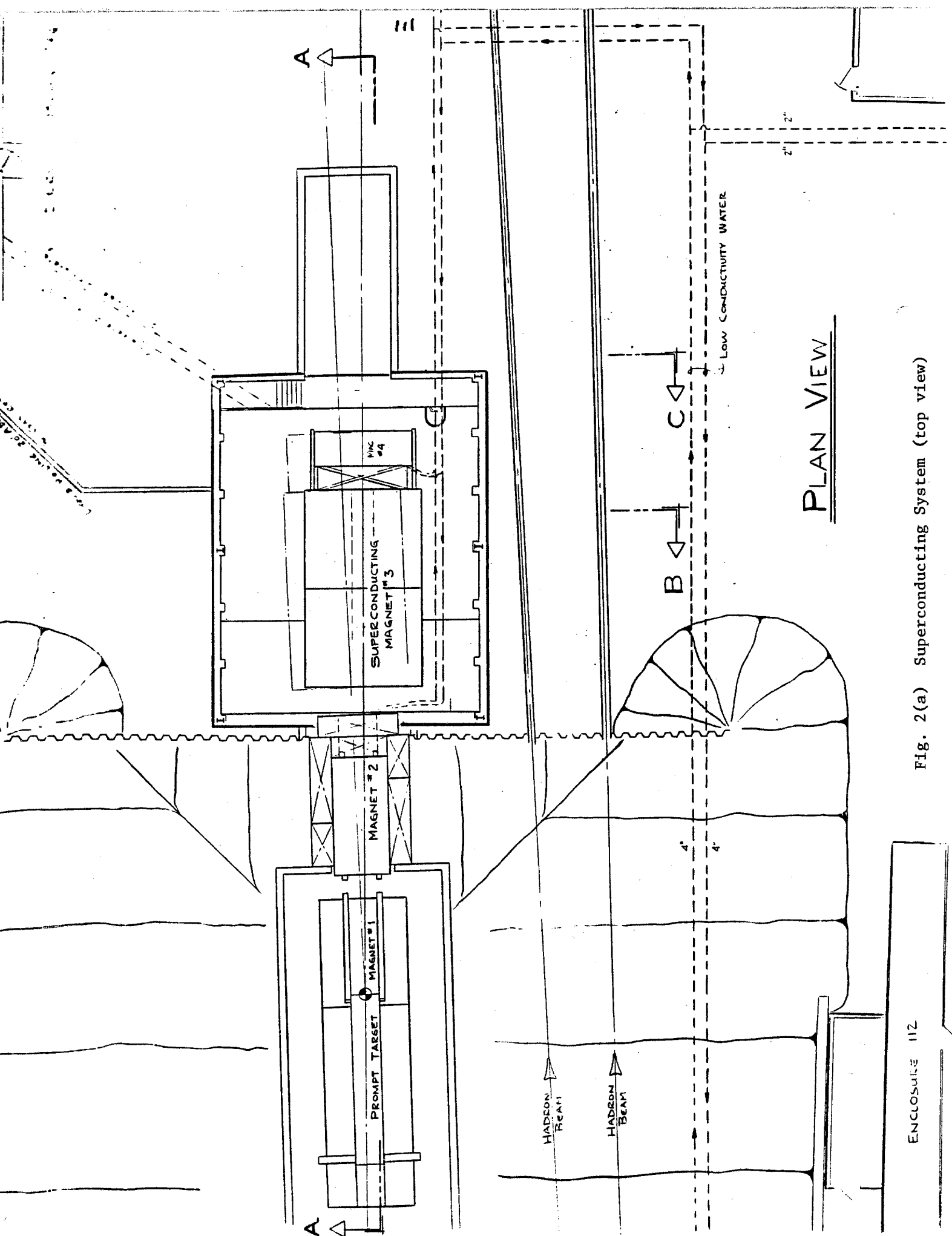


Fig. 2(a) Superconducting System (top view)

ENCLOSURE 112

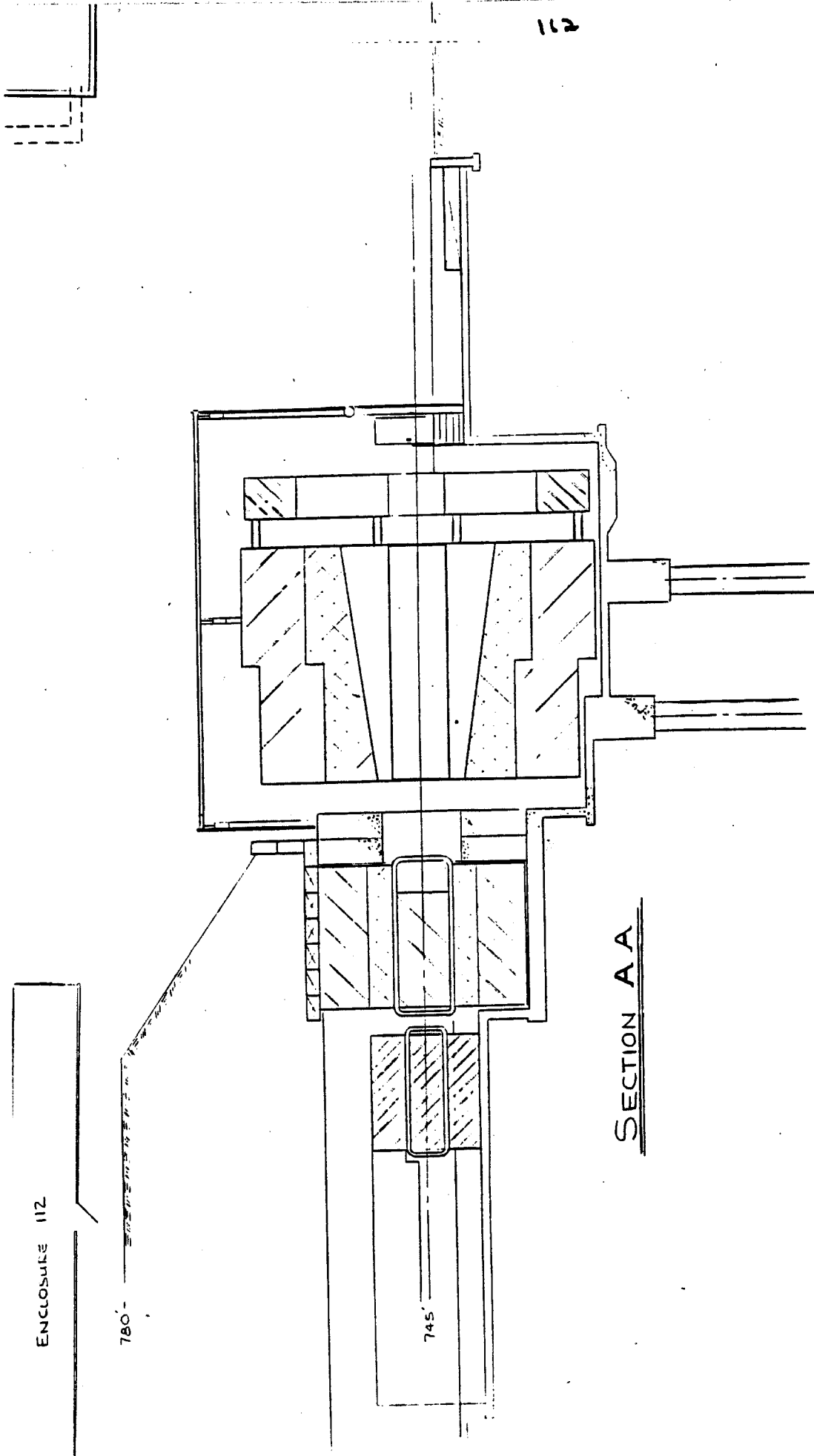


Fig. 2(b) Superconducting System (side view)

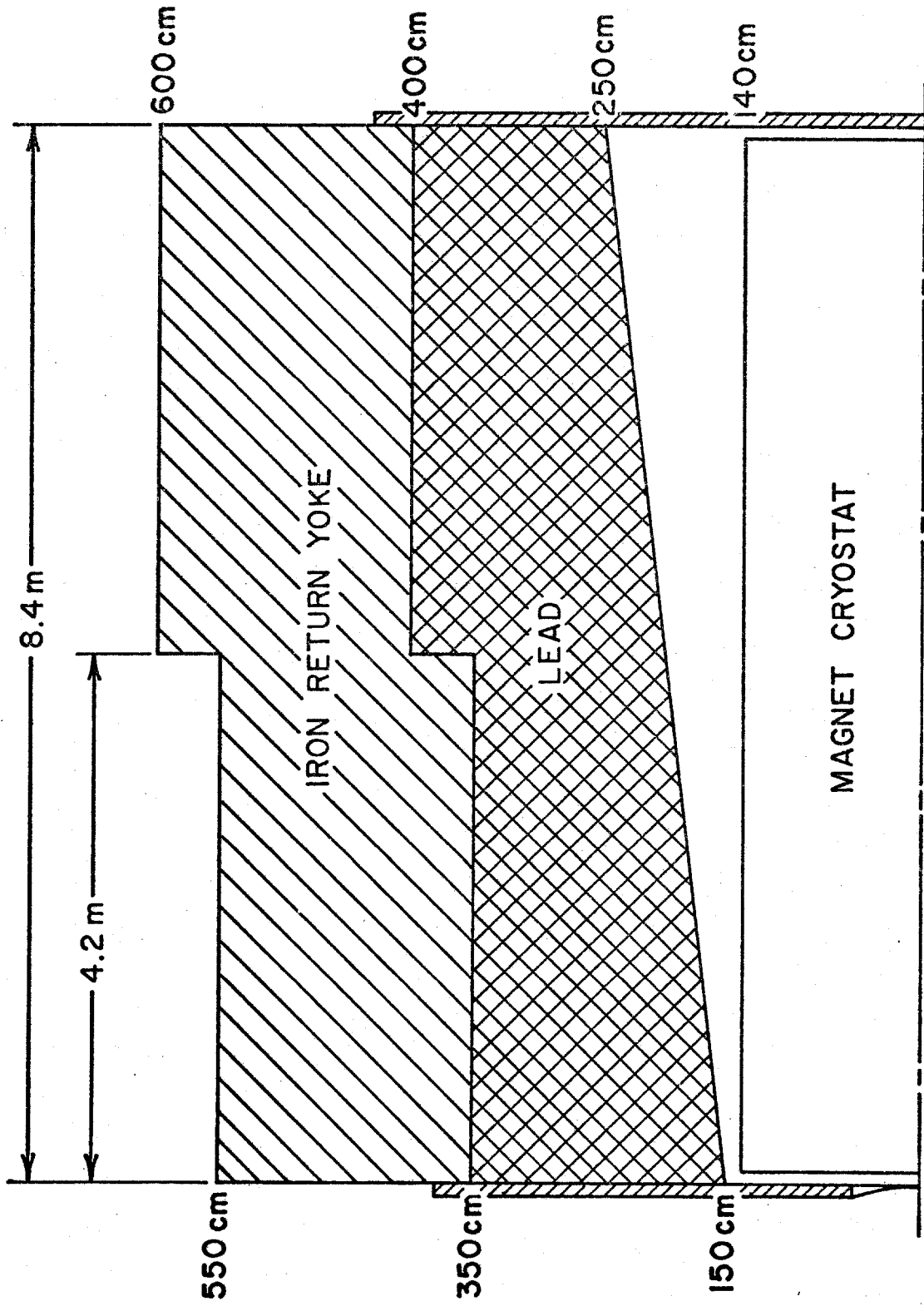


Fig. 3(a) Longitudinal Section of Magnet

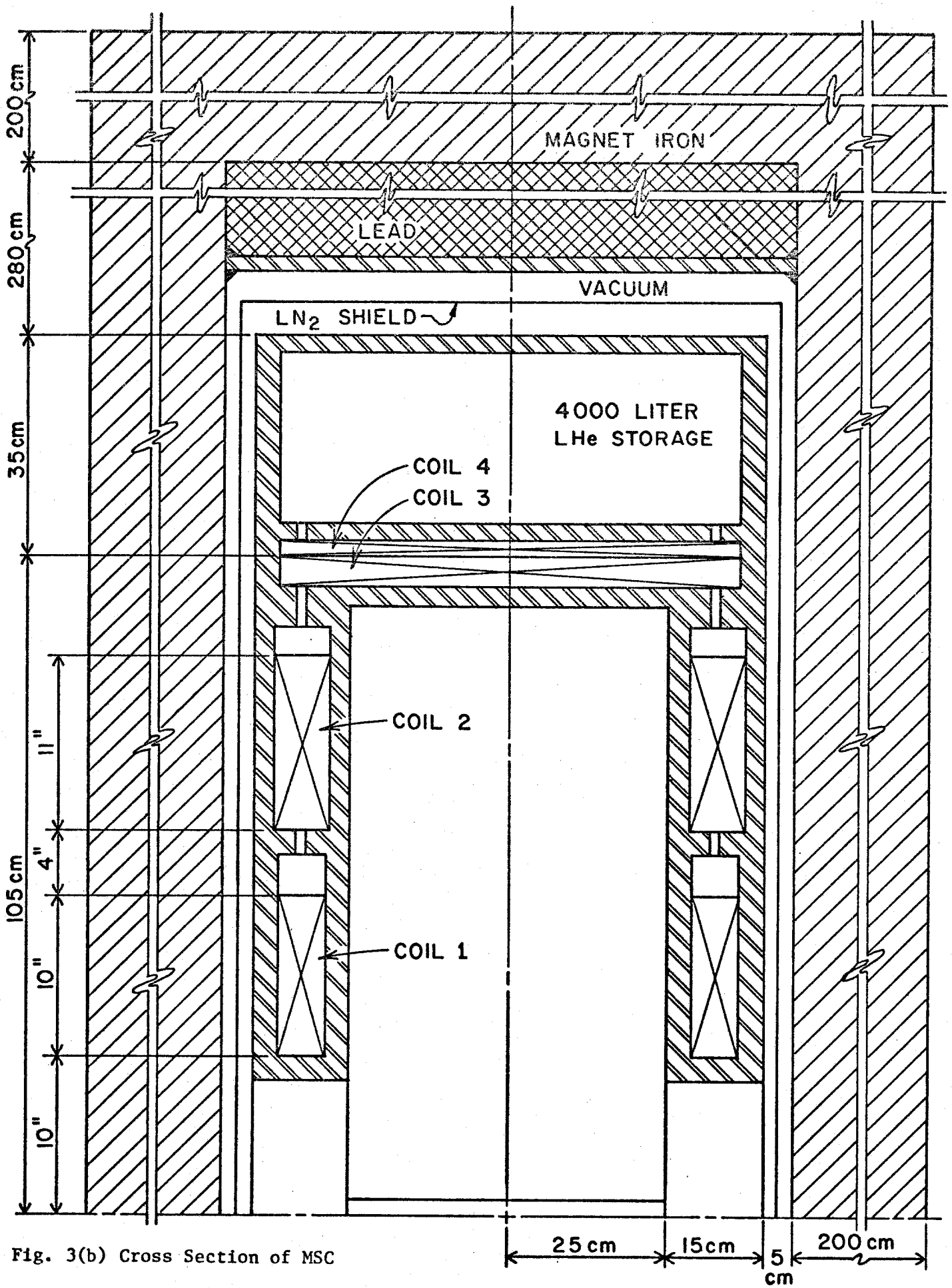
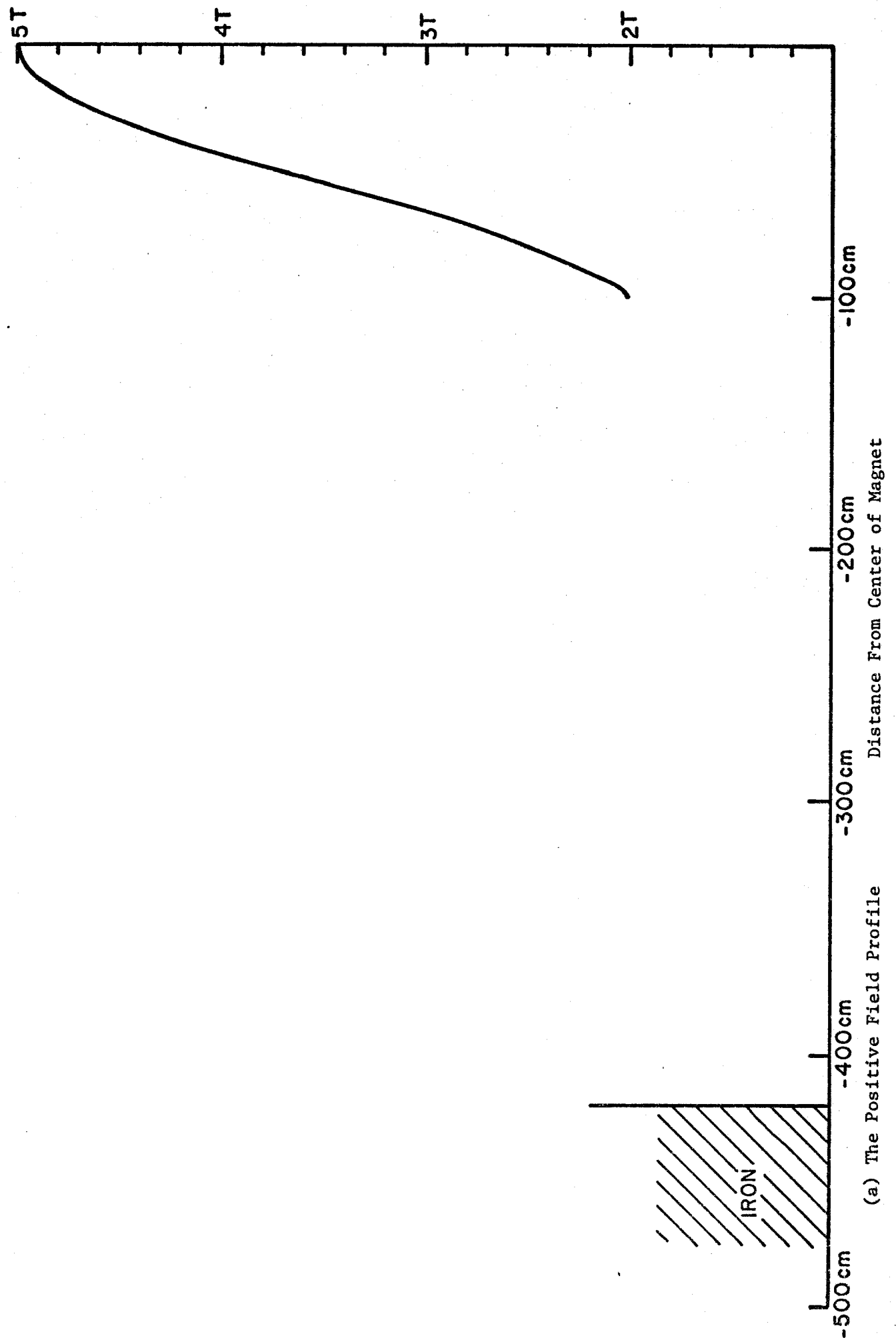


Fig. 3(b) Cross Section of MSC

Magnetic Field

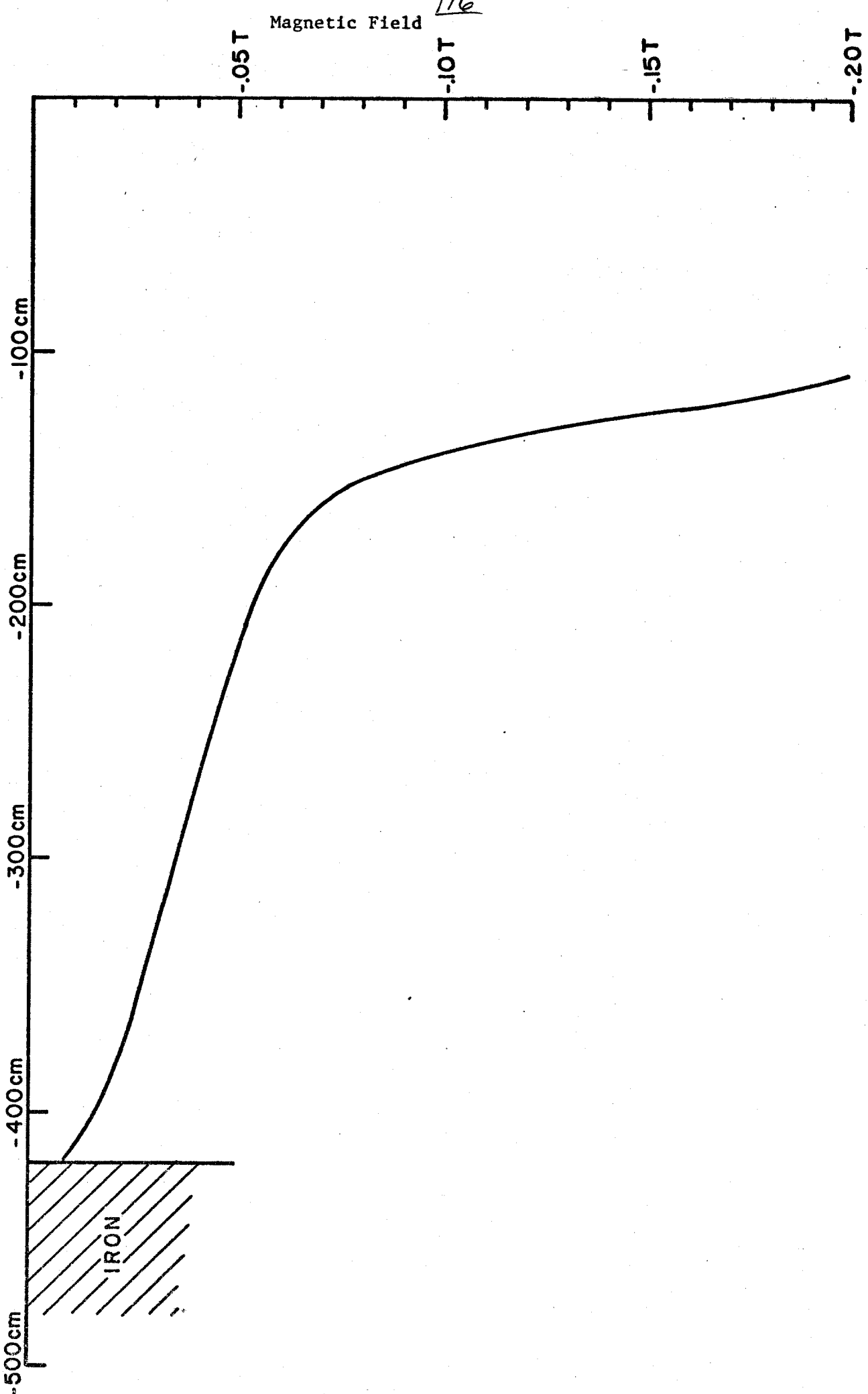
Fig. 4. The Vertical Distribution of Horizontal Field on the Mid-Plane



(a) The Positive Field Profile

(b) The Return Field Above the Coils

Distance From Center of Magnet



Magnetic Field

-.05T

-.10T

-.15T

-.20T

-100cm

-200cm

-300cm

-400cm

-500cm

IRON

116

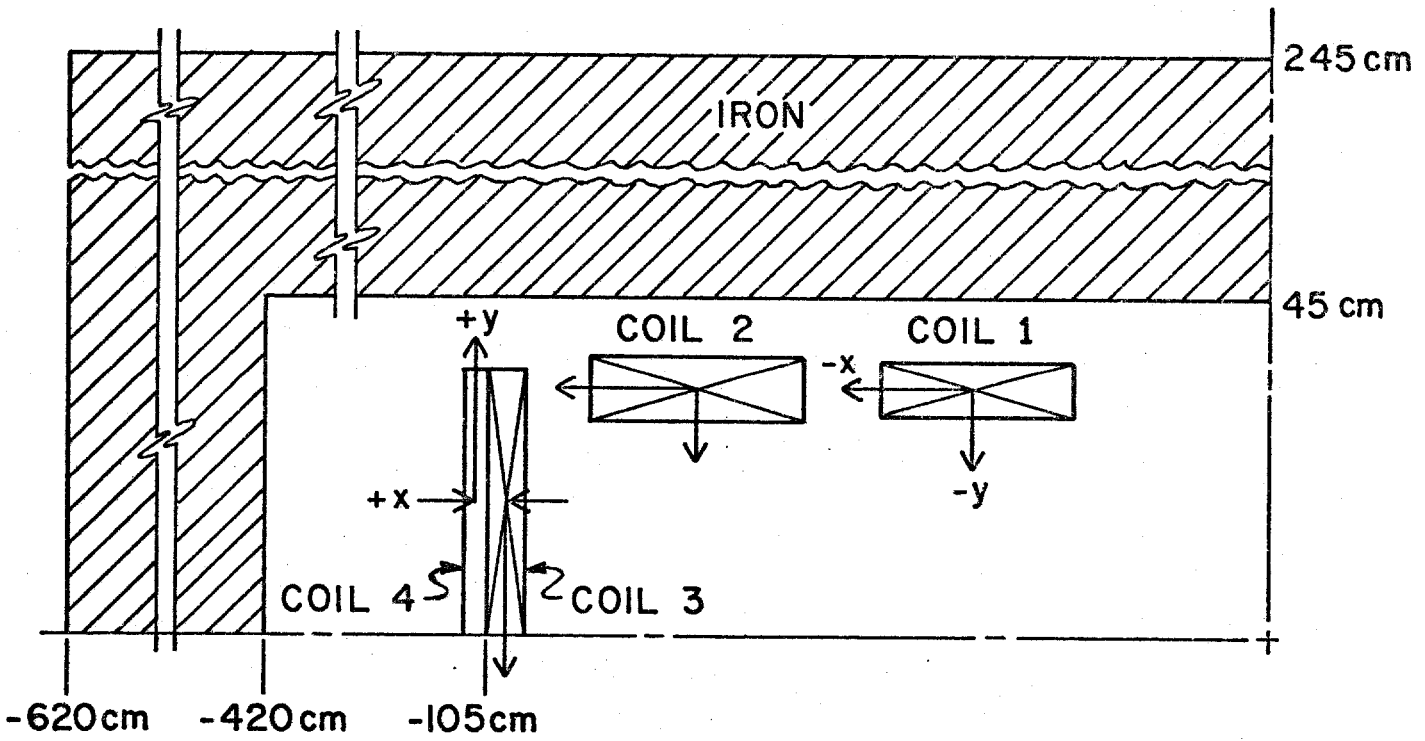
Using a unit cost of \$8/lb, the total conductor cost would be about \$318 K. A quotation obtained from AIRCO, Ltd. for a viable conductor design is \$318 K. We shall use this number for estimation of the conductor cost.

### Structural Calculations

The magnitude and direction of the forces acting on the various coils are given in Fig. 6. The horizontal forces acting on coils #3 and #4 are supported against the internal coil structure while those on coil #1 and coil #2 are reacted against the helium cryostat. The forces are high but by reacting the forces internally, we can cut down the heat leak into the helium compartment. Similarly, we can support the vertical forces acting on the various coils. An ANSYS (3D finite element structural code) run is being performed to check the analytic calculations performed so far (App. B).

Twenty short I-beam shaped rollers on rail and side G-10 bumpers are used to support the 110,000 lbs magnet cold mass and the magnet de-centering forces. Cost of the supports total \$50 K.

Preliminary thickness calculation for the various walls of the helium cryostat were performed and the results summarized in Fig. 3(b). The upper half of the cryostat provides a storage capacity of 4000 liters of liquid helium. A total of 70,000 lbs of stainless steel 304 is required for the construction of the helium shell. The material cost would be \$2.5/lb and the fabrication cost an additional \$7.5/lb. The helium vessel cost



<u>Items</u>	<u>Coil #1</u>	<u>Coil #2</u>	<u>Coil #3</u>	<u>Coil #4</u>	<u>Units</u>
Fx	$-2.33 \times 10^4$	$-1.47 \times 10^4$	-2832	+3318	lbs/in
Fy	-698.5	-1659	-1796	+583.6	lbs/in
Px	-7767	-4200	-192	+225	psi
Py	-69.85	-150.8	-898	+583.6	psi

Fig. 6 Forces on Coil

\$700 K.

Radiation Shield and Vacuum Box

The LN<sub>2</sub> temperature radiation shield is to be constructed out of 3/64" thick copper. With a surface area of 1800 ft<sup>2</sup>, the weight of copper required is 3600 lbs; at \$5.5/lb (material and fabrication), the cost is \$20 K. Adding \$4 K for fabrication of standoffs and \$8 K for purchase of NRC-2 thermal insulation and aluminum tape. Total cost √ \$32 K.

For the vacuum box, it is proposed to use part of the iron return yoke as part of the box (6" on each side, except 12" on the bottom where the cold mass supports also have to be housed in). The end plates are constructed out of 2" thick steel plate. The weight required is 40,000 lbs. At \$6/lb (material and fabrication) total cost for the vacuum box √ \$240 K.

Fixtures

It is difficult to estimate the cost for fixturing at this stage, but the following are perhaps representative:\*

Coil winding fixture	\$ 50 K
Assembly fixture	\$ 25 K
Handling fixture	\$ 25 K
Total	<u>\$100 K</u>

\*The in-house fixtures used for the assembly of the coils for E-605 M 1/2 magnet cost \$84 K.

### Thermal Analysis

(1) Radiation heat transfer from  $LN_2$  temperature radiation shield: Applying the new 77 K+4.2 K insulation scheme† as that used in CCM and 32" B.C. (3M #425 pure aluminum tape on the helium cryostat plus an additional 12 layers of NRC-2 - 500°A thermal insulation on the outside), we can use a heat leak number of 2 mW/ft<sup>2</sup> for calculation. A surface area of 1800 ft<sup>2</sup> will yield a heat load of 3.6 W.

(2) From current leads: Calculated energy of the magnet is  $\approx$  81 MJ. Choosing a current of 2000 A, the calculated inductance of the magnet is  $\approx$  40.5 H and a terminal voltage of 333 volts would appear for an L/R of  $\approx$  2 minute. This is reasonable. So we would nominally choose 2000 A to be our operating current. For extra flexibility in doing physics, it is requested that each of the 4 pairs of coil to have separate current leads. Using AMI<sup>∇</sup> leads, the heat load is 2.8 l/hr/1000 A pair; hence total heat leak via the current leads during operation is  $2.8 \times 2 \times 4 = 22.4$  l/hr and when the current is off, equals to  $\approx .4 \times 22.4 \approx 8.96$  l/hr. This is a rather high price to pay. We can always have the option of using 1000 A coils #3 and coil #4, in this case, corresponding LHe boil-off numbers would be 16.8 l/hr during operation and 6.72 l/hr when the current is off.

(3) Heat leak down the chimney and misc. paths

$\approx$  1 W

†E. Leung, R. Fast, J. Heim and H. Hart, Advances in Cryogenic Engineering, Vol. 25, p. 489 (1981).

∇American Magnetic Incorporated.

(4) Heat leak through the 5" cold mass supports

$$\leq 1 \text{ W}$$

Total heat load into the helium system

$$\approx 17 \text{ W (or } 24.2 \text{ l/hr)}$$

## Magnet Cost Summary

The above costs are summarized:

Superconductor	\$ 318 K
Helium cryostat	\$ 700 K
Coil support structure	
Cold mass support structure	\$ 50 K
Radiation shield	\$ 30 K
Fixtures	\$ 100 K
Vacuum box	\$ 240 K
Total	<u>\$1438 K</u>

Manpower Required

Assuming a project duration of 2 years, the following manpower is required:

<u>Personnel</u>	<u>Man-yr.</u>	<u>Annual Cost</u>	<u>Cost</u>
Project Manager/ engineer	2	\$45 K	\$ 90 K
Engineers (2)	4	\$45 K	\$180 K
Vendor liason	2	\$35 K	\$ 70 K
Designer	2	\$35 K	\$ 70 K

Draftsman	2	\$30 K	\$ 60 K
Technicians (2 in 1st half year) (6 in last 1-1/2 year)	10	\$26 K	\$260 K
Tech. Specialist	2	\$35 K	\$ 70 K
Machinist	1-1/2	\$28 K	\$ 42 K
Welder	1-1/2	\$28 K	\$ 42 K
			---
Total			\$884 K

The successful completion of the project within 2 years depends very much so on the availability of the right number and kind of personnel at the correct time.

#### Iron Yoke

Figure 3(a) shows a longitudinal section of the magnet with iron. 3814 tons of iron are required for flux return. Field calculations have been done to optimize the use of the iron such that the field inside iron is  $\approx 1.73$  T. At a cost of \$500/ton, total cost of iron = \$1907 K. Cost of rigging, piling the iron and surveying at \$60/ton would amount to another \$229 K.

#### Refrigeration, Power Supply and Instrumentation

(a) Refrigeration: Wes Smart of the Experimental Facility suggested that the most economic way is to have a satellite for both MSC and the 32" B.C. Total cost for a satellite (and control) is  $\approx$  \$650 K. Appropriating \$150 K to the 32" B.C. project, the cost here is \$500 K. Allowing \$50 K for building of transfer lines and dewars, the total is \$550 K.

(b) Power Supply: At 2 KA, the inductance of the magnet is 40.5 H. In order to charge the magnet in 1 hour, approximately 40 V is required. Four such power supplies would cost \$100 K, the dump resistor, dc contractor and cable would probably cost \$15 K and \$10 K respectively.

(c) Instrumentation: This includes the various current, voltage, temperature, pressure, stress and refrigerator parameters to be monitored and read. An interlock and quench protection system has to be installed also. The whole system (sensing, readout and interlock) could cost \$60 K. (Breakdown: \$7 K for current leads, \$43 K for control system and \$10 K for other instrumentations).

#### Excavation

Civil engineering figures are provided by Norm Bosek of the Experimental Facility. This includes a thin metal building, preparation of foundation for magnet and all the necessary civil construction items. The total cost is \$357 K.

#### Total System Cost Breakdown

Coils	\$1438 K	±20%
Iron	\$1907 K	±10%
Manpower	\$ 884 K	±15%
Power Supply & Instrumentation	\$ 185 K	±10%
Refrigeration & Cryogenic System	\$ 550 K	±10%
Excavation	\$ 357 K	± 5%
Rigging, Surveying	<u>\$ 229 K</u>	± 5%
Total Capital Cost:	\$ 5550 K	

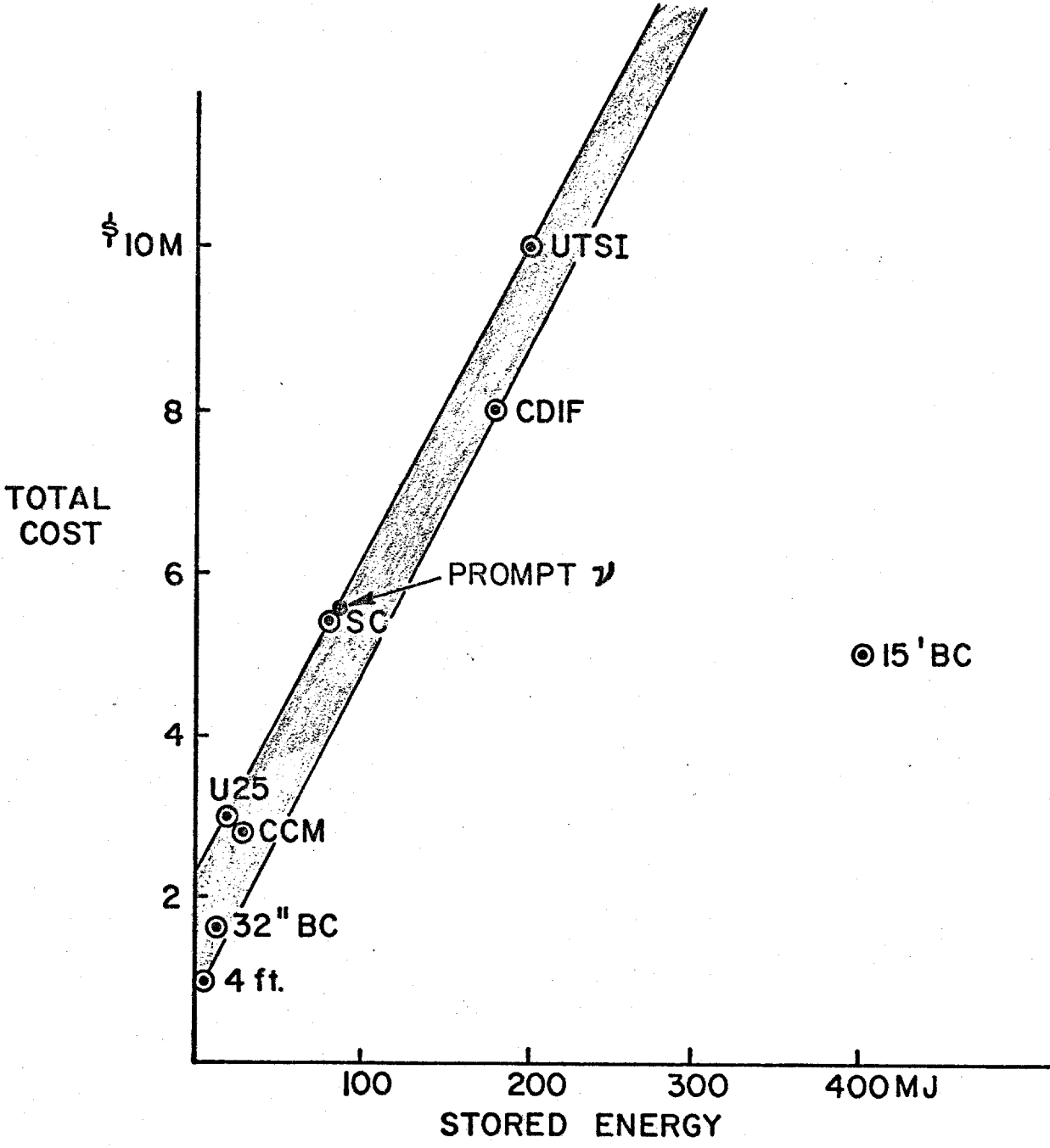
5 year operating cost at 250 KW x 50% duty factor  $\approx$  \$225 K

Total Project Cost = \$5550 + \$225 = \$5775 K

This cost estimate number is probably accurate to  $\pm$  15%.

#### Cost Comparison to Other Magnets

The capital costs for a number of magnets either of similar configuration (UTSI, CDIF, SC and U25 are all MHD type dipoles) to MSC or that we have concrete cost numbers on because they were built in Fermilab (CCM, 4 ft., 32" B.C. and 15' B.C.), are plotted against their respective stored energy in Fig. 7. With the exception of the 15' B.C. which was designed in ANL and which utilized most of the engineering development and research of the 12' B.C., we can see that there is a positive linear correlation between the two parameters considered and that the capital price tag of \$5.55 M for the superconducting version of the Prompt Neutrino Magnet System is a reasonable one.



Capital Cost of Magnets vs Stored Energy

Prompt Neutrino Facility  
Conventional Magnets M1 and M2

The M1, or target magnet, is the same whether the muon spoiler system is conventional or superconducting. The magnet is all iron except for a stainless steel portion between the coils, as shown in Fig. 1. Since the M1 magnet is very close to the target, the coil and associated water plumbing must be radiation resistant. The iron in the center portion should be magnetized to 2.1 T.

The M2 magnet is somewhat different for the conventional and superconducting cases. For the conventional case M2 is an all-iron magnet shown in Fig. 2. If the system is superconducting the downstream 1 m of the useful volume is air. The field in the useful region is 2.0 T.

The coil parameters are given in Table 1. To reduce the power required, the current density is quite low,  $\sim 600$  A/in<sup>2</sup> (93 A/cm<sup>2</sup>) and the coils are operated DC.

A preliminary cost estimate is given in Table II, using \$500 per ton for the iron yoke, \$2.00 per pound for conductor, and \$4.00 per pound for coil fabrication.

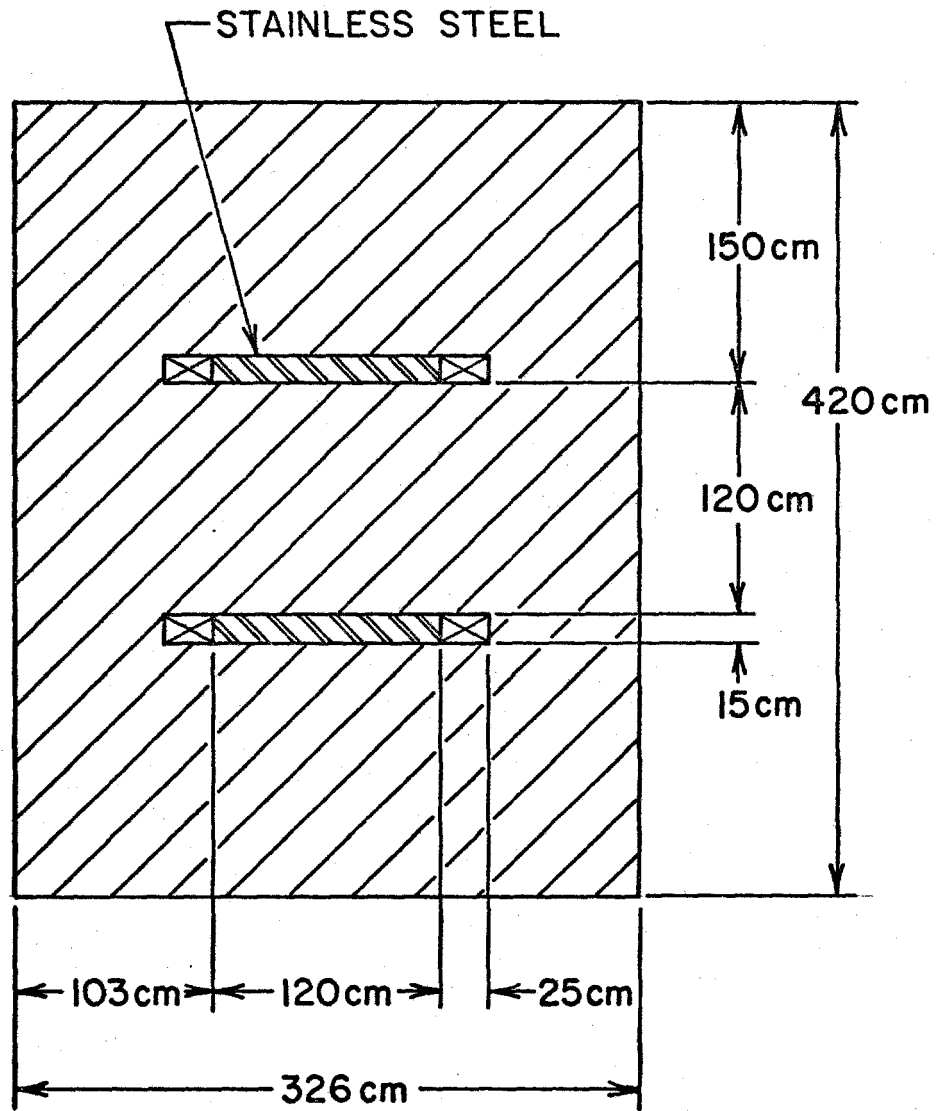
TABLE I  
Coil Parameters,  
M1 and M2 Magnets

<u>Magnet</u>	M1	M2	Total
kNI per half	25	25	--
Coil size (cm - horizontal x cm - vertical)	25 x 15	25 x 15	--
N per half	15	15	--
I (A)	1667	1667	--
L (H)	0.091	0.179	0.27
R ( $\Omega$ )	0.0027	0.0036	0.0063
$\tau = L/R$ (S)	33.7	50.0	42.9
$J_{\text{cond}}$ (A/cm <sup>2</sup> )	93	93	--
PDC (kW)	7.5	10.0	17.5
Conductor weight (short tons)	5.5	7.3	12.8

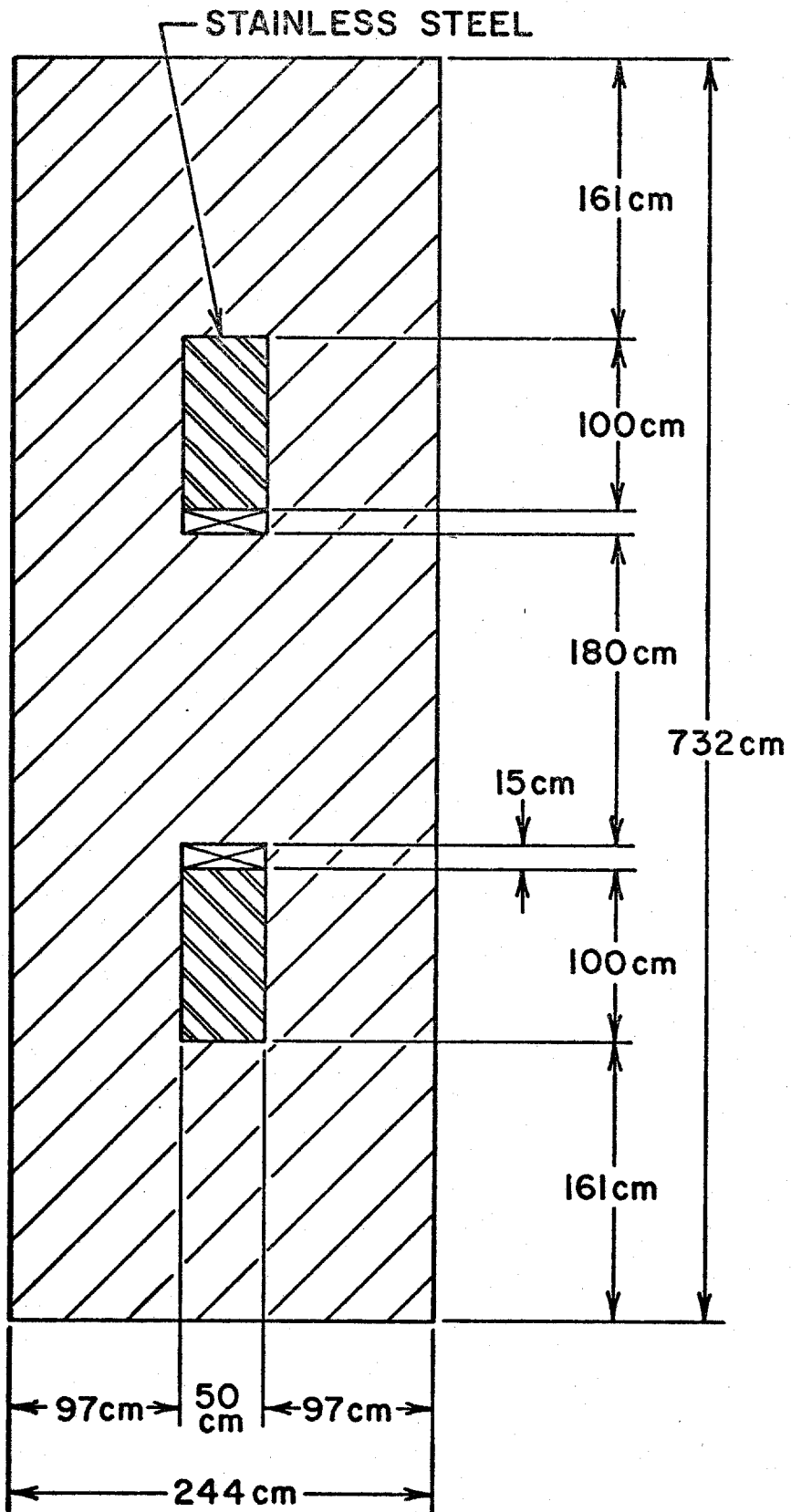
TABLE II  
Preliminary Cost Estimate  
M1 and M2 Magnets

Magnets	M1	M2	Total	<u>Units</u>
Iron weight	430	750	1180	tons
Iron cost, \$500 per ton	215	375	590	K\$
Stainless weight	11.3	47	58.3	tons
Stainless cost, @\$2.5 per lb	57	--	292	K\$
Conductor weight	5.5	7.3	12.8	tons
Conductor cost, @\$4000 per ton, plus 10% extra	24.2	32.1	56.3	K\$
Coil fabrication @\$8000 per ton	44	58.4	102.4	K\$
Manpower - engineering and design of coils and iron	--	--	25	K\$
Power supply (2000 A, 20 V)	--	--	20	K\$
Cooling water system, closed cycle	--	--	25	K\$
Rigging, @\$60 per ton	--	--	75	K\$
			1186	K\$
Capital Cost			1186	K\$
Escalation and contingency (20%)			237	K\$
Total capital cost			1423	K\$

M1  
4m LONG



# M2 5m LONG



Comparison of Cost of Conventional  
and Superconducting System

R.W. Fast, E.M.W. Leung  
October 14, 1982

<u>ITEMS FOR COMPARISON</u>	<u>CONVENTIONAL M3C→M6C</u>	<u>SUPERCONDUCTING MSC</u>
Coils (including radiation shield and cryostat and vacuum box in superconducting case)	1140 K\$	1438 K\$
Iron (at \$500/ton)	3308 K\$	1907 K\$
Manpower (including only design and engineering manpower for conventional case)	250 K\$	884 K\$
Power supply and instruments	100 K\$	185 K\$
Refrigeration for S/C	---	550 K\$
Cooling water for conventional	10 K\$	---
Conventional construction	400 K\$	357 K\$
Rigging, cost in piling iron and surveying (at \$60/ton)	404 K\$	229 K\$
Capital cost	5612 K\$	5550 K\$
Escalation and contingency (20%)	1122 K\$	1110 K\$
Total capital cost	6734 K\$	6660 K\$
5 year operation cost	at 1.5 MW (pulsed) & 50% duty factor - ~1530 K\$	at 250 KW x 50% duty factor ~225 K\$
Total cost (C + O)	8264 K\$	6885 K\$

## Energy Deposition in the Superconducting Active Muon Shield

Michael W. Peters

11/4/82

In the preferred design for the active muon shield in the prompt neutrino beam the deflected muons pass through superconducting coils 3 and 4 where they close over the upstream and downstream ends of the magnet (See Figure 1). These coils are well shielded against neutrons by the solid magnets M1 and M2 but the muon flux must be examined to insure that the energy deposition does not exceed the quench point for the superconducting material used.

Figure 2 of this note gives the vertical distribution of muons in narrow vertical band extending  $\pm 5$  cm horizontally about the midline. In the coil region the maximum number of muons per  $10^{13}$  incident protons is  $0.8 \cdot 10^9$  in a 20 cm by 10 cm bin. Thus the peak areal density is  $0.4 \cdot 10^7$  muons/cm<sup>2</sup>. Using an energy loss rate of 12.9 MeV/cm (Cu), we calculate an energy deposition of  $5.2 \cdot 10^7$  MeV/cm<sup>3</sup> or .008 mJ/cm<sup>3</sup> per beam burst. This would result in a local temperature rise of the conductor of about 0.1 Kelvin which is completely acceptable.

Figure 1

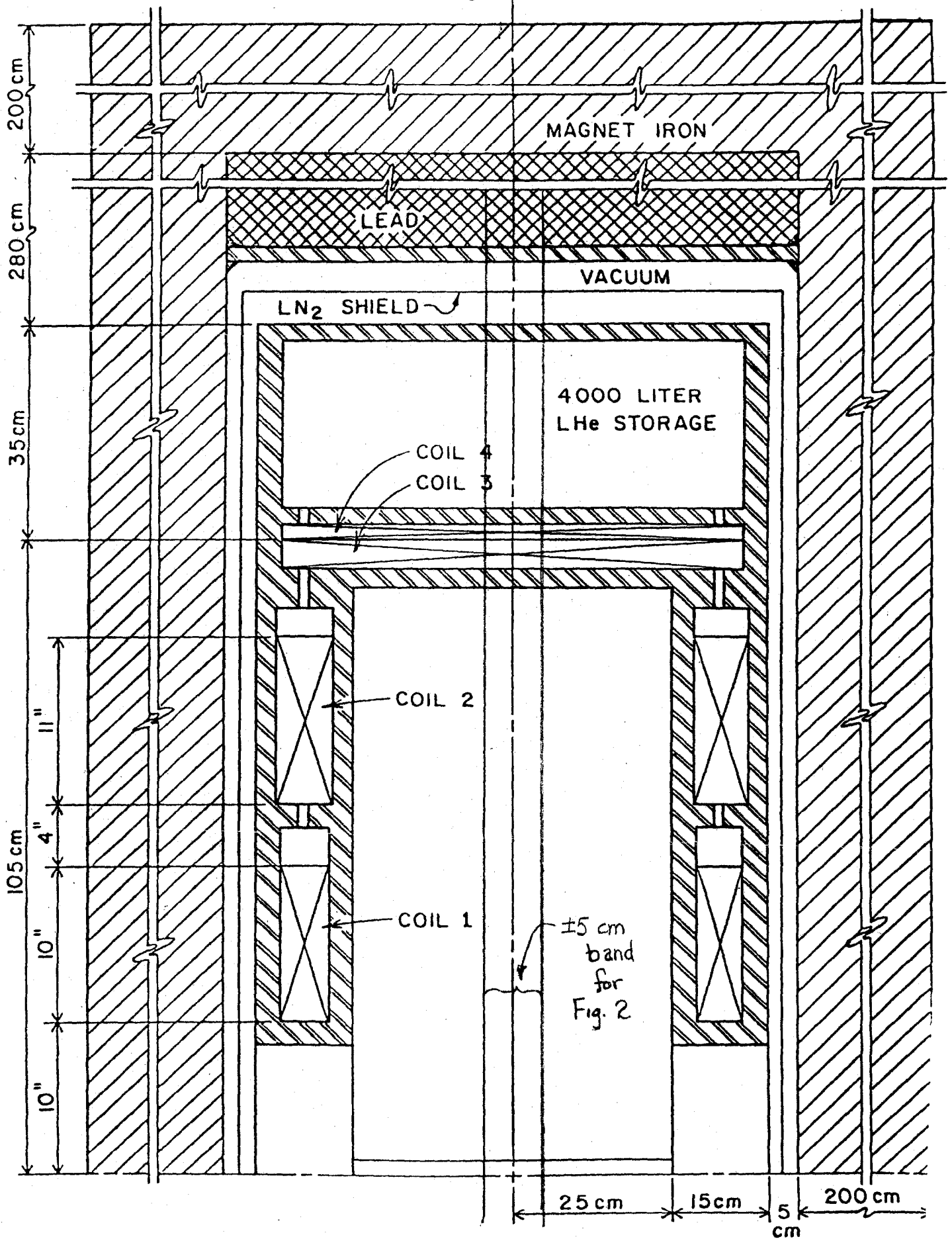


Figure 2

Number of  $\mu^+$  in  $\pm 5$  cm  
Vertical Band on  $\downarrow$

of  
Superconducting Magnet

End coils  $\overline{344}$

$\times 10^8$   
#  $\mu^+$

y (cm)

